UNIVERSITY OF CALIFORNIA,
IRVINE

Fossil Fuel Emissions of Carbon Dioxide: Feedbacks and Forecasting

DISSERTATION

submitted in partial satisfaction of the requirements
for the degree of

DOCTOR OF PHILOSOPHY

in Earth System Science

by

Dawn L. Woodard

Dissertation Committee:
Professor James T. Randerson, Chair
Professor Steven J. Davis, Co-chair
Professor Michael L. Goulden
Professor Nathan M. Mueller

2020

DEDICATION

This thesis is dedicated to the teachers who taught me to be curious and who gave me the tools to begin answering all my questions.

"Every major national science academy in the world has reported that global warming is real, caused mostly by humans, and requires urgent action. The cost of acting goes far higher the longer we wait — we can't wait any longer to avoid the worst and be judged immoral by coming generations."

– James Hansen

TABLE OF CONTENTS

LIST OF FIGURES

LIST OF TABLES

ACKNOWLEDGMENTS

This dissertation is based upon work in part supported by the National Science Foundation Graduate Research Fellowship Program under Grant DGE-1321846.

I would like to express so much gratitude to my committee chair, James Randerson, who has had patience throughout all of my ups and downs the past five and a half years, and who was always interested in whatever idea I had for a research topic, no matter the subject, and provided me with so many opportunities to advance my career and build professional connections. He has constantly been there to advocate for me and provide support when needed and has always helped me find the story in my research and the interesting direction to pursue in my analysis whenever I was floundering.

I also want to thank my committee co-chair Steven Davis for all of his advice and support, particularly for his creativity and design ideas for making my figures interesting and readable, and his suggestions for structuring papers for flow and a clear story.

I want to thank the other members of my committee, Nathan Mueller and Michael Goulden, for providing additional perspectives on this work, and for their useful input and advice along the way.

And I could not have done any of this without my friends, partners, and of course my parents. My friends have kept me sane, commiserated over stress and deadlines and coding errors, and provided much needed distractions after work. My partners have been endlessly supportive throughout everything and I cannot put into words how much their constant presence and faith in me has meant. And, finally, my parents who have been there in all the little ways like cards and care packages and encouragement and listening to my venting about whatever hurdle I was currently facing, but also throughout my life in all the bigger ways, like providing me with all the best educational opportunities and always believing in me and supporting me in whatever direction my interests turned.

VITA

Dawn L. Woodard

EDUCATION

Doctor of Philosophy in Earth System Science **2020**
University of California, Irvine *Irvine, California*

Master of Science in Earth System Science **2018**
University of California, Irvine *Irvine, California*

Bachelor of Science in Mathematics **2010**
Appalachian State University *Boone, North Carolina*

RESEARCH EXPERIENCE

Graduate Student Researcher Fall 2014 - Winter 2020
University of California, Irvine, Irvine, CA

Research Assistant Fall 2012 - Summer 2014
Appalachian State University, Boone, NC

Student Researcher Summer 2013
Bishop Heber College, Tiruchirapalli, Tamil Nadu, India

REU Student Summer 2012
National Institute of Mathematical and Biological Synthesis
University of Tennessee Knoxville, Knoxville, TN

REU Student Summer 2011
North Carolina Agricultural and Technical State University, Greensboro, NC

RESEARCH PUBLICATIONS

Woodard, D. L., Davis, S. J., & Randerson, J. T., (2019). Economic carbon cycle feedbacks may offset additional warming from natural feedbacks. *Proceedings of the National Academy of Sciences*, 116(3), 759-764.

Hogue, S., Marland, E., Andres, R. J., Marland, G., & **Woodard, D.** (2016). Uncertainty in gridded CO2 emissions estimates. Earth's Future, 4(5), 225-239.

LoPresti, A., Charland, A., **Woodard, D.**, Randerson, J., Diffenbaugh, N., Davis, S. (2015). Rate and velocity of climate change caused by cumulative carbon emissions. *Environmental Research Letters*, 10 (9), 095001.

Woodard, D., Branham, M., Buckingham, G., Hogue, S., Hutchins, M., Gosky, R., Marland, G., Marland, E. (2014). A spatial uncertainty metric for anthropogenic CO_2 emissions. *Greenhouse Gas Measurement and Management*, 4(2-4), 139-160.

Singer, A., Branham, M., Hutchins, M., Welker, J., **Woodard, D.**, Badurek, C., Ruseva, T.,

Marland, E., Marland, G. (2014). The Role of CO2 Emissions from Large Point Sources in Emissions Totals, Responsibility, and Policy. *Environmental Science and Policy*, 44, 190-200.

TEACHING EXPERIENCE

Teaching Assistant Spring 2017
The Sustainable Ocean
University of California Irvine,

Departmental Teaching Seminar Winter 2016
University of California Irvine,

Teaching Assistant Winter 2016
Advanced Data Analysis
University of California Irvine,

Teaching Assistant Fall 2016
GIS For Environmental Science
University of California Irvine,

RESEARCH GRANTS

NASA Carbon Monitoring System Flux Pilot Project [$10142] 2012-2014
North Carolina Space Grant [$4000] Academic Year 2013-2014
Office of Student Research Travel Grant [$250] Fall 2013
Honors International Travel Grant [$400] Spring 2013
National Science Foundation REU Grant NIMBioS [$3500] Summer 2012
National Science Foundation REU Grant NC A&T State University [$4500] Summer 2011

AWARDS AND HONORS

NSF Graduate Research Fellowship 2015-present
NSF Machine Learning and Physical Sciences (MAPS) Program Honorary Fellow 2016-2018
Caesar Cruz Award (for work with the Law Enforcement Accountability Network) 2017
UC Irvine Grad Slam Semifinalist 2017
Ralph J. & Carol M. Cicerone Endowed Graduate Fellowship Fall 2014
UCI Diversity Recruitment Fellowship Fall 2014
Honorable Mention in Appalachian Energy Summit 2014 Poster Competition Summer 2014
COMAP MCM Honorable Mention Award Spring 2014
Sigma Xi Interdisciplinary Research Award for poster presentation Spring 2013
COMAP MCM Meritorious Award Spring 2011

PROFESSIONAL AFFILIATIONS

Ecological Society of America 2018-present

American Geophysical Union	2013-present
Society for Neuroscience	2013
Society of Mathematical Biology	2012

RESEARCH PRESENTATIONS

Oral Presentations

"Improving our understanding of anthropogenic carbon-climate feedbacks: mechanisms, theory, and application." Chapman Conference on Understanding Carbon Climate Feedbacks, San Diego, CA.	Aug. 2019
"Understanding Future Fossil Fuel Emissions." American Geophysical Union Fall Meeting, San Francisco, CA.	Dec. 2018
"Human carbon-cycle feedbacks to global warming may offset natural feedbacks." Ignite oral presentation. Ecological Society of America Annual Meeting, New Orleans, LA.	Aug. 2018
"Human Carbon-Cycle Feedbacks to Global Warming May Offset Natural Feedbacks." NSF NRT Graduate Trainee Symposium on Machine Learning and the Physical Sciences (MAPS), Irvine, CA.	May. 2018
"Let's Turn Down The Heat: Improving Models to Prevent Climate Change." AGS Graduate Student Symposium, Irvine, CA.	April. 2017
"An Uncertainty Metric for Anthropogenic Carbon Dioxide Emissions." Biomathematics, Ecology: Education and Research, Arlington, VA.	Oct. 2013
"A Strategy for VHF Repeater Packing." Celebration of Student Research, Boone, NC.	Apr. 2011

Poster Presentations

"Quantifying Economic Carbon Cycle Feedbacks." Swiss Climate Summer School, Ascona, Switzerland.	Sept. 2019
"Predictability of U.S. Fossil Fuel Emissions." American Geophysical Union Fall Meeting, San Francisco, CA.	Dec. 2018
"Human and natural carbon feedbacks to global warming may be of similar magnitude." GCAM Community Modeling Meeting, College Park, MD.	Nov. 2017

"Human and natural carbon feedbacks to global warming may be of similar magnitude." 10th International Carbon Dioxide Conference, Interlaken, Switzerland.	Aug. 2017
"Comparing Natural and Economic Carbon Cycle Feedbacks." American Geophysical Union Fall Meeting, San Francisco, CA.	Dec. 2016
"Drivers and Methods of Addressing Uncertainty in Large Point Sources of CO_2." Appalachian Energy Summit, Boone, NC.	July, 2014
"Characterization and Analysis of Anthropogenic Point Source CO2 Emissions." Celebration of Student Research, Boone, NC.	Apr. 2014
"Resolution and Uncertainty in Spatial CO2 Emissions Estimates." American Geophysical Union Fall Meeting, San Francisco, CA.	Dec. 2013
"An Uncertainty Metric for Anthropogenic Carbon Dioxide Emissions." State of North Carolina Undergraduate Research and Creativity Symposium, Charlotte, NC.	Nov. 2013
"A Decade of the Journal IMPULSE: Growth and Impact." Society for Neuroscience Annual Meeting, San Diego, CA.	Nov. 2013
"IMPULSE: The Premier Undergraduate Neuroscience Journal." Poster presentation, workshop. SYNAPSE, Charleston, SC.	Apr. 2013
"Characterizing Uncertainty in Power Plant Emissions." Celebration of Student Research, Boone, NC.	Apr. 2013
"Effects of Constituent Monoterpenes of Monarda on Sporulation and Germ Tube Growth of *Beauveria bassiana*." Poster presentation, session moderator. Society for Mathematical Biology Annual Meeting, Knoxville, TN.	Jul. 2012

SELECT WORKSHOPS AND CONFERENCES ATTENDED

Intro to Linux Workshop	May 2017
Predictive Modeling with Python Workshop	April 2017
Climate Data Science Short Course	March 20-22, 2017
Advanced Predictive Modeling with Python Workshop	March 2017
Data Science Initiative-Machine Learning and Human Behavior Symposium	March 10, 2017
2017 UC Women's Caucus Leadership Conference	Feb. 10-12 2017

ABSTRACT OF THE DISSERTATION

Fossil Fuel Emissions of Carbon Dioxide: Feedbacks and Forecasting

By

Dawn L. Woodard

Doctor of Philosophy in Earth System Science

University of California, Irvine, 2020

Professor James T. Randerson, Chair
Professor Steven J. Davis, Co-chair

The key role that atmospheric carbon dioxide plays in climate warming makes it particularly relevant to understand the human and natural processes that increase or decrease carbon in the atmosphere. Contributing fluxes from the ocean, land, and various anthropogenic sources have been estimated by previous research but large uncertainties remain. As the only component directly under our control, the human contribution is critical to understand for policy decisions seeking to mitigate and prevent climate impacts. In this dissertation I have focused on a few aspects of understanding future fossil fuel emissions on both short and long timescales.

I started with the long term, exploring carbon feedbacks on fossil fuel emissions. In my first research chapter I conceptualize and estimate the size of several economic mechanisms that generate a carbon-climate feedback, using the Kaya Identity to separate a net economic feedback into components associated with population, GDP, heating and cooling, and the carbon intensity of energy. In a fossil fuel intensive future scenario, I found that such decreases in economic activity due to warming reduced fossil fuel emissions by 13% this century, lowering atmospheric CO_2 by over 100 ppm in 2100. The natural carbon-climate feedback, in contrast, increased atmospheric CO_2 over this period by a similar amount, and thus the net effect including both feedbacks was nearly zero. Importantly, although these

impacts of climate warming on the economy may offset weakening land and ocean carbon sinks, a loss of economic productivity will have high societal costs, potentially increasing wealth inequity and limiting resources available for effective adaptation.

The uncertainty in my estimation of a potential economic carbon feedback effect is high, however, motivating a need for improved understanding of these feedbacks within more sophisticated models. To that end, in my second study I have extended a framework previously developed for calculating natural carbon feedback parameters to include anthropogenic feedback effects, so it can be used to compare a larger set of carbon feedbacks across models as more human-driven mechanisms are incorporated. I then illustrate some of these calculations using a the model from the previous chapter and a modified version of the Dynamic Integrated Climate-Economy (DICE) model. This work demonstrates a framework that can be applied to evaluate model representation of both anthropogenic and natural feedbacks in integrated assessment models, aiding further model development and improving policy-relevant model outputs.

In my final research chapter I turn to a shorter-term analysis of fossil fuel emissions, exploring the use of autoregression models to make forecasts of emissions in the United States over intervals of a few months to a few years. I focus on freely available and frequently updated predictors including climatic and socioeconomic variables and test several different modeling approaches across all subsets of the predictors. The approach with the most predictive power for out-of-sample forecasts of up to a few months was a vector autoregression (VAR) model, which had a mean absolute percent error of 3.2% for an out-of-sample forecast one month ahead and was able to outperform an existing annual forecast from the EIA by an average of 20%. The model demonstrates the potential of simpler statistical models for short term emissions forecasts and provides a foundation for producing similar global forecasts.

The combined results from these analyses help support improved modeling efforts on short and long timescales of a critical climate driver: carbon dioxide emissions from fossil fuels.

Chapter 1
Introduction

1.1 Climate and the carbon cycle

Climate change is currently a key topic of concern among science communities, policymakers, public health officials, disaster relief organizations, and in news headlines around the world. And this is a subject that at its core is centered around carbon. There are many species of gases that absorb infrared radiation and warm the planet, but gaseous carbon compounds make up the largest fraction. Atmospheric carbon is found in two forms: methane and carbon dioxide (CO_2). While both are important, I have focused this dissertation on carbon dioxide as it is still today the most significant greenhouse gas in the atmosphere contributing to climate change (Myhre et al., 2013). This gas is cycled to and from the atmosphere through other carbon pools on Earth in a process known as the carbon cycle.

The majority of carbon is stored beneath the Earth's crust, but on centennial timescales the most significant of stores of carbon are marine and terrestrial biota, organic material in soils, and dissolved and particulate matter in the ocean (Suarez et al., 2019). The rate of exchange between these carbon pools determines the amount of carbon left in the atmosphere to affect global climate, as well as the amount in the ocean contributing to acidification. The exchanges between pools are affected by various factors, including the amount and type of biomass on the planet, soil types and levels of disturbance, and, importantly, air temperature and atmospheric carbon concentrations (Ciais et al. (2014), Figure 1.1).

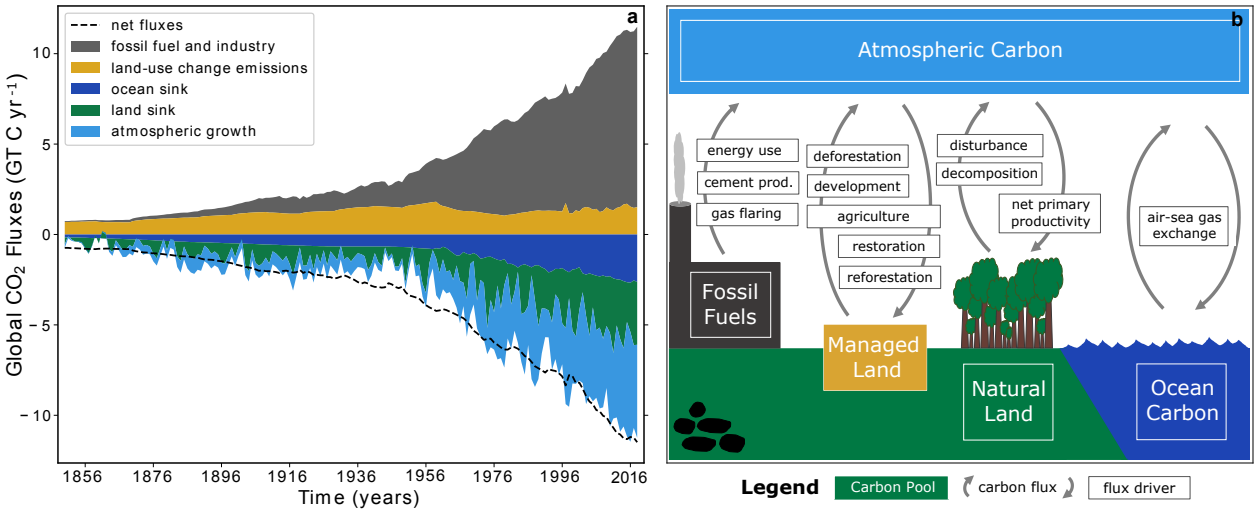

Figure 1.1: Global carbon cycle fluxes from 1850 to 2010, adapted from Friedlingstein et al. (2019) (a). The difference between the sum of the fluxes (black dashed line) and the atmospheric carbon line represents the budget imbalance and the limitations of current understanding of the carbon cycle. Panel b shows a corresponding diagram of the various carbon pools, the fluxes between them, and their driving mechanisms.

These last two factors set up two different types of feedback mechanisms. The first operates through changing carbon concentrations in the atmosphere which directly change the rate of uptake of carbon into the land or ocean pools, and then in turn change the amount of carbon in the atmosphere. This is called a carbon-concentration or carbon-carbon feedback in the literature, though I will be using the former nomenclature. Examples of mechanisms that drive this feedback include higher uptake of carbon into plants at higher CO_2 concentrations, an effect known as 'CO_2 fertilization,' and increased carbon uptake in the ocean due to higher partial pressure of carbon at the air-sea interface. In both cases, an increase in atmospheric carbon results in increased carbon storage in these two carbon pools, consequently decreasing carbon in the atmosphere. Because the net effect of this complete cycle is self-dampening and acts to reduce the initial increase in atmospheric CO_2, this cycle is called a 'negative' feedback. Not all carbon-concentration feedbacks are necessarily negative, but the primary examples of these feedbacks on land and in the ocean do fit into that category (Ciais et al., 2014).

The second feedback mechanism, called a carbon-climate feedback, refers mecha-

nisms affecting the exchange of carbon between various pools and the atmosphere that are not directly driven by a change in atmospheric CO_2, but instead are driven by changes in temperature. For example, carbon solubility in the ocean decreases at higher temperatures resulting in lower uptake. So when an increase in atmospheric carbon raises temperatures, carbon solubility in the ocean decreases, and as a result more carbon ends up in the atmosphere on top of the initial increase. With this mechanism, and with many other marine and terrestrial carbon-climate feedbacks, it acts to amplify any change in atmospheric carbon, whether an increase or a decrease. Feedbacks that have this self-reinforcing effect are referred to as 'positive' feedbacks.

The importance of the carbon cycle to Earth's climate and to the life living here cannot be overstated. Four of the five largest mass extinction events on the planet are thought to have been caused by large perturbations to the carbon cycle from geologic events known as large igneous provinces (LIPs) (Suarez et al., 2019) and carbon cycle feedbacks are likely important drivers of Earth's glacial-interglacial cycles (Montañez et al., 2016; Torres et al., 2017). One need only look to the scorching surface temperatures of Venus to understand just how consequential changes in a planet's carbon cycle can be (Bullock and Grinspoon, 1999).

1.2 Fossil fuel emissions of carbon dioxide

Historically, humans primarily affected the carbon cycle through deforestation and agriculture, but today fossil fuel emissions represent the most rapid large-scale perturbation to the carbon cycle in human history. Prior to the industrial revolution and the increasing use of fossil fuels to power growing economies, atmospheric carbon dioxide concentrations oscillated between around 200 to 280 ppm for hundreds of thousands of years as the Earth moved between glacial and interglacial periods (Friedlingstein and Prentice, 2010; Siegenthaler et al., 2005). In fact atmospheric CO_2 has never exceeded 300 ppm over the past 800,000 years of available data (Lüthi et al., 2008). Ice core records reveal increases in atmospheric CO_2

of around 80 to 100 ppm between each of the past four glacial to interglacial transitions (Monnin et al., 2001), and these past carbon changes coincided with a temperature change during the last glacial maximum of around 4.9 °C below the interglacial average (Shakun and Carlson, 2010). However over the last century and a half atmospheric CO_2 has risen to over 400 ppm, more than 100 ppm above its maximum over the past quarter million years, and global temperatures have increased nearly 1 °C as a result.

This massive perturbation to the carbon cycle is thanks to the more than 400 Pg C that humans have put into the atmosphere over the same time period from burning fossil fuels (Boden et al., 2017; Friedlingstein et al., 2019). By 2018, total global fossil fuel emissions had increased to a rate of around 10 Pg C $\cdot$ yr^{-1}, up from less than 7 Pg C $\cdot$ yr^{-1} in 2000 (Friedlingstein et al., 2019). For comparison, during LIPs, carbon emissions averaged up to only around 3 Pg C yr^{-1}, and the increase in atmospheric CO_2 of 76 ppm following the last glacial maximum occurred over 6000 years (Monnin et al., 2001). It has taken humanity since only 1975 to raise atmospheric CO_2 by that same amount (Friedlingstein et al., 2019).

Humanity's fossil fuel consumption is driven by a variety of sources. The primary source globally is from energy uses including electricity generation from coal, oil, and natural gas fired power plants, non-electric heat generation in private homes and manufacturing industries, as well as cargo and personal transportation. Emissions from non-energy sources include CO_2 released during cement production and natural gas flaring (Krey et al., 2014). Despite growing international concern about the effects of climate change and multiple international agreements to reduce carbon emissions, global emissions are continuing to rise.

As with marine and terrestrial carbon fluxes, there are climate-driven mechanisms that may also generate feedbacks on fossil fuel emissions. These include climate effects on various drivers of emissions such as energy demand, population growth, economic growth, development and adoption of energy efficient technologies, climate policies and individual behavior, and society's dependence on carbon-emitting versus zero-carbon energy generation. To the extent that any of these and other drivers of emissions are affected by a changing

climate, they become mechanisms that generate carbon-climate feedbacks on the fossil fuel CO_2 flux to the atmosphere. Such feedbacks have received almost no attention in the literature, however, so little is known about their potential significance or impacts on climate. I should also note that while there may be a small carbon-concentration driven feedback as well through CO_2 fertilization of agriculture, this is likely to have only a minimal net effect on emissions and climate and as such I neglect it in the following chapters.

1.3 Modeling the carbon cycle

While our understanding of the carbon cycle can be greatly advanced by analyses of current and historical data, modeling is a critical tool in furthering knowledge of this system, particularly for making projections of its future evolution under the current perturbation from fossil fuels. Various models of different degrees of complexity have been developed to represent the behavior of the climate and carbon cycle, particularly the effect of fossil fuel emissions on natural systems, as well as to provide diagnostic information about the functioning of key components.

Earth system models (ESMs) combine a physical climate model with representations of land and ocean biogeochemical processes, importantly including the natural carbon cycle fluxes and key carbon cycle feedbacks. These models perturb their climate with exogenous fossil fuel emissions trajectories and calculate the effects of that ongoing perturbation on the physical climate system and on marine and terrestrial biogeochemistry (Flato, 2011; Dunne et al., 2012). It is these models that have provided the public and policymakers with estimates of future physical and biogeochemical changes to the climate under different policy scenarios by the end of the century.

Integrated assessment models (IAMs) are the models responsible for generating the fossil fuel emissions trajectories that are used as inputs to ESMs. These economic and energy-system models give researchers tools to project future impacts of climate change on the economy, evaluate the effectiveness of future climate policies, and estimate future green-

house gas emissions based on assumptions about future growth and development. IAMs vary in structure depending on their intended purpose, ranging from technologically driven models with explicit representations of a variety of technologies to models focusing on macroeconomic feedbacks. These models can be run with different policy options and are fed assumptions about future quantities such as population, economic growth, or technological progress (Kriegler et al., 2015).

Both classes of models serve important roles in understanding past, current, and future climate conditions, but they still have many limitations in their ability to represent key carbon cycle processes. Most integrated assessment models have only very rudimentary climate modules and do not include two-way coupling between these modules and their economic and energy components, so carbon-climate feedbacks on emissions are not considered and the natural carbon cycle in these models is missing many critical mechanisms (Weyant, 2017). While earth system models do have a much more sophisticated representation of the natural carbon cycle, many are still lacking representation of certain natural feedback components, such as fires and permafrost, and none have the ability to include policy and economic responses to climate change (Arora et al., 2019). Model intercomparison projects have been used extensively by the earth system modeling community to aid in development and compare representation of processes between models, but the integrated assessment modeling community has been less active in pursuing this type of analysis and what has been done has been focused on economic and emissions outcomes rather than carbon and climate behavior (Kriegler et al., 2015).

1.4 Organization of research

The goal of this work is to further understanding of the fossil fuel carbon flux and its dynamics. This research supports modeling efforts of fossil fuel emissions by laying a foundation for improved representation of feedbacks on fossil fuel emissions and exploring the use of simple statistical techniques combined with up-to-date data to forecast near-term fossil fuel

emissions. The rest of this dissertation is organized into an additional four chapters and an appendix of supplementary methods for Chapter 2.

In Chapter 2 I share results exploring the relative magnitude of anthropogenic and natural carbon-climate feedbacks in a carbon cycle box model I developed. I also introduce a simple approach to the representation of anthropogenic feedbacks in this model. In this analysis I sought to understand the potential drivers of a carbon-climate feedback on fossil fuel emissions and to estimate the relative magnitude of the net economic feedback compared to the net natural feedback. This work has been published in PNAS as

"Woodard, D. L., Davis, S. J., & Randerson, J. T. (2019). Economic carbon cycle feedbacks may offset additional warming from natural feedbacks. Proceedings of the National Academy of Sciences, 116(3), 759-764."

In Chapter 3 I describe a mathematical framework that had previously been developed for estimating natural carbon cycle feedbacks in models, but which I here extend to include anthropogenic feedbacks such as those on fossil fuel emissions. I provide concrete examples to support the application of this framework to carbon cycle analysis within integrated assessment models and demonstrate its application to estimate feedbacks in a modified version of the Dynamic Integrated Climate Economy (DICE) model and in the model from Chapter 2. The goals of this research were to support model development and representation of carbon cycle processes by building out a more comprehensive framework for comparing carbon cycle feedbacks between models that includes both natural and anthropogenic mechanisms.

Chapter 4 describes a forecasting system I developed for near term fossil fuel emissions using a vector autoregression (VAR) model, addresses forecasting with data on different temporal availability, and demonstrates that this statistically simple model can outperform more complex emissions forecasting systems for U.S. fossil fuel emissions, at least on short timescales. Finally, in Chapter 5 I discuss the overall implications and future directions of this work.

Chapter 2
Economic carbon cycle feedbacks may offset additional warming from natural feedbacks

2.1 Introduction

Changes in the Earth system as the planet warms are likely to make it progressively more difficult to stabilize the climate (Field et al., 2014). For example, decreases in carbon uptake by terrestrial and marine ecosystems could reduce cumulative CO_2 emissions allowable under a 2 °C climate target by 6-29% (Jones et al., 2013; Ciais et al., 2014). On land, climate models show a positive carbon-climate feedback primarily from decreases in net primary production in response to warming and drying in the tropics, along with enhanced carbon losses from soils (Arora et al., 2013; Friedlingstein et al., 2006; Davidson and Janssens, 2006). In the oceans, increasing stratification weakens anthropogenic carbon flow into the ocean interior, while rising temperatures simultaneously reduce CO_2 solubility (Schwinger et al., 2014). Previous studies have quantified the relative importance of different natural feedback processes by using Earth system models to isolate and estimate the gain of the carbon-climate feedback as a function of the models' climate sensitivity, the sensitivity of ocean and land carbon reservoirs to warming, and the sensitivity of these same reservoirs to rising atmospheric CO_2 (Gregory et al., 2009). Yet although there are a number of mechanisms by which fossil fuel emissions may be affected by temperature (see, for example, Roson and van der Mensbrugghe 2012), emissions remain an exogenous, temperature-insensitive

input to most Earth system models (Arora et al., 2013; Friedlingstein et al., 2006). Though some integrated assessment models have explored the connection between temperature and emissions (Roson and van der Mensbrugghe, 2012; Zhou et al., 2014; Nordhaus, 2017; Beckage et al., 2018), the feedback effect from this relationship has not been systematically assessed. As a result, the magnitude of the carbon cycle feedback related to human systems is not well-understood.

Climate change will affect human activity, different sectors of the economy, and types of energy infrastructure in different ways, each with the potential to alter fossil fuel CO_2 emissions (Figure 2.1). Each of these impacts has been analyzed separately to varying degrees by previous studies. Rising temperatures will have direct effects on human mortality through various avenues including heat exposure, disease spread, extreme weather events, and food and water scarcity (McMichael et al., 2006). Climate change will also alter economic productivity through direct impacts on labor productivity from heat stress, infrastructure damage, and resource diversion and losses (Libecap and Steckel, 2011). These effects on population and economic output overall tend to indirectly decrease energy use and thus fossil CO_2 emissions. Increased temperatures will also change energy use more directly by influencing heating and cooling demands in residential and commercial sectors, the balance of which determines the overall sign of this effect (Santamouris et al., 2015). Additionally, rising temperatures will impact thermoelectric power production, electricity distribution, and transportation systems by decreasing energy efficiency and thereby increasing emissions from fossil fuel-burning infrastructure (Aivalioti, 2015; Sathaye et al., 2011; Mideksa and Kallbekken, 2010).

Integrating various economic effects across different sectors, empirical modeling has recently suggested that temperature may have a strong influence on economic activity, reducing gross domestic production (GDP) by as much as 20% worldwide by 2100 (Burke et al., 2015). Such large economic impacts would in turn decrease energy use and fossil fuel CO_2 emissions. Although other estimates of economic damages under climate change are

much smaller ranging from -1.5% to +2.3% change in GDP per °C (Nordhaus, 2017; Tol, 2009), such estimates often rely on theoretical and sometimes arbitrary damage functions (Ackerman et al., 2009; Burke et al., 2016; Ackerman and Stanton, 2012; Weitzman, 2012) rather than historical observations.

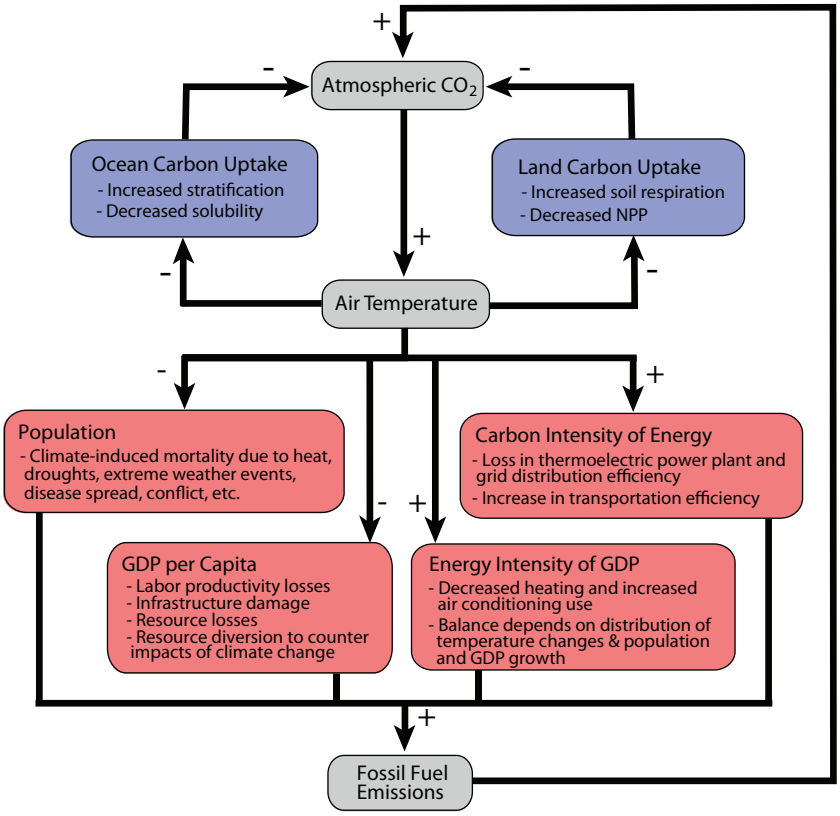

Figure 2.1: Diagram of the relationship between the economic and natural carbon cycle processes considered in this analysis. In our model, we included carbon-climate feedbacks on the natural carbon cycle from ocean stratification, soil decomposition, and NPP. We then used this base model to explore effects from global temperatures on the economic carbon cycle through population, GDP, the energy intensity of GDP, and the carbon intensity of energy. These effects translate into a temperature-driven impact on fossil fuel emissions through the Kaya Identity (Eqn. 2.1) in our model, which then has consequences for atmospheric CO_2 and land and ocean uptake of carbon, as well as temperature. The signs shown indicate a net direct (+) or inverse (-) relationship between each upstream and downstream process in our model. Further discussion of the uncertainty of the signs of the economic relationship is given in the appendix.

The combination of temperature-driven effects on population, energy, and GDP generates an economic carbon-climate feedback because of the direct connection between

economic activity and fossil fuel emissions. This feedback is an economically-driven parallel to the natural carbon-climate feedback operating through land and ocean processes. Through its influence on atmospheric carbon dioxide, the economic carbon-climate feedback may subsequently modify processes regulating natural carbon-concentration and climate-carbon feedbacks, including, for example, changes in photosynthesis and air-sea gas exchange that are sensitive to rising CO_2 and climate warming.

Here, we systematically compare economic and natural carbon cycle feedbacks in order to estimate the carbon cycle implications of human responses to climate change, and especially the recent estimates of climate-related economic damages (Burke et al., 2015). We conceptualize drivers of the economic carbon-climate feedback through the Kaya Identity, using a set of scenarios to isolate feedbacks on population (hereafter referred to as our Population scenario), GDP per capita (GDP scenario), the energy intensity of GDP (Energy Intensity), and the carbon intensity of energy (Carbon Intensity) individually, as well as a scenario combining GDP and carbon intensity processes (Net Economic). We also include a baseline scenario (No Feedbacks), which allows natural carbon fluxes in our model to respond to rising CO_2, but not to rising temperatures, and a scenario which includes only natural carbon-climate feedback processes (Net Natural). Previous work has referred to this latter scenario as a "fully-coupled" scenario (for example, Arora et al. 2013; Friedlingstein et al. 2006), but we reserve the term Fully Coupled here for our final scenario, which is the combination of the Net Natural and Net Economic scenarios (see Table A.1 for more detail on our simulation design).

For our baseline data, we use historical socioeconomic data and assume future fossil fuel CO_2 emissions and energy and population projections from the Global Change Assessment Model (GCAM) simulation for Representative Concentration Pathway 8.5 (RCP8.5) (Moss et al., 2008, 2010). Relationships between temperature and each economic component are derived from a literature synthesis, whereas for the natural carbon cycle we optimize a box model to match the mean carbon cycle behavior of fully coupled Earth system models

(Arora et al., 2013; Friedlingstein et al., 2013).

2.2 Materials and methods

Details of our analytic method are available in the appendix. All data and code used to generate the results are available on Github (https://github.com/dawnlwoodard/econ-feedbacks.git). Briefly, we represent the natural carbon cycle, including key carbon-climate and carbon-concentration feedbacks using a global box model of the atmosphere, land, and ocean carbon system (see Appendix). We tuned the model to within one standard deviation of the mean behavior of Earth system models from the 5th Phase of the Coupled Model Intercomparison Project (CMIP5) (Tables A.4 and A.5) and it reasonably reproduces observations of the carbon cycle and temperature over the past two centuries (Figure A.1). Economic feedback effects are explicitly incorporated in the model as impacts on different factors of the Kaya identity:

$$F = P \cdot \frac{G}{P} \cdot \frac{E}{G} \cdot \frac{F}{E} \tag{2.1}$$

where F represents global fossil fuel CO_2 emissions, P is population, G is world GDP or gross world product, E is global energy consumption, and E/G and F/E are the energy intensity of GDP and the carbon intensity of energy, respectively. As a baseline, we use historical socioeconomic data (Table A.6; Figure A.2) and assume future fossil fuel CO_2 emissions and energy and population projections from the Global Change Assessment Model (GCAM) simulation for Representative Concentration Pathway 8.5 (RCP8.5) (Moss et al., 2008, 2010). Relationships with temperature for each economic component are derived from previous studies (see Appendix, Figure A.3).

We isolate and estimate the magnitude of carbon cycle feedbacks by restricting in turn the various components of the coupled model following methodology established for natural carbon cycle analysis (Friedlingstein et al., 2006; Gregory et al., 2009). All scenarios

include natural carbon-concentration feedback processes, but carbon-climate feedbacks are isolated in different scenarios as summarized in Table A.1. The No Feedbacks scenario is our baseline for comparison and includes only natural carbon cycle responses to rising atmospheric CO_2, neglecting both human responses as well as land and ocean climate sensitivity. The Net Natural scenario corresponds to the fully-coupled scenario in previous analyses of the natural carbon cycle (Arora et al., 2013; Friedlingstein et al., 2013) in which all natural feedbacks are allowed to operate, but all economic responses to warming are excluded. The Population scenario adds estimates of climate-related deaths (but no other human responses) (World Health Organization, 2014) onto the baseline scenario. The Energy Intensity scenario includes only modeled changes in energy demand for heating and cooling of residential and commercial buildings (following Isaac and van Vuuren (2009)) on top of the baseline. The Carbon Intensity scenario includes only temperature-related changes in the efficiency of electricity production, electricity distribution, and transportation (Aivalioti, 2015; Sathaye et al., 2011; Basha et al., 2012; Burnard and Bhattacharya, 2011) (see Appendix, Figure A.4 and Table A.7 for details) in addition to the baseline. The GDP scenario incorporates economic damages due to climate change, using using the non-linear relationship found by Burke et al. (2015) as a best estimate. The Net Economic scenario is the economic parallel to the "Net Natural" and includes carbon intensity responses and GDP responses (i.e., effects on the Kaya factors G/P and F/E, which influence emissions in opposite directions as temperature increases) but excludes our independent estimates of population and energy intensity responses because these may be subsumed into GDP damages. Finally, our Fully Coupled scenario combines the Net Natural and Net Economic scenarios to include both economic and natural carbon-climate feedbacks on top of the baseline scenario.

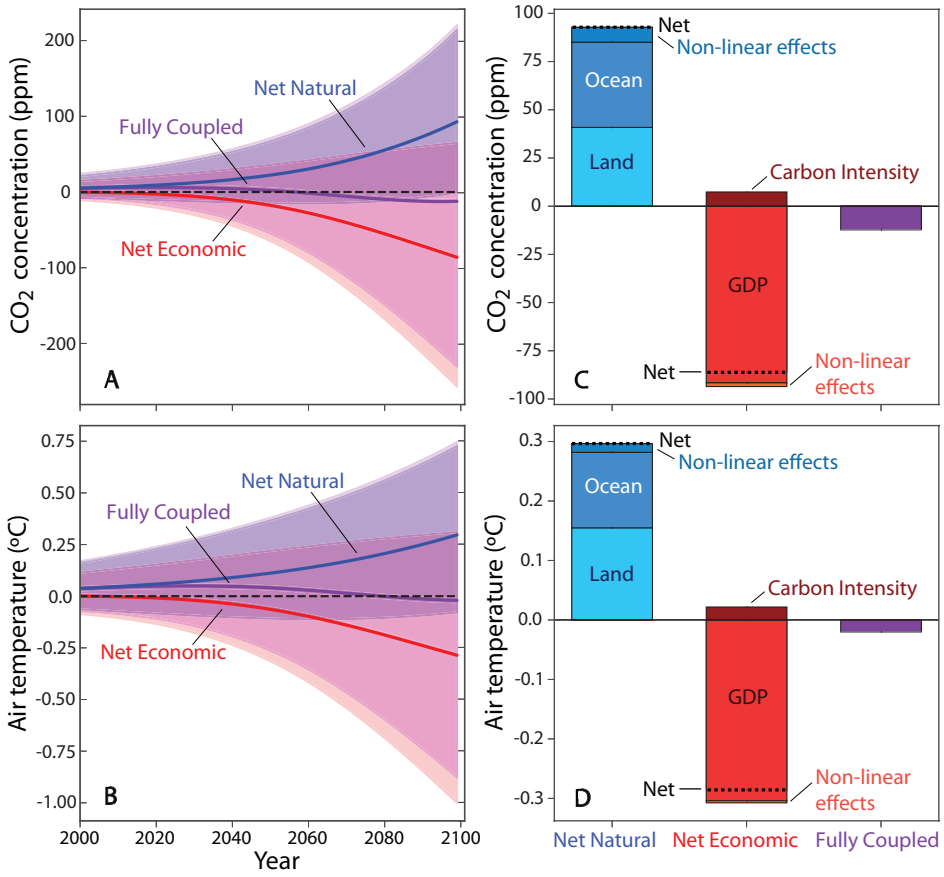

Figure 2.2: Net effects of including only natural, only economic, or both sets of feedbacks in our model compared to the baseline, No Feedbacks, scenario. All values shown are given as the difference between the baseline and that scenario. Panels A and B show air temperature and atmospheric CO_2 over the 21st century with uncertainty bounds on the Fully Coupled and Net Economic scenarios. Natural carbon-climate feedbacks (Net Natural) increased atmospheric CO_2 and temperature, while economic feedback processes (Net Economic) decreased them. The net economic effect more than offset the net natural, so the Fully Coupled scenario showed an overall negative effect on temperature and atmospheric CO_2. Panels C and D show the change in temperature and atmospheric CO_2 from 1800 - 2100 for these scenarios along with decompositions of the contributions to each net effect. For the natural carbon cycle, effects from the land and ocean in our model were similar in magnitude. Temperature effects on GDP drove the net economic effect strongly down, and while the carbon intensity of energy (Carbon Intensity) feedback caused a slight increase, the overall effect was dominated by GDP. Both net natural and net economic results also had some non-linear interaction effects that were not captured by our decoupled scenarios.

2.3 Results

2.3.1 Climate and carbon cycle impacts

Relative to our baseline scenario, the natural carbon-climate feedback (Net Natural) increased atmospheric CO_2 by 92 ppm (56 - 152 ppm), or about 15%, and temperature by 0.30 °C (0.19 °C - 0.44 °C) from 1800 to 2100, while the economic feedback (Net Economic) decreased them by 85 ppm (ranging from an increase of 3.3 ppm to a decrease of 204 ppm), or 14%, and 0.29 °C (ranging from an increase of 0.01 °C to a decrease of 0.76 °C) over the same period. The combination of these two sets of effects in our Fully Coupled scenario reduced CO_2 by about 12 ppm (ranging from an increase of 156 ppm to a decrease of 179 ppm) and had only a minor effect on temperature (Figure 2.2; Table A.3). Here, the response of economic processes to climate warming has not only compensated for the positive feedback from natural carbon-climate interactions but has driven the entire system toward a small negative feedback.

For both economic and carbon cycle parameters we derived upper and lower uncertainty bounds and propagated them through our model. Our upper bound on the relationship between GDP and temperature comes from the highest impact scenario in Burke et al. 2015, and our lower bound is the damage function from the Dynamic Integrated Climate-Economy (DICE) model (Nordhaus, 2017). For uncertainty related to climate effects on carbon intensity, we derived upper and lower bounds from estimates reported in the literature (see Appendix for details). For our population and energy intensity scenarios we assumed upper and lower uncertainty bounds of ± 50% as significant uncertainties exist in the current understanding of these relationships in the literature.

Natural carbon cycle uncertainty estimates were derived from fitting to ± one standard deviation of the CMIP5 multi-model mean ocean and land carbon storage by 2100. A more detailed description of uncertainty in each scenario is available in the appendix.

Our results demonstrate the potentially comparable magnitude of an economic

carbon-climate feedback and indicate that this may act to substantially counter warming from the natural carbon-climate feedback. Importantly, this apparent benefit to the climate is driven by large economic losses, so while we find that economic feedback processes do have the capacity to balance the additional warming from the natural carbon-climate feedback, this is achieved only through damages to the global economy.

Carbon fluxes, atmospheric CO_2 levels, and global mean surface temperatures in our Fully Coupled scenario were lower than the Net Natural values, particularly as temperatures increased more rapidly after 2050 (Figure 2.3A-C). By 2100 economic damages from climate warming reduced GDP by 22% (5.9 - 61%) (Table A.2), which in turn lowered cumulative fossil fuel emissions by 298 Pg C (ranging from a decrease of 764 Pg C to an increase of 8 Pg C) or 14% in the GDP scenario (Figure 2.3D). Temperature-driven decreases in the efficiency of energy production from fossil fuels increased the carbon intensity of energy in our model by 2.4% (ranging from a decrease of 0.51% to a decrease of 6.6%), which alone (in the Carbon Intensity scenario) drove a 24 Pg C increase (ranging from a 6 Pg C decrease to a 58 Pg C increase) in cumulative emissions (1%) relative to the baseline by the end of the century. This positive influence on emissions associated with temperature effects on the carbon intensity of energy was more than offset by the negative effect of temperature on GDP, so that together economic processes in our Fully Coupled scenario reduced atmospheric CO_2 by 104 ppm (ranging from a decrease of 235 ppm to an increase of 3 ppm), or 15% , and global mean air temperature by about 0.32 °C (ranging from a decrease of 0.82 °C to an increase of 0.01 °C) from 1800 to 2100 relative to the Net Natural scenario (Figure 2.3). This impact on the carbon cycle is comparable in magnitude, but opposite in sign, to potential losses in permafrost over the next century (Schuur et al., 2015).

In two other decoupled economic scenarios, we examined how climate change impacts on energy demand and population may influence carbon cycle processes. In our analysis, the contribution of each of these two components to economic effects on the carbon cycle was only very slight (Figure 2.3D-F).

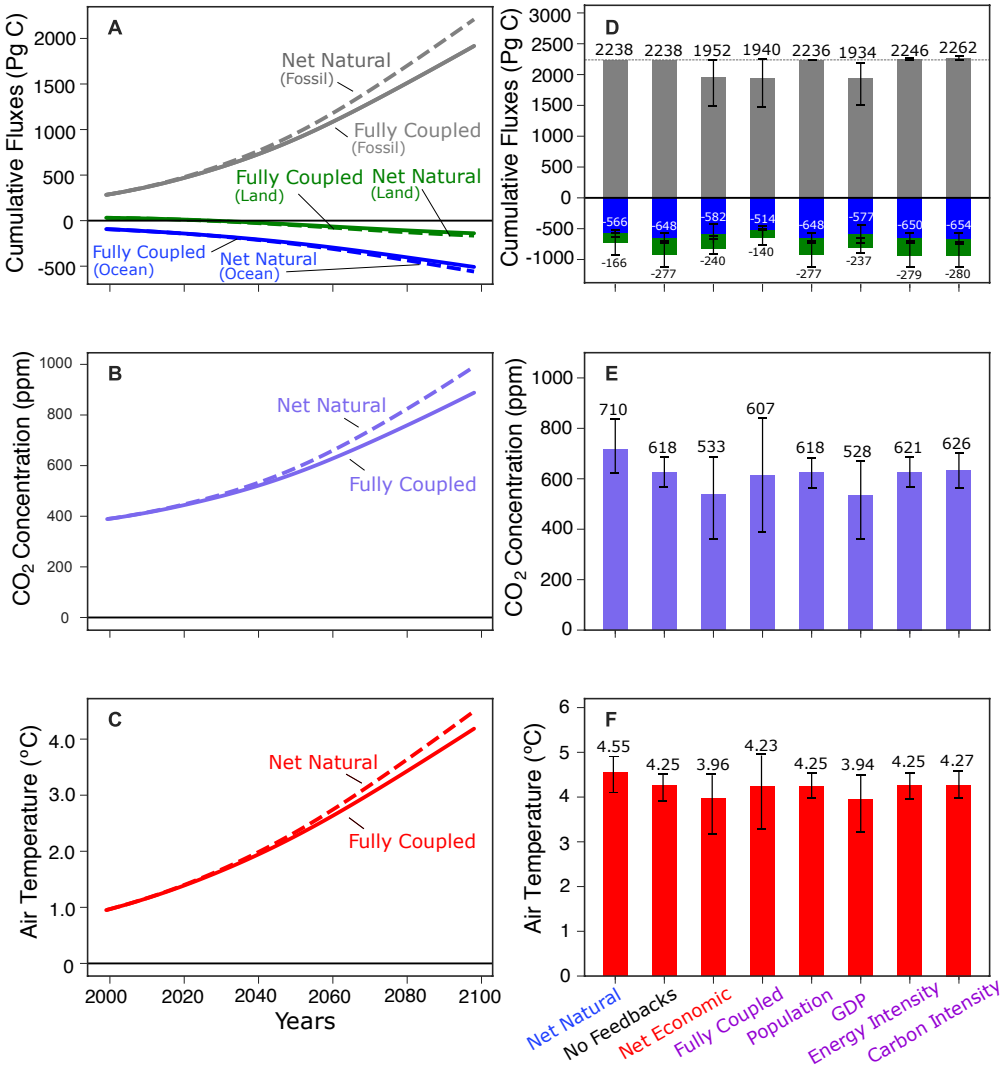

Figure 2.3: Model results compared across all scenarios from 1800-2100. Panels A-C show the effect on the carbon cycle of including economic feedback effects over the 21st century. Our Fully Coupled scenario (solid), which includes both natural and economic carbon-climate feedbacks, has lower emissions, atmospheric CO_2, and temperature than our Net Natural scenario (dashed), which includes no temperature effects on fossil fuel emissions. These effects are seen most strongly in the latter half of the century when temperature increases are higher. Panels D-F show changes in cumulative fluxes, atmospheric CO_2 concentration, and temperature for each scenario from 1800 to 2100. The Net Natural carbon-climate feedback drives atmospheric CO_2 and temperature above the No Feedbacks scenario baseline, while the Net Economic lowers these values below baseline. Our GDP and Population scenarios both result in negative effects on emissions, though the GDP effect is considerably more pronounced, while our Energy Intensity and Carbon Intensity scenarios contribute to slight increases in fossil fuel emissions.

2.3.2 Feedback effects

Integrating economic processes into our model changed the sign and magnitude of the gain of the carbon-climate feedback because of the relatively strong temperature sensitivity of fossil fuel emissions. We illustrate this sensitivity in Figure 2.4. In our model, a 1% decline in fossil fuel emissions per °C of climate warming corresponded to a decrease in the gain of the carbon-climate feedback of about 0.05, a decrease in atmospheric CO_2 of 28 ppm compared to our Net Natural scenario, and a feedback-driven temperature decline of 0.1 °C by 2100. Although the sensitivity function was non-linear, we fit a linear model through our upper and lower bounds from our Fully Coupled scenario to estimate this unit effect. Because our Fully Coupled scenario had an average emissions sensitivity of about -3% per °C, this reduced the gain of the carbon-climate feedback from a positive value in our Net Natural scenario (+0.13) to slightly below zero in our Fully Coupled scenario (-0.02) (Figure 2.4, Table A.3).

2.4 Discussion

Our results indicate that the economic feedback has the potential to reverse the sign of the overall carbon-climate feedback, but the significance of the impact is highly sensitive to the relationship between climate and GDP. If the effect of climate on GDP is large and dominates the feedback, the economic carbon feedback counteracts the response of the natural carbon cycle. However, if this temperature-GDP effect is more in line with estimates like those in the 2016 version of DICE model (Nordhaus, 2017), we can expect that the economic contribution to the carbon-climate feedback will instead add slightly to the natural positive gain (Figure 2.4), somewhat increasing future temperatures and atmospheric carbon dioxide (Figure 2.3A).

Our estimate of climate impacts on fossil emissions is substantially higher than a previous analysis from the ENVISAGE model, which found a reduction in CO_2 emissions

of 4.7% from their economic feedbacks by 2100 (Roson and van der Mensbrugghe, 2012). This is likely driven by the choice of economic damage function. The damages found by Burke et al. 2015 are larger than that used in ENVISAGE as well as those used in many other models, as Burke's analysis broadly includes any climate-driven impacts that would be reflected in GDP over the past half century. The sum of the effects considered in ENVISAGE we expect to be lower as only certain economic sectors were included. For example, both extreme weather and catastrophic events are not included in the ENVISAGE results (van der Mensbrugghe, 2010), whereas the GDP damages from Burke et al. 2015 are general enough to include such effects.

By propagating upper and lower uncertainty bounds for each term in the Kaya identity through our model, we have attempted to illustrate the spread of potential outcomes. Additionally, while we have made every effort to use reasonable values, it was necessary to make several major assumptions in order to maintain the simplicity of our model and not attempt to replicate a full integrated assessment model, as that is beyond the scope of this work. A key future challenge is to quantify economic carbon-climate feedbacks within and across integrated assessment models that account for more complex interactions among different sectors and processes.

Improving estimates of the economic carbon-climate feedback is particularly relevant because important tradeoffs exist with respect to the societal impacts of strong versus weak economic damage functions. While a stronger damage function in response to rising temperature appears to imply that it may be easier to match emissions reductions targets, this comes at an economic cost that would likely make it more difficult for vulnerable regions to respond to climate change impacts (Rose, 2004). Moreover, such economic and social costs entailed by stronger damage functions are likely to be large and inequitably distributed, as climate change is expected to worsen already existing economic vulnerabilities (Otto et al., 2017). Natural disasters, for example, have higher death tolls in lower income areas and in countries without democratic institutions (Kahn, 2005). In our globally averaged model, the

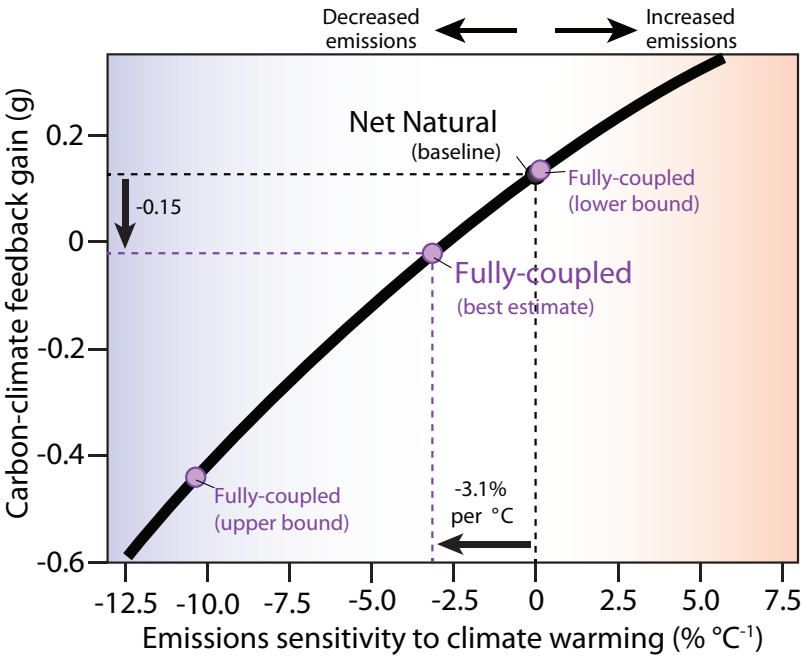

Figure 2.4: Generalized comparison of the carbon cycle response to economic damages in our model under RCP8.5. The black curve was derived from inputting a range of potential emissions damages per degree (shown along the x-axis) into our model and computing the resultant cumulative carbon-climate feedback gain over the period from 1800-2100 for each. The steep slope of the curve suggests that even small changes in the temperature-sensitivity of fossil fuel emissions may have significant consequences for the carbon cycle. Overlaid on the curve are points showing specific results from our Fully Coupled and Net Natural scenarios. Comparing these scenarios shows the overall effect on the carbon cycle of including an economic carbon-climate feedback in our model. The Fully Coupled scenario has an approximate fossil fuel temperature sensitivity of -3.1% per °C, resulting in a decrease in the gain of 0.15 from the Net Natural scenario.

Burke et al. relationship led to GDP losses of 22% by 2100 (Table A.2). In just the United States by the end of the century, the poorest third of counties are predicted to experience losses of 2% to 20% of income while the richest third may experience losses of only 7% up through potential benefits of 1.2% of income (Hsiang et al., 2017). Any potential benefit in terms of lower emissions from a negative economic feedback only exists because nations necessarily lose so much productivity, in the form of human lives, agriculture, infrastructure, and labor, that this reduction in economic activity lowers their fossil fuel emissions.

Strong versus weak economic damage functions also may have implications for the

distribution of climate impacts across natural and human systems. A weaker economic damage function, for example, would allow more CO_2 to accumulate in the atmosphere, causing higher surface air temperatures. Accelerated warming, in turn, would cause greater damages in terrestrial and marine ecosystems, including losses of net primary production and biodiversity on land (Diffenbaugh and Field, 2013) and the disruption of critical nutrient supply pathways in the ocean (Moore et al., 2018). Thus, although natural and economic feedbacks are likely opposite in sign, carbon-climate feedbacks driven by higher temperatures have net damaging effects on both natural and human systems.

The strength of both economic and natural feedbacks varies significantly over the globe, so regional carbon cycle impacts may be considerably stronger or weaker than the global mean (Burke et al., 2015; Boer and Arora, 2010). Economic activities driving the carbon-climate feedback at the local level will include changes in tourism revenue, damages from sea level rise and wildfires, and locally varying patterns of energy use. For example, Isaac and van Vuuren 2009 found that India showed a very strong impact of temperature on energy demand, in contrast to their finding of a much less significant effect globally. The economic climate feedback from energy use would overall be expected to be higher in areas with quickly increasing GDP and population as well as larger predicted climate impacts.

In the model used here, we have considered a limited number of both natural and economic processes. We tuned our simple natural carbon cycle model to match the mean behavior of the CMIP5 models, but these models are missing key natural processes such as the permafrost carbon reservoir and its sensitivity to thaw (Schuur et al., 2015) and are weak in their representation of other drivers of the carbon-climate feedback including the representation of ecological tipping points within the Amazon (Cox et al., 2013). On the economic-driven side, we do not include any feedbacks associated with climate effects on land use. Recent work indicates these would be expected to contribute to a positive economic carbon-climate feedback (Thornton et al., 2017), mitigating slightly the negative effects of the GDP feedback described here. It is also worth acknowledging that there are

other human-driven feedbacks that fall outside of the carbon-climate feedback. One example is an economic carbon-concentration feedback associated with the benefits of increasing atmospheric CO_2 on crops. There are also potential economic impacts associated with climate-driven human migration, which could have varied impacts on climate through both carbon and non-carbon pathways. Beyond carbon feedbacks entirely, there may be policy-driven feedbacks that influence aerosols and albedo.

Our results provide a baseline effort to assess the economic carbon-climate feedback and compare it to the natural feedback by unifying the different contributing mechanisms and processes within a single framework. More broadly, we show how methodology for carbon cycle feedback analysis can be extended to the economic sector, for future assessment of integrated assessment models. Our model results have demonstrated that an economic carbon-climate feedback has the potential to significantly counteract the warming contribution of land and ocean feedbacks; however, the benefits of this negative economic feedback in terms of the carbon cycle are heavily balanced by substantial economic costs. Earth system models that neglect these economic feedback processes may significantly overestimate the carbon-climate feedback. Future research to better characterize the nature and scale of economic disruptions from climate change will reduce uncertainty and allow this feedback to be better incorporated into integrated assessment and Earth system models.

Chapter 3
Estimating Carbon Cycle Feedbacks on Fossil Fuel Emissions

3.1 Introduction

Cycling of carbon between the land, ocean, and atmospheric carbon pools is a critical driver of future climate change, and the processes that regulate flows between these reservoirs have been the subject of considerable experimental investigation and model analysis. By and large that work has been focused on the sign and magnitude of naturally occurring fluxes from terrestrial and marine carbon pools through mechanisms such as carbon and climate effects on photosynthesis (Díaz et al., 1993; Zaehle et al., 2014; Zhu et al., 2017), disturbance and decomposition (Arora and Melton, 2018; Crowther et al., 2016; Davidson and Janssens, 2006; Lasslop et al., 2019; Lombardozzi et al., 2015; Ruppel and Kessler, 2017; Schuur et al., 2015; Zhou et al., 2009), ocean biogeochemistry (Behrenfeld et al., 2006; Bopp et al., 2005; Boyd and Doney, 2003; Kemp and Villareal, 2013), and changes in ocean circulation (Lopes et al., 2015; Toggweiler and Russell, 2008). Experimental results have provided a better understanding of temperature and atmospheric CO_2 controls on uptake and emissions of carbon from important Earth system components, while models have given estimates of the resulting feedbacks and the relative sensitivities of these components to changes in temperature and atmospheric CO_2.

However, human-driven feedback mechanisms have been largely absent from these

analyses. Recent work has shown that such a feedback may play a significant role in the future carbon cycle, but further study is necessary. A feedback on land use change emissions has been explored in previous work linking the Global Change Assessment Model (GCAM) to the Community Earth System Model (CESM) (Jones et al., 2018; Thornton et al., 2017). Analysis of a potential feedback on fossil fuel emissions is still relatively limited, but some papers reporting results from integrated assessment models have mentioned such effects (Roson and van der Mensbrugghe, 2012), and a recent study used a simple global scale model to explore the potential mechanisms and magnitude of this feedback (Woodard et al., 2019). The influence of climate on fossil fuel emissions may operate through a variety of mechanisms including impacts on population, economic productivity, energy use, and the efficacy of energy production and delivery systems. Additionally significant drivers of an anthropogenic feedback may also include human behavioral responses to climate change caused by changes in perceived risk (Beckage et al., 2018).

These examples suggest potential mechanisms for a human-driven feedback that may be more or less predictable largely depending on the human agency involved. For example, climate effects on crop yields or hurricane damages in coastal areas may in theory be directly understood based on analysis of current and historical data, including the impacts of such effects on the economy and fossil fuel emissions. On the other hand, policy responses to climate change are subject to unpredictable human decision making across a range of scales and may therefore be best assessed in the future by comparing over a range of scenarios.

As a conceptual starting point for integrating these anthropogenic feedbacks in carbon cycle analyses, we consider the carbon cycle in terms of exchange of carbon between the atmosphere and four carbon pools: two natural carbon pools, natural land and ocean carbon, and two human carbon pools, managed land and fossil fuels. Each pool has uptake from and emissions to the atmosphere, though the flux of atmospheric carbon to fossil fuels operates on such long timescales that it can reasonably be neglected with respect to contemporary climate change. Carbon-climate and carbon-concentration feedbacks influence both

directions of carbon fluxes between these pools and the atmosphere (Figure 3.1). Although human activity also affects lateral carbon flows among these pools, as suggested in Figure 3.1, in the rest of this chapter we will neglect these lateral flows due to current lack of sufficient representation in models, focusing instead on atmospheric fluxes, as a direct extension of previous carbon cycle feedback analyses.

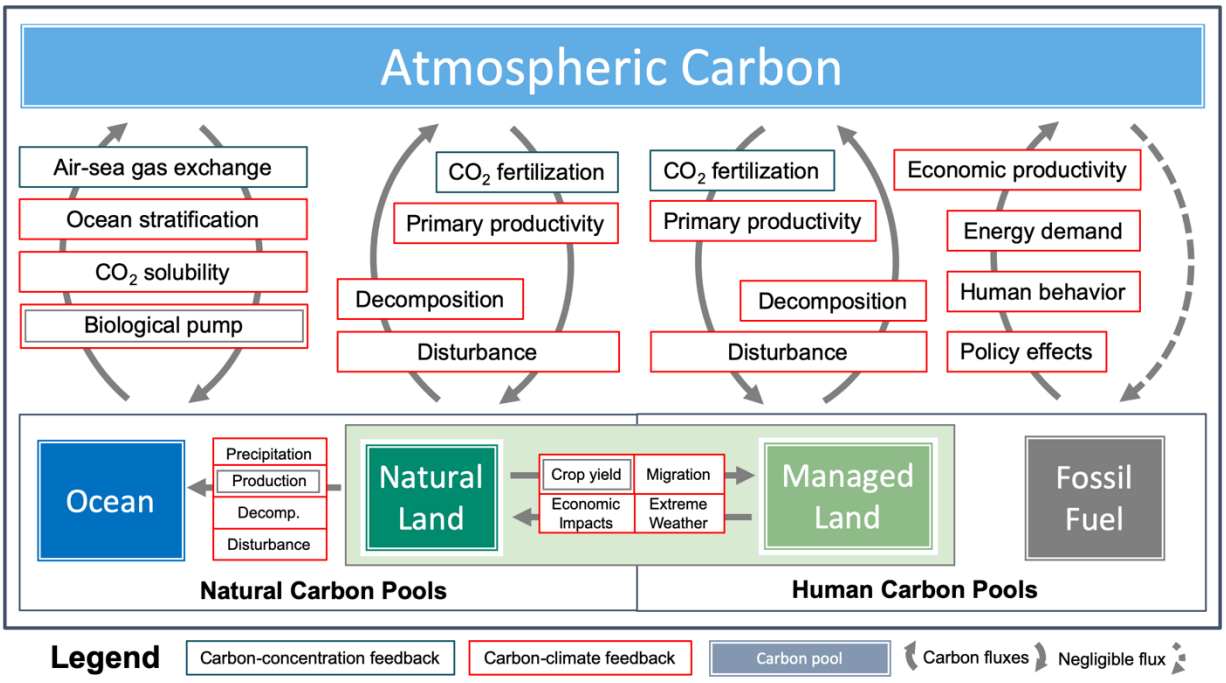

Figure 3.1: Carbon-climate and carbon-concentration feedbacks on both human and natural carbon fluxes between the atmosphere and each of four carbon pools: ocean, natural land, managed land, and fossil fuel. The returning flux from the atmosphere to the fossil fuel carbon pool is negligible on relevant timescales so we do not consider feedbacks on this term. While most feedback effects are fall into either the carbon-climate (red outline) or carbon-concentration (gray outline) category, some fall into both, indicated by a double outline. We additionally show carbon and climate feedback factors affecting the partitioning of land use and natural land carbon pools and feedbacks affecting the dissolved organic carbon flux from land to the ocean. While the feedbacks shown are not an exhaustive list, they cover the broad categories considered to date in carbon feedback analyses in the literature. We omit a carbon-concentration feedback on fossil fuel emissions, as the effect on emissions due to carbon-dioxide fertilization of agriculture is relatively insignificant compared to the land storage consequences from this feedback process.

In the natural land carbon pool, there are both carbon-concentration and carbon-

climate feedbacks on net primary productivity (NPP) through CO_2 fertilization and climate-induced stress, respectively, influencing the net flow of carbon into this pool (Devaraju et al., 2016; Zhu et al., 2017). In both simple box models of the carbon cycle and fully-coupled Earth system models (ESMs), loss of carbon from this pool is regulated primarily by the effects of temperature and moisture availability heterotrophic respiration from soil decomposition processes as well as climate effects on disturbance, both of which increase carbon losses from soils and land biomass (Arora and Melton, 2018; Crowther et al., 2016; Davidson and Janssens, 2006; Lasslop et al., 2019; O'Connor et al., 2010; Schuur et al., 2015; Zhou et al., 2009). Disturbance processes also have influence on carbon uptake through changing biomass in carbon stocks (Arora and Melton, 2018; Lu et al., 2015).

The ocean-atmosphere carbon flux is primarily affected by atmospheric CO_2 concentration, which influences the rate of air-sea gas exchange, and by rising temperatures, which drive increases in ocean stratification and a reduction in CO_2 solubility. Additionally, carbon uptake in the ocean responds to changing export rates of carbon from the surface through climate and carbon impacts on marine biological productivity, an effect known as the biological pump (Boyd and Doney, 2003; Tréguer et al., 2018). Climate warming may also increase the ocean carbon flux to the atmosphere through the destabilization of methane hydrates (Ruppel and Kessler, 2017), although recent work tracking the plume from the Deep Horizon spill suggests rapid microbial responses may limit these methane sources (Valentine et al., 2010; YvonLewis et al., 2011). There are also potential feedback effects on the flux of carbon from land to the ocean in the form of dissolved organic carbon (DOC) transported by freshwater to the ocean and impacted by the condition of coastal ecosystems such as mangroves (Pendleton et al., 2012; Raymond et al., 2016; Tian et al., 2015). The DOC flux is affected by the same feedback mechanisms changing the productivity and decomposition of biomass on land, as well as by changes in factors controlling runoff including precipitation, erosion, and disturbance (Raymond et al., 2016).

Managed land carbon also responds to changes in atmospheric composition and

climate by means of mechanisms similar to those that affect the natural land pool, but the magnitude of the effects is different and is mediated by human decisions regarding, for example, fertilizer use, crop type, irrigation, and disturbance prevention measures (Thornton et al., 2017; Mahowald et al., 2017). Human land use may even determine the sign of the net feedback on a given parcel of land (Fleischer et al., 2016). Importantly, the fraction of land carbon that is managed is also affected by carbon and climate feedbacks. Climate impacts on crop yield may drive the abandonment of agricultural areas in some parts of the world and deforestation in others, as regional and global trade adjusts to new optima for production. The carbon cycle implications of deforestation are particularly large because they include both immediate losses of carbon and limits on potential carbon storage of the deforested land over longer timescales (Mahowald et al., 2017).

There has been relatively little work assessing the combined climate feedbacks of both land use and land cover change, but a recent study estimated both the net carbon-climate and carbon-concentration feedback effects from these processes (Jones et al., 2018). Although that analysis found a very small carbon-concentration feedback related to land use and land cover change, the carbon-climate feedback from these processes in their model was slightly over 25% of the magnitude of the natural terrestrial carbon-climate feedback but opposite in sign, thus significantly offsetting the natural feedback. The authors found that this negative feedback effect was driven by increasing carbon storage due to reductions in agricultural area from climate change (Jones et al., 2018).

Finally, we consider fossil fuels as a fourth carbon pool. We only include feedbacks operating on carbon emissions from fossil fuels, since carbon uptake into this pool does not operate on timescales relevant for current modeling efforts. This emissions term can be impacted by climate-driven changes in economic productivity, policy, energy use, and behavioral choices (Beckage et al., 2018; Burke et al., 2015, 2018; Isaac and van Vuuren, 2009; Kjellstrom et al., 2009). A 2019 study estimated that the net carbon-climate feedback on fossil fuel emissions has the potential to have a magnitude similar to that of

the natural carbon-climate feedback but opposite in sign, such that the two net feedback effects substantially offset each other when both are active (Woodard et al.). In this analysis, losses of economic productivity from future climate warming considerably reduces fossil fuel consumption for a fossil fuel intensive future scenario (RCP8.5). Other feedbacks involving population and the carbon efficiency of energy infrastructure were predicted to have much smaller impacts at a global scale, with climate change impacts on energy demand for heating and cooling largely canceling one another. However, the limitations of the model used in Woodard et al. (2019) highlight a need for improved estimates of this feedback from integrated assessment models that are able to represent more complex economic dynamics including potential effects from policy and human behavior.

Both the natural and human carbon cycle feedback processes outlined in Figure 3.1 have been considered to varying degrees in the literature, but not all are integrated within individual models and no model we are aware of at the time of this publication has a representation of feedback mechanisms in all four carbon pools shown. We also acknowledge that some may never be found to be significant enough to dedicate computational resources to including, but as models continue to improve the representation of key processes, it will be increasingly important to expand the discussion of carbon cycle feedback analysis to include a broader array of feedback processes from both human and natural systems.

For the past decade and a half, the Coupled Climate-Carbon Cycle Model Intercomparison Project (C4MIP) framework has provided a standardized approach for comparing carbon cycle feedbacks across Earth system models (Arora et al., 2013; Friedlingstein et al., 2006). This framework involves using coupled and decoupled simulations to isolate carbon-climate and carbon-concentration feedback components and estimate the magnitude and sign of these processes. There are limitations in using a linearized set of equations to represent these nonlinear processes, but the linear estimation has been found to be a reasonable assumption sufficient for the purpose of making comparisons between models (Boer and Arora, 2012; Gregory et al., 2009; Zickfeld et al., 2011). This framework has also been previously

applied to understand causes of uncertainty in model output derived from different modeling centers.

Since the C4MIP protocol is focused on feedbacks on land and ocean carbon fluxes, fossil fuel emissions and land use change have been considered non-interactive components of the Earth system. Recently, this framework has been expanded to incorporate climate and carbon-concentration sensitivity of land use and land cover change emissions (Jones et al., 2018) but to date has not been updated to include a carbon cycle feedback on fossil fuel emissions. Here we extend it a step further to include a fossil fuel climate sensitivity and demonstrate how the integrated assessment modeling community can use this framework to diagnose the various human-driven feedback components in these models. As an example, we compare carbon-climate feedback parameters in a simple integrated assessment model commonly used for climate policy to the feedback effects in Woodard et al. (2019).

3.2 An extension of the feedback framework

Analysis using the C4MIP framework has provided useful estimates of natural carbon cycle feedback mechanisms but the framework is limited by the assumption that anthropogenic carbon dioxide emissions and land use and land cover change emissions are insensitive to temperature or atmospheric CO_2. Removing these assumptions generalizes this carbon cycle feedback estimation methodology to include feedback effects on fossil fuel and land use and land cover change emissions, so it can be extended to models that are considering these additional linkages.

Building on the work of Friedlingstein et al. (2006) for the natural carbon cycle, here we add the human contribution to both carbon-concentration and carbon-climate feedbacks. While Friedlingstein *et al.* consider three carbon pools: land, ocean, and atmospheric carbon, we include fossil fuels as a fourth carbon pool that exchanges with the atmosphere (2006). We also subdivide the land into components with natural and managed land pools, to allow for the separate consideration of land use and land cover change emissions following Jones

et al. (2018) (Figure 3.1).

To estimate the strength of the carbon-climate feedback in a model, decoupled simulations need to be generated that systematically exclude key feedback mechanisms. In past work on the natural carbon cycle, this set has included a biogeochemically-coupled simulation and a fully coupled simulation. The biogeochemically-coupled scenario attempts to isolate the carbon-concentration feedback on carbon fluxes from the ocean and land by eliminating the radiative effects of carbon dioxide so that only rising atmospheric CO_2 influences land and ocean submodels. The fully-coupled simulation, in contrast, involves no decoupling of the model. These scenarios have been generated by models under both emissions-driven and concentration-driven simulations. For emissions-forced simulations of the natural carbon cycle, atmospheric CO_2 dynamically evolves in response to prescribed emissions, while in concentration-forced simulations, responses in land and ocean carbon fluxes are driven by prescribed changes in atmospheric CO_2.

The relative magnitude and sign of a carbon-climate feedback is commonly estimated by the feedback gain, g, which, for this set of simulations, can be calculated directly from the difference in atmospheric CO_2 between the fully-coupled and biogeochemically-coupled simulations (Friedlingstein et al., 2006):

$$g = 1 - \frac{\Delta C_A^{UC}}{\Delta C_A^{FC}} \tag{3.1}$$

where ΔC_A^{UC} is the change in atmospheric CO_2 from the biogeochemically-coupled simulation, and ΔC_A^{FC} is the change in atmospheric CO_2 from the fully-coupled simulation. A positive gain corresponds to a positive feedback and vice versa, and the magnitude of the gain corresponds to the relative strength of the feedback in terms of amplifying or dampening the influence of a perturbation. Equation 3.1 can also be used to estimate the gain of the carbon-climate feedback for the anthropogenic system alone as well as the combined natural and anthropogenic system. For the combined gain, the fully coupled simulation would include the coupling between climate and land use as well as between climate and

the processes regulating fossil fuel emissions, in addition to natural couplings. For the anthropogenic gain alone, the fully-coupled simulation in Equation 3.1 would exclude natural carbon-climate feedback mechanisms. There are different pathways for generating this decoupling in a model that includes processes representing both natural and human systems, and these options will be described below in further detail.

We note that for the natural carbon cycle, concentration-forced simulations have also been used to estimate the gain of the carbon-climate feedback. For this class of simulations, the gain can be estimated directly from differences in compatible fossil fuel emissions from fully-coupled and biogeochemically-coupled simulations (Arora et al., 2013). Compatible fossil fuel emissions for these simulations are deduced as the flux necessary to balance the carbon accumulation rate in the atmosphere, ocean, and land reservoirs (Jones et al., 2013). When fossil fuel and land use emissions also are sensitive to atmospheric CO_2 and climate, as may be typical for next generation integrated assessment models, the utility of concentration-forced simulations may be limited. For this reason, here we focus on the conceptual extension and analysis of simulations in which emissions dynamically respond to atmospheric forcing.

3.3 Decomposing the gain of the carbon-climate feedback

To diagnose drivers of the gain of the carbon-climate feedback (Equation 3.1), the gain has been linearly decomposed into terms representing sensitivity of carbon storage to changing CO_2 (β), a term representing the sensitivity of carbon storage to climate (γ), and the sensitivity of climate to atmospheric CO_2 (α). Here we extend this framework to include interactive human system terms.

For example, equations 2-5 below describe how a climate-decoupled (denoted with 'UC' for 'uncoupled') natural and anthropogenic simulation can be used to estimate the relevant β sensitivity terms:

$$\Delta C_O^{UC} = \beta_O \Delta C_A^{UC} \tag{3.2}$$

$$\Delta C_{L,N}^{UC} = \beta_{L,N} \Delta C_A^{UC} \tag{3.3}$$

$$\Delta C_{L,H}^{UC} = \beta_{L,H} \Delta C_A^{UC} - E_{LUC} \tag{3.4}$$

$$\Delta C_F^{UC} = \beta_F \Delta C_A^{UC} - E_F;\ \beta_F = 0 \tag{3.5}$$

For equations 2-5, the ocean carbon reservoir is denoted with an 'O' subscript, land with an 'L', fossil fuels with an 'F'. Natural and human managed components of the terrestrial biosphere are further separated with an 'N' (for natural) or 'H' (for human-managed), following Figure 3.1 and the notation in Jones et al. (2018). We assume above in equation 3.5 that the sensitivity of the fossil reservoir to rising atmospheric CO_2 is negligible, given the likely minimal effect of CO_2 fertilization on emissions and our exclusion of any flux into the fossil fuel carbon pool on these timescales.

While with natural land and ocean carbon it may be reasonable to assume that changes in the flux from these pools to the atmosphere are largely driven by sensitivities to atmospheric CO_2 and climate (Boer and Arora, 2009), the same is not true of fossil fuel emissions and managed land both of which are influenced by climate but driven primarily by other factors, namely, human behavior. We include the term E_F in equation 3.5 to account for this portion of fossil fuel emissions not driven by carbon feedbacks, as well as an equivalent term, E_{LUC}, in equation 3.4.

Once the β terms have been estimated from the climate-uncoupled simulation, the γ terms can be estimated from this information and an equivalent, fully-coupled simulation with the same model by rearranging the following equations:

$$\Delta C_O^{FC} = \beta_O \Delta C_A^{FC} + \gamma_O \Delta T^{FC} \tag{3.6}$$

$$\Delta C_{L,N}^{FC} = \beta_{L,N} \Delta C_A^{FC} + \gamma_{L,N} \Delta T^{FC} \tag{3.7}$$

$$\Delta C_{\mathrm{L,\,H}}^{FC} = \beta_{L,H} \Delta T^{FC} + \gamma_{L,H} \Delta T^{FC} - E_{LUC} \tag{3.8}$$

$$\Delta C_F^{FC} = \gamma_F \Delta T^{FC} - E_F \tag{3.9}$$

This approach can also be used to estimate the net effects on atmospheric carbon from the different feedback components where the atmosphere change is defined as:

$$\Delta C_A^{FC} = -(\Delta C_O^{FC} + \Delta C_{L,N}^{FC} + \Delta C_{\mathrm{L,\,H}}^{FC} + \Delta C_F^{FC}) \tag{3.10}$$

Substituting equations 6-9 into 10, we get:

$$\begin{aligned} \Delta C_A^{FC} = -((&\beta_O \Delta C_A^{FC} + \gamma_O \Delta T^{FC} + \beta_{L,N} \Delta C_A^{FC} + \gamma_{L,N} \Delta T^{FC}) + \\ &(\beta_{L,H} \Delta T^{FC} + \gamma_{L,H} \Delta T^{FC} - E_{LUC}) + (\gamma_F \Delta T^{FC} - E_F)) \end{aligned} \tag{3.11}$$

which can then be reorganized to derive an expression for β_A^{FC} and γ_A^{FC} in terms of the land, ocean, and fossil fuel components for a model scenario with all natural and anthropogenic feedbacks active. We also combine the insensitive emissions components into the term E.

$$\Delta C_A^{FC} = -(\beta_{L,N} + \beta_{L,H} + \beta_O + \beta_F) \cdot \Delta C_A^{FC} - (\gamma_{L,N} + \gamma_{L,H} + \gamma_O + \gamma_F) \cdot \Delta T^{FC} + E \tag{3.12}$$

$$\Delta C_A^{FC} = \beta_A \Delta C_A^{FC} + \gamma_A \Delta T^{FC} + E \tag{3.13}$$

$$\gamma_A^{FC} = -(\gamma_{L,N}^{FC} + \gamma_{L,H}^{FC} + \gamma_O^{FC} + \gamma_F^{FC}) \tag{3.14}$$

$$\beta_A^{FC} = -(\beta_{L,H}^{FC} + \beta_{L,H}^{FC} + \beta_O^{FC}) \tag{3.15}$$

A final parameter necessary for decomposing the gain is the sensitivity of climate to atmospheric carbon dioxide (α). This parameter, which is closely related to the transient climate

sensitivity, can be computed from the following equation:

$$\alpha = \frac{\Delta T^{FC}}{\Delta C_A^{FC}} \tag{3.16}$$

Equation 3.1, the approach for directly computing the gain, can then be expressed as a combination of the α, β, and g parameters,

$$g = \frac{\alpha \cdot \gamma_A}{(m - \beta_A)} \tag{3.17}$$

where m is the conversion between Pg C and ppm (2.1 Pg C/ppm). In practice there may be differences in the gain estimated from equation 3.1 from that computed from equation 3.18 due to non-linearity, with the former providing a direct measure of feedback strength and the latter providing mechanistic insight about the drivers (Friedlingstein et al., 2006). In simpler models like Woodard et al. (2019) they are nearly equivalent.

3.4 Decoupling models

There are many ways to decouple models to estimate the feedback effects of interest, and we have laid out several that we consider to be the most directly useful in Table 3.1, based on a hypothetical model with active feedbacks on carbon fluxes from ocean, managed and natural land, and fossil fuel emissions. For ease of reference, we will describe biogeochemically-coupled scenarios as 'carbon' and radiatively-coupled scenarios as 'climate' in the rest of this text. Both involve carbon-driven effects, but this nomenclature refers to the type of feedback (carbon-carbon or carbon-climate) that is primarily influencing effects on atmospheric carbon in each.

Table 3.1: A set of scenarios to estimate carbon feedbacks that extends the three scenarios described by the natural carbon cycle literature. The Natural Carbon, Natural Climate, and Natural Fully Coupled correspond to the biogeochemical, radiative, and fully coupled runs from previous analyses (Arora et al., 2013). Additional scenarios are necessary for the separate estimation of land use and fossil fuel carbon cycle feedbacks in models. Columns 2-5 indicate whether a component has the potential for active feedback processes driven by biogeochemical responses to atmospheric CO_2 concentration changes (BGC) or by radiative effects of atmospheric CO_2 (RAD). If neither set of feedback processes were active, this is indicated by '—'. Not all models include all sensitivities on all components, but for each scenario the table indicates the effects that could be active in the model based on where the decoupling is done. Column 7 indicates the connections (numbered from Figure 3.2) that need to be decoupled to create each scenario.

Scenario Number	Scenario	Natural Carbon Fluxes		Human Carbon Fluxes		Active Feedbacks	Pathways for Decoupling from Fig. 3.2
		Land ($F_{L,N}$)	Ocean (F_O)	Land Use ($F_{L,H}$)	Fossil Fuel (F_F)		
1	Natural Carbon	BGC	BGC	—	—	Ocean and land carbon-concentration	3 & 5 or 3, 6, 8, & 10
2	Natural Climate	RAD	RAD	—	—	Ocean and land carbon-climate	1, 3, 8, & 10
3	Natural Fully Coupled	RAD, BGC	RAD, BGC	—	—	Ocean and land carbon-concentration and carbon-climate	3, 8, & 10
4	Natural + Anthro Carbon	BGC	BGC	BGC	—	all carbon-concentration	5 or 6, 8, & 10
5	Land Use Climate Only	BGC	BGC	RAD, BGC	—	all carbon-concentration + land use carbon-climate	6, 12
6	Land Use Climate Decoupled	RAD, BGC	RAD, BGC	BGC	RAD	All active except land use carbon-climate	3
7	Fossil Climate Only	BGC	BGC	BGC	RAD	Natural + Anthro Carbon and fossil carbon-climate	6, 8, 11
8	Fossil Climate Decoupled	RAD, BGC	RAD, BGC	RAD, BGC	—	All except those affecting fossil fuel emissions	12
9	Natural Climate Decoupled	BGC	BGC	RAD, BGC	RAD	All except land and ocean carbon-climate	6
10	Natural + Anthro Fully Coupled	RAD, BGC	RAD, BGC	RAD, BGC	RAD	all carbon-concentration and carbon-climate	none

The linkages between atmospheric carbon, temperature, and each carbon pool from Figure 3.1, in a model with active feedbacks on each, is shown in Figure 3.2. The natural and managed land carbon-concentration feedback pathways on land are described by {1, 2} and {3, 4}, respectively, while the natural, land use, and fossil carbon-climate feedback pathways are described by {5, 6, 7}, {5, 8, 9, 11} + {5, 10, 11, 9}, and {5, 10, 12, 13}. Decoupling models requires cutting off one or more of these pathways. For example, to estimate a natural fully-coupled scenario (Table 3.1 - 3) in a model with active anthropogenic feedbacks, the model would need to be decoupled at linkages 3, 8, and 10 to isolate the natural feedbacks.

Different scenarios may be more or less helpful depending on the model structure and the ease of decoupling certain mechanisms, as well as which parameters are of interest. We will focus here on fossil fuel and combined anthropogenic and natural feedback parameters as examples, but net natural, net anthropogenic, and managed land parameters may also be relevant to separately isolate.

The combined Natural + Anthropogenic carbon-climate gain can be best estimated from equation 3.1 with the Natural + Anthropogenic Carbon scenario (Table 3.1 - 4) and Natural + Anthropogenic Fully Coupled scenario (Table 3.1 - 10) as the uncoupled and fully-coupled scenarios, respectively. For the fossil fuel carbon-climate feedback gain, we consider using scenarios 8 and 10 from Table 3.1 to be likely the simplest approach to estimate this in most models, where scenario 8 is considered the uncoupled and 10 is the fully-coupled. Scenario 8 requires decoupling only the fossil fuel feedback, for example by feeding constant temperature values to relevant economic modules or setting any temperature-sensitive parameters to zero, while scenario 10 includes all feedback processes and needs no decoupling.

This approach to estimation of a feedback effect by decoupling only the feedback of interest and comparing to a fully-coupled baseline is in contrast to feedback estimation based on comparison to a decoupled baseline, where the desired feedback effect is isolated by decoupling all or most other feedbacks. For example, to calculate a fossil carbon-climate feedback gain with a decoupled baseline, a carbon-only run (scenario 4) can be used as the

uncoupled run in Equation 3.1, and a scenario that adds only the fossil fuel coupling on top of this baseline (scenario 7) would then be the fully-coupled run. While both typically produce similar results, these two approaches are not necessarily equivalent. A 2014 analysis found that the net natural carbon-climate feedback parameter, γ_A, calculated from a radiatively coupled scenario (Table 3.1 - 2) against a decoupled baseline may be underestimating the decrease in ocean carbon uptake from higher carbon dioxide combined with warming, compared to using the difference between the natural fully-coupled baseline and the biogeochemically-coupled scenario (Table 3.1 - 1 and 3). This is because having only the natural carbon-climate feedback active necessarily neglects the effects of ocean stratification on the carbon flux into the ocean (Schwinger et al., 2014).

To estimate the decomposed parameters for the gain, additional scenarios are needed. The feedback-insensitive fossil fuel flux, *E,* can be estimated from equation 3.9 with any scenario that does not include a fossil fuel feedback coupling, e.g., scenarios 1-5 and 8 in Table 3.1 because γ_F is zero in each. Using this value of E, the combined carbon-concentration effect on the atmosphere, β_A^{FC} (defined in equation 3.16), can be estimated from the Natural + Anthropogenic Carbon scenario (Table 3.1 - 4) and equation 3.14, where $\gamma_A^{FC} = 0$. There is no carbon-concentration feedback on fossil fuel emissions, so $\beta_F = 0$ in this case.

The fossil fuel carbon-climate feedback parameter, γ_F, can be estimated using equation 3.9 directly from the Natural + Anthropogenic Fully Coupled scenario (scenario 10) or any scenario that includes a fossil fuel coupling, as well as an uncoupled scenario necessary to estimate E. Equation 3.14 then gives the combined natural and anthropogenic carbon-climate feedback parameter (γ_A^{FC}) from scenario 10, once β_A^{FC} is known.

To calculate the full set of parameters described here, models would need to be able to generate a Natural + Anthropogenic Carbon scenario, a Fossil Climate Decoupled scenario, and a Natural + Anthropogenic Fully Coupled scenario (Table 3.1 - 4, 8, and 10), but others may be desired to isolate other feedback effects.

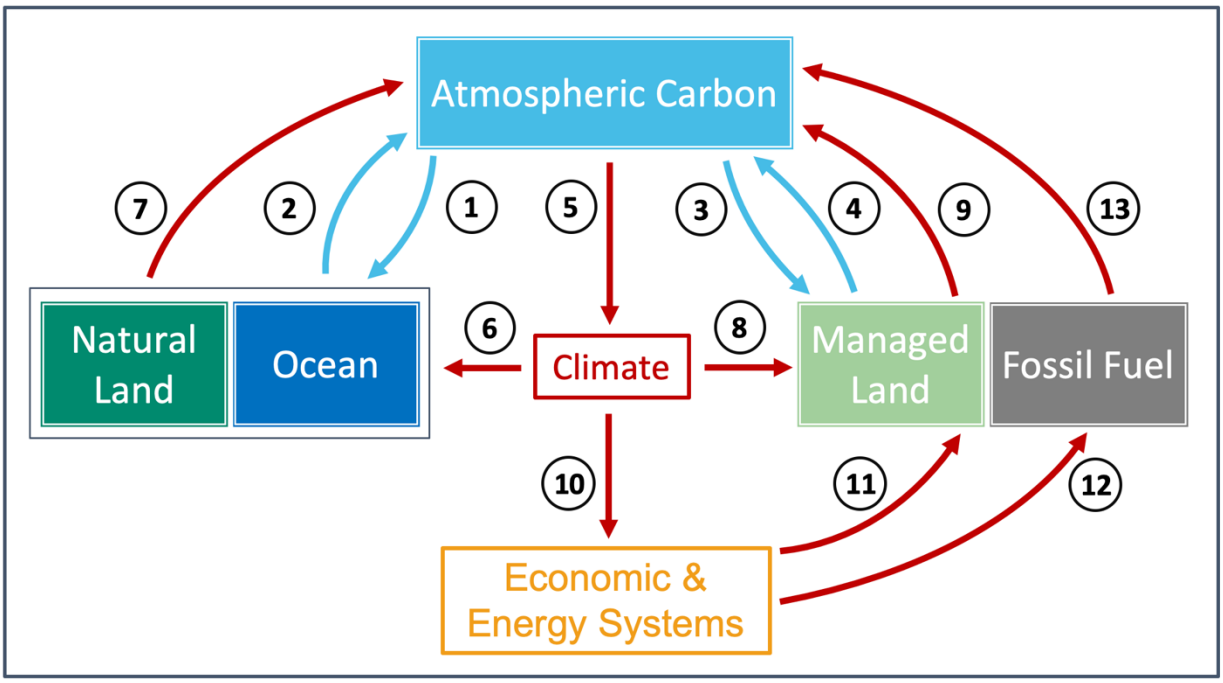

Figure 3.2: Diagram showing the pathways of carbon-climate and carbon-concentration feedbacks on the various carbon pools. Arrows represent the influence of one box on another such that pathways of influence can be traced through the diagram, but do not directly represent a carbon flux. Red arrows correspond to pathways of carbon-climate feedbacks, while all light blue arrows correspond to carbon-concentration feedbacks. For simplicity we only show arrows to and from the entire natural carbon pool, although most models do handle carbon feedbacks separately in marine and terrestrial systems. While there is some potential for a carbon-concentration feedback through CO_2 fertilization to affect fossil fuel emissions, it is likely small and thus is also not shown here. In the Woodard *et al.* model, land use change is an exogenous term, so 3, 8, and 9 are inactive, but all other pathways shown are active. In DICE-Burke, the only pathways that exist are {1, 2} and {5, 10, 12, 13} as there is no responsive land use term, nor any natural carbon-climate feedbacks. Additionally, there is no land carbon pool in DICE-Burke so {1, 2} only affects ocean carbon.

An important note is that we define the scenarios referenced in this analysis based on the potential feedback effects that could be active based on where the model is decoupled, rather than on which feedbacks are necessarily included in the model. In practice this means that for a given model, a Natural Fully Coupled scenario, for example, might only include carbon feedbacks on ocean but not land fluxes, and would still be considered 'fully-coupled' because the only decouplings needed to generate it would be between temperature and

atmospheric CO_2 and the anthropogenic carbon fluxes.

3.5 Estimates from simple models

We investigated feedbacks on fossil fuels and land use change in two simple models: the Kaya-based model described in Woodard et al. (2019) and a modified version of the Dynamic Integrated Climate-Economy (DICE) model we refer to as DICE-Burke.

The Woodard *et al.* model has carbon-climate feedbacks on land, ocean, and fossil fuel carbon fluxes, and carbon-concentration feedbacks on land and ocean carbon fluxes and does not include any land use change effects. For consistency we used the same climate-driven damage function on fossil fuel emissions for this analysis as the one reported in Woodard et al. (2019) but our conclusions are not affected by this choice and the resulting magnitudes are only illustrative.

The DICE-Burke version of the DICE model includes the default DICE2016 climate damages, which are represented as direct losses of Gross World Product (GWP) at each timestep based on a quadratic relationship with temperature (Nordhaus, 2017) but additionally includes a separate scenario that affects economic growth through total factor productivity and the capital depreciation rate parameterized Burke et al. (2015) relationship between temperature and GDP. We used the latter relationship for more direct comparison to the Woodard *et al.* results.

Fossil fuel emissions in the DICE-Burke model are estimated as a function of economic output so that climate damages have direct consequences for the level of emissions. The model's natural carbon cycle is simple, including only deep and mixed layer ocean components and no land carbon pool. The ocean carbon flux is a function of atmospheric carbon and exchange between the two ocean boxes. Without a land pool at all, and without any carbon-climate feedbacks in the ocean, the model has only one carbon-climate feedback component, that of fossil fuel emissions, and only one carbon-concentration feedback component, that of ocean carbon uptake.

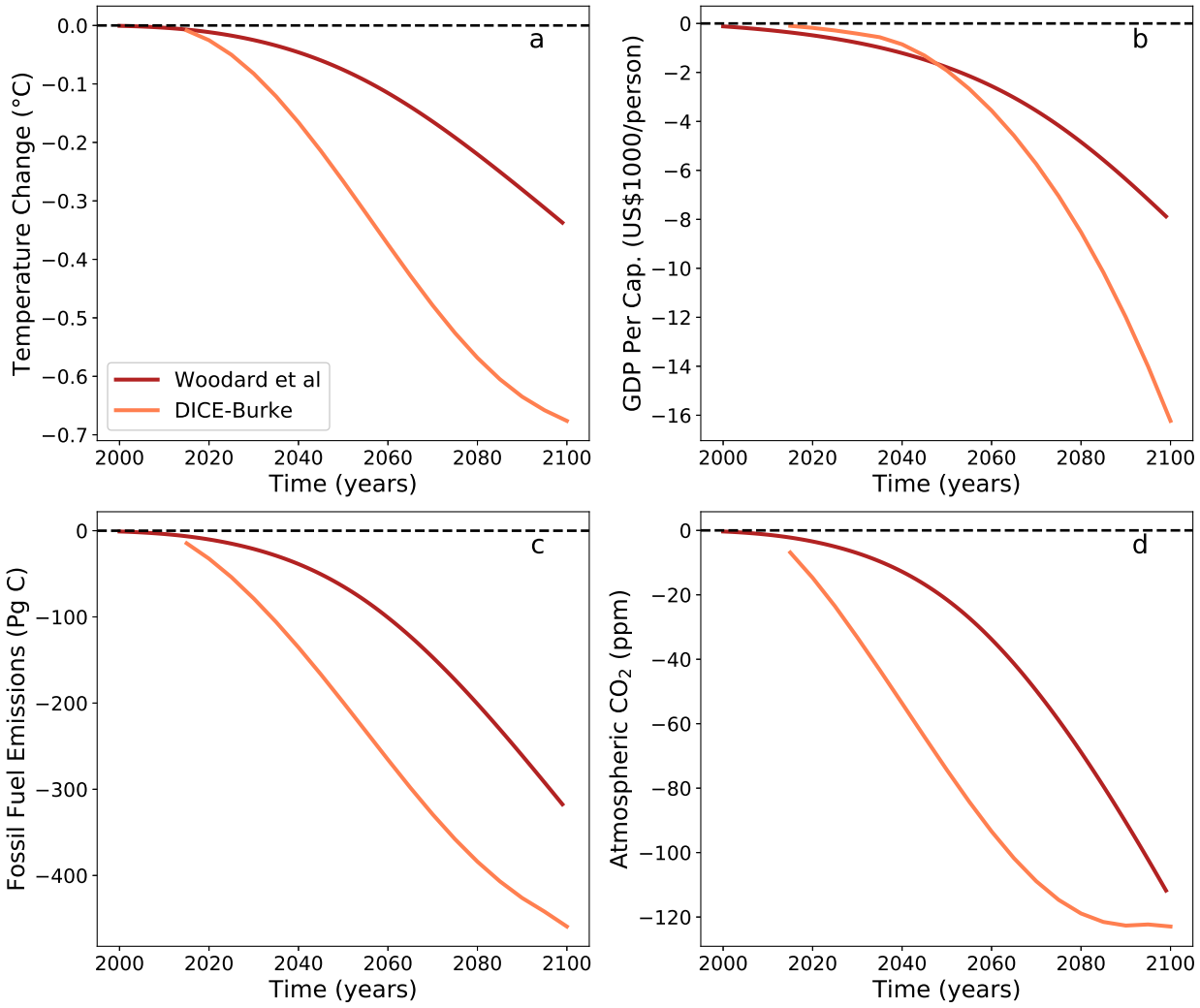

Figure 3.3: Fossil fuel feedback effect on model output in DICE-Burke (orange) and Woodard *et al.* (red). Each line is the difference between a Natural + Anthropogenic Fully Coupled scenario and a Fossil Climate Only scenario in the model and represents the isolated effect of the coupling of fossil fuel emissions to climate on each component.

We compared the net effect of the fossil fuel carbon-climate feedback on several variables across these two models, estimated as the difference between the Natural + Anthropogenic Fully Coupled scenario and the Fossil Climate Only scenario. In both models this feedback mechanism was driven by rising temperatures, which reduced fossil fuel emissions due to economic damages, generating a net negative feedback effect. This translated to reductions in temperature, GDP per capita, fossil fuel emissions, and atmospheric CO_2

compared to a Fossil Climate Only scenario in both models (Figure 3.3). In DICE-Burke, the fossil fuel feedback was responsible for reducing temperature by nearly 0.7 °C, GDP by over US$16,000 per capita, cumulative fossil fuel emissions by more than 450 Pg C, and atmospheric CO_2 by over 120 ppm. In the Woodard *et al.* model, the effects were considerably smaller on all but CO_2, as the effect on DICE-Burke atmospheric CO_2 leveled off by the end of the century. The fossil fuel feedback effect in the Woodard *et al.* model reduced temperatures by a little over a third of a degree Celsius, GDP by nearly US$8000 per capita, fossil fuel emissions by over 300 Pg C, and atmospheric CO_2 by 112 ppm. Relative to other feedbacks in the Woodard *et al.* this cooling from the fossil fuel feedback was around 15% the strength of the net carbon-concentration feedback, and entirely counteracted the warming from the natural carbon-climate feedbacks (Figure 3.4, Table 3.2).

As a more direct metric of feedback strength, we estimated the gain and carbon-climate and carbon-concentration feedback parameters in both models (Figure 3.5). While the magnitudes of the carbon cycle feedback parameters are not directly comparable between the two sets of model results due to differences in the emissions scenario, they display significantly different dynamics, which raises important questions about the role of model structure in the size of carbon feedbacks on fossil fuel emissions.

The beta parameters across the models both decrease steadily over the century, but the carbon-climate feedback parameters follow very different paths. While the Woodard *et al.* model has an anthropogenic gain and gamma that decrease through the end of the century, proportional to the rise in temperature, these same parameters in the DICE-Burke model reach a minimum near the end of the century before beginning to increase (Figure 3.5). This behavior suggests that damages from rising climate change reach a threshold beyond which the model optimization routine begins to limit emissions, thus reducing the sensitivity of the carbon cycle to temperatures. In theory various other mechanisms could similarly dampen the response of the human carbon cycle to climate change. A few possible examples include policy measures to curb emissions, human behavior changes in response

to perceived climate risk, and technological innovations that reduce the carbon intensity of GDP. Human behavioral responses have been found to potentially affect future climate change projections by a degree or more but are not well-constrained (Beckage et al., 2018).

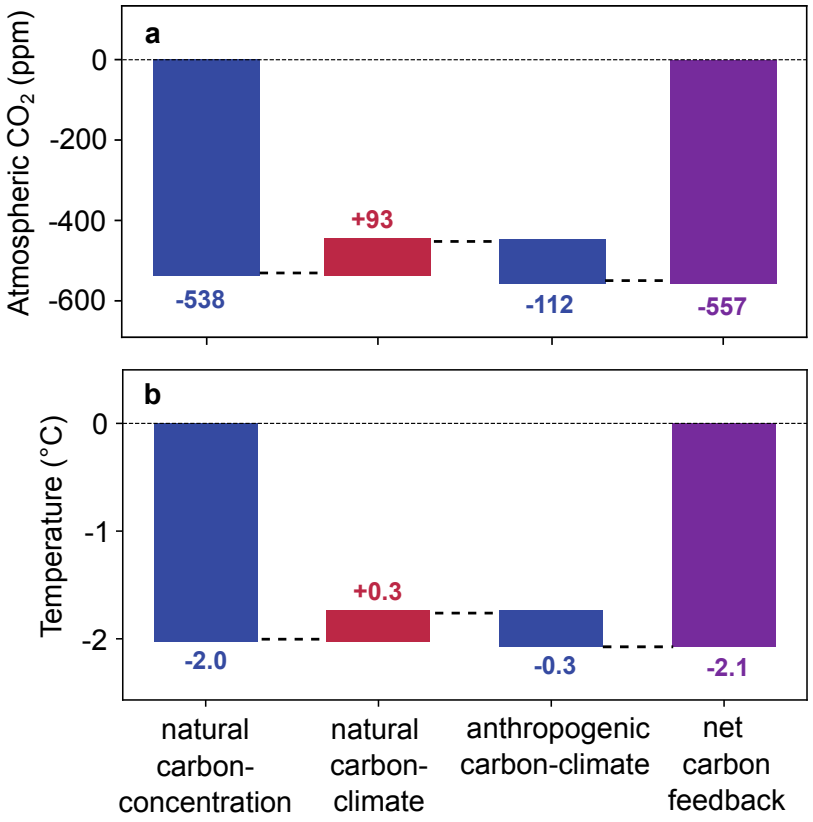

Figure 3.4: A comparison of carbon-climate and carbon-concentration feedback effects in the Woodard *et al.* model. Blue bars represent negative contributions to the net feedback effect, while red represent positive. These sum to the net effect of all active feedbacks in the model (purple). The carbon-concentration feedback is estimated relative to a control run with no active carbon feedbacks, while the carbon-climate feedbacks are estimated with relative to a fully-coupled baseline.

We additionally used the Woodard *et al.* model to assess the equivalence of estimating natural and anthropogenic carbon-climate feedback parameters using a fully-coupled or a decoupled baseline, and we found the results to be nearly identical in this simple model (Figure 3.6). We first compared the difference in our model between two approaches to estimating the natural carbon-climate gain. In models that include anthropogenic feedbacks,

Table 3.2: Results across carbon and climate variables in the model as well as feedback parameters for the DICE-Burke model and the Woodard *et al.* model. The numerical columns are estimated over the entire model period (2010-2100 for DICE-Burke, 1800-2100 for Woodard *et al.*). All scenarios are fully coupled within each system indicated, although carbon-concentration feedback parameters were calculated using decoupled scenarios. The beta values are estimated from the biogeochemically-coupled versions of each scenario, the gammas and carbon-climate feedback gain from the fully-coupled.

Model	Scenario	ΔT (°C)	ΔGDP (US$1000/ person)	ΔFF (Pg C)	ΔC_{atm} (ppm)	α (°C/ ppm)	γ (Pg C/ °C)	β (Pg C/ ppm)	Gain (g)
DICE-Burke	Natural	2.89	66.6	1246	305	0.0045	—	-0.85	—
DICE-Burke	Natural +Anthro	2.21	50.4	787	182	0.0057	-119	-0.85	-0.21
Woodard	Natural	4.55	28.2	2238	1506	0.0030	63.7	-1.02	0.13
Woodard	Natural +Anthro	4.21	25.7	1921	1271	0.0033	-14.0	-1.02	-0.03

what we here describe as estimating the natural carbon-climate gain against a *decoupled* baseline is the equivalent of what in previous natural carbon cycle analyses was effectively estimating against a *fully-coupled* baseline. For this approach the gain is estimated from equation 3.1, using atmospheric carbon changes in the Natural Fully Coupled scenario (Table 3.1 - 3; previously, 'fully-coupled') and the Natural Carbon scenario (Table 3.1 - 1; previously, 'biogeochemically-coupled') (Friedlingstein et al., 2006; Arora et al., 2013). However, in a model that includes anthropogenic feedback effects as ours does, this estimation requires separate decoupling of the anthropogenic feedbacks and the natural carbon-climate to get both of the necessary model runs. In past analyses on Earth system models that only include natural feedbacks, the only decoupling that has been required for the same calculation is on the radiative effects of temperature in order to isolate the biogeochemical feedbacks in the Natural Carbon scenario. This means in practice that with a model that includes carbon cycle feedbacks on human systems, it requires less decoupling of the model to estimate the feedback gain compared to a fully-coupled baseline. To do this, the natural carbon-climate gain is estimated from the difference between a Natural + Anthropogenic

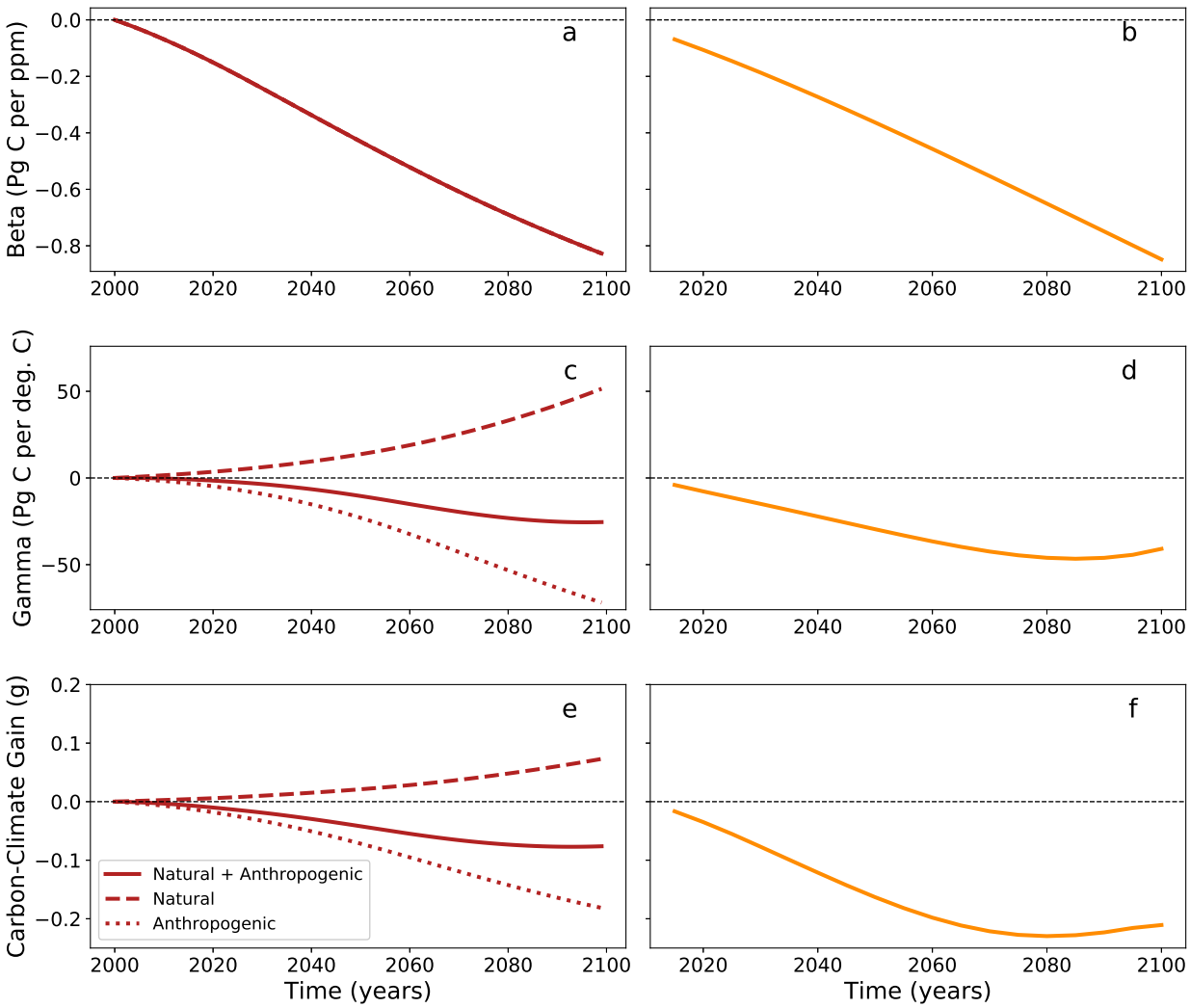

Figure 3.5: A comparison of feedback responses and dynamics between the Woodard *et al.* model (A-C) and the DICE-Burke model (D-F). Panels A and D show the carbon-concentration feedback parameter, beta, over the 21st century. Panels B and E show the carbon-climate feedback parameter, gamma, and panels C and F show the change in the carbon-climate feedback gain over the over the same time period. The gain results include three different net feedback effects: natural, anthropogenic, and natural + anthropogenic. The results from the DICE-Burke model include only one time series for each parameter as there is only a natural beta effect and anthropogenic gamma effect and thus only a single carbon-climate gain. The Woodard *et al.* results include all three feedback effects for everything except beta, as there are only natural carbon-concentration feedbacks active in this model, so beta does not change between scenarios.

Fully Coupled scenario (Table 3.1 - 10) and a Natural Climate Decoupled scenario (Table 3.1 - 9), which only requires decoupling the radiative effects of temperature on the natural

carbon cycle to create the latter scenario. Both approaches gave very similar results (Figure 3.6a), though the gain estimated against a decoupled baseline is slightly larger because it does not include the dampening effect of the negative carbon-climate feedback on fossil fuel emissions.

Comparing the anthropogenic carbon-climate gain between these same methods (from Table 3.1, decoupled baseline: 7 - 4; fully-coupled baseline: 10 - 8) showed similarly equivalent results (Figure 3.6b), although estimating from a decoupled baseline in this case produced a smaller magnitude gain due to the lack of an amplifying effect from the natural carbon-climate feedbacks which increases the difference between Scenarios 8 and 10. Finally, we made the same comparison for fossil fuel carbon-climate feedback parameter (γ_F), where the difference between the different approaches reflected the same pattern as we found with the anthropogenic gain (Figure 3.6c). From Scenario 4 we estimated the climate-independent fossil fuel emissions flux, E_F, from equation 3.5, and this was used in equation 3.9 to directly calculate γ_F. Estimating γ_F against a fully-coupled baseline still requires a decoupled scenario such as 4 or 8 to get E_F and then Scenario 10 can be used to estimate γ_F using equation 3.9.

3.6 Discussion

The evaluation of carbon cycle feedbacks becomes more complex with the addition of anthropogenic feedback mechanisms, requiring additional steps to decouple the models and compute the same feedback parameters that have been previously estimated by the Earth system modeling community. The extended mathematical framework presented here provides a practical approach to these calculations that can be used to compare feedback strengths between models and isolate individual contributions to net feedback effects.

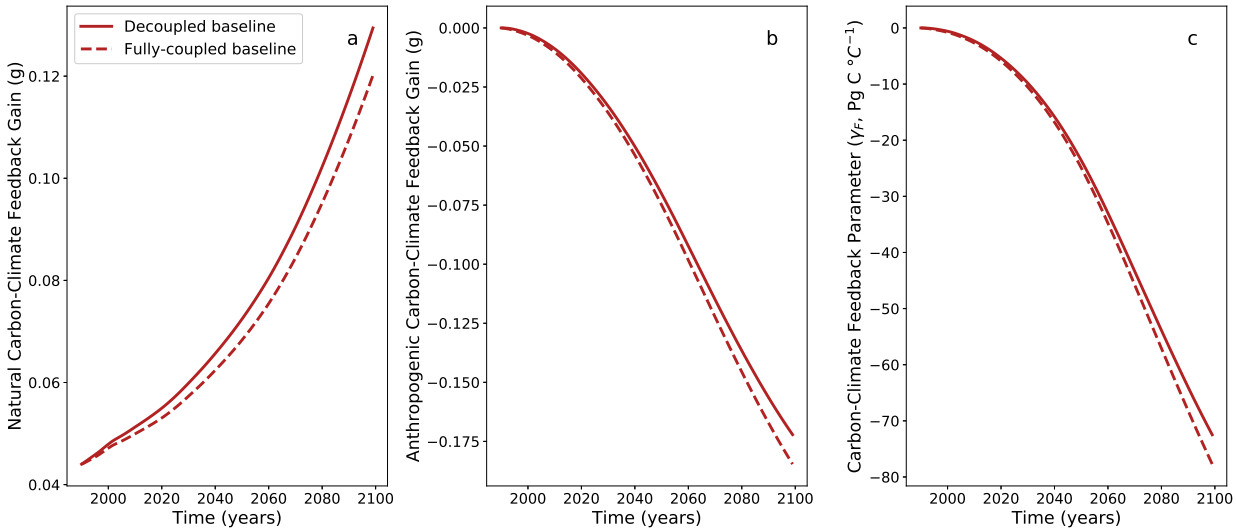

Figure 3.6: Output from the Woodard *et al.* model showing the natural (a) and anthropogenic (b) carbon-climate feedback gains and the fossil fuel carbon-climate feedback parameter (c) estimated based on a decoupled (solid line) or fully-coupled (dashed line) baseline. The small differences show the effect of the interaction between the different feedbacks active in the model in the two approaches.

We have demonstrated two different approaches to calculating feedback parameters in models, which may be useful in different cases. Estimating the carbon-climate feedback parameter from a decoupled baseline may be simpler if a carbon-only scenario is needed anyway to estimate the carbon-concentration feedback parameter, but in general this approach requires more decoupling of the model and will miss interactive feedback effects. Estimating parameters against a fully-coupled baseline, on the other hand, requires only decoupling the feedback of interest and is sufficient estimate the gain and carbon-climate feedback parameter of each feedback and the net feedback effect on various model outputs. This approach also provides a more accurate representation of the effect of a particular feedback in the context of others in the model since only the feedback mechanism of interest is turned off.

An important future step will be systematic intermodel comparisons of carbon cycle feedbacks within integrated assessment models. One goal of such comparisons is to evaluate the size of the net anthropogenic carbon feedback in models that include this mechanism and to push forward development of the relevant climate-economic relationships to reduce uncer-

tainty on this term. Not only is the magnitude of the carbon feedback on fossil fuel emissions highly dependent on the choice of economic damage function, which is still a much-debated quantity in the literature, but is also dependent on the relationship between the economy and emissions. Using the Kaya Identity to translate changes in GDP directly into changes in fossil fuel emissions (Woodard et al., 2019), or, similarly, combining output with a carbon intensity factor, as in the default DICE parameterization, relies on the assumption that any change in GDP affects emissions in the same way, regardless of the sector of the economy affected by climate. More complex integrated assessment models may be able to remove this assumption and shed light on more of the underlying dynamics of this relationship in the future.

Another goal is to assess the effect of natural carbon cycle feedbacks on model results and support improved representation of this significant component. In DICE-Burke, the model has a strongly net negative carbon-climate feedback effect, which acts to somewhat mitigate climate change, while that of the Woodard *et al.* model was near neutral due to the inclusion of positive natural carbon-climate feedbacks (Table 3.2). The net natural carbon-climate feedback is generally expected to contribute to a net increase in atmospheric CO_2 for a given amount of emissions and would likely reduce the magnitude of the net negative gain in a fully-coupled scenario in a model like DICE, by offsetting some of the negative feedback effects. This has important consequences for policy-relevant outputs from this and similar models such as the social cost of carbon. The stronger moderation of climate change in DICE-Burke due to lack of natural positive carbon-climate feedbacks would be expected to lead to a lower estimated social cost of carbon than would be predicted in a model that included a more complete set of key feedback effects. This translates to reduced incentives for climate mitigation policy and other economic and social preventative efforts.

Integrated assessment model intercomparisons will be additionally important to understand the impact of specific policies and different future development scenarios on anthropogenic carbon feedbacks, to better define the potential range of these feedback effects.

Policies penalizing carbon emissions can encourage economies to decarbonize, reducing the impact of changes in GDP on emissions by reducing the carbon intensity of economic productivity. Depending on which sectors reduce their dependence on fossil fuels, the effects of those changes on carbon feedbacks may vary. For example, deep decarbonization of energy systems would leave feedbacks related to land use as the predominant human-driven feedback effect, while resource-intensive future development may increase the strength of both land use and fossil fuel feedback mechanisms.

As previous work has indicated, anthropogenic carbon feedbacks have not only potentially large consequences for climate and the carbon cycle but also come at high economic costs, so reducing uncertainty around their magnitude and understanding their interactions with policy are important goals moving forward. Here we have laid out a standardized approach to make comparisons of carbon cycle feedback components across models that include more than just natural carbon cycle feedback mechanisms and illustrated its application to evaluate carbon cycle feedbacks in a simple integrated assessment model commonly used for climate policy. Hopefully further comparisons of these feedbacks within integrated assessment models can facilitate future development and understanding of anthropogenic feedback mechanisms and advance their consideration in new generations of models.

Acknowledgements

This material is based upon work supported by the National Science Foundation Graduate Research Fellowship Program under Grant DGE-1321846. J.T.R. and S.J.D. received support from NASA's Interdisciplinary Science Program. J.T.R. received additional support from NASA's Carbon Monitoring System (CMS) Program; the Gordon and Betty Moore Foundation (GBMF 3269); and the Reducing Uncertainty in Biogeochemical Interactions Through Synthesis and Computation (RUBISCO) Science Focus Area in US Department of Energy's Office of Science, Division of Biological and Environmental Research.

Chapter 4
Near Term Forecasts of US Fossil Fuel Emissions with a Vector Autoregression Model

4.1 Introduction

As the world wrestles with policy decisions and mitigation strategies in the face of climate change, a lot rests on scientific understanding of how the rate of anthropogenic fossil fuel emissions will change in the future and how that trajectory can be influenced. Different aspects of this question have been addressed in the literature, including analysis breaking down key drivers of emissions (Peters et al., 2017; Raupach et al., 2007), creating detailed emissions inventories (e.g. Gurney et al. 2009; Boden et al. 2017; Oda et al. 2018), looking at feedbacks on emissions (Beckage et al., 2018; Woodard et al., 2019), generating future emissions scenarios (van Vuuren et al., 2011; Riahi et al., 2017), and a variety of near and long term forecasting over different regions (see, for example, Köne and Büke 2010; Pao et al. 2012; Wu et al. 2015). Forecasting emissions can be used to aid in near real time estimation and short term forecasting of net carbon cycle changes, as well as supporting national and regional efforts to curb fossil fuel emissions through climate policy. As of 2017, the United States still has the highest per capita carbon dioxide (CO_2) emissions of any nation in the world and the second highest total CO_2 emissions behind only China as of 2018 (Le Quéré et al., 2018), so accurate prediction of US emissions is a critical step toward a global forecast.

The availability of US emissions data also has a three month delay, a gap that any forecast must first fill before estimating future values.

Fossil fuel CO_2 emissions in the US come primarily from energy, with around two percent from non-energy sources such as cement manufacturing, limestone consumption, natural gas production, and other industrial processes (Figure 4.1D) (Conti and Holtberg, 2011). While oil-based energy continues to dominate the energy sector, in the past decade declines in the use of coal and a rise in natural gas have combined to allow natural gas to replace coal as the second largest source of energy-related fossil fuel emissions in the United States (Figures 4.1A, 4.1B). This shift has lead to an overall decline in the carbon intensity of the US energy sector over the past decade and a half, since the average carbon intensity of coal in the US (95 Mt CO_2 per EJ) is much higher than that of natural gas (65 Mt CO_2 per EJ). Oil has an even lower mean carbon intensity (52 Mt CO_2 per EJ) but has contributed to a relatively constant fraction of US fossil fuel emissions over recent history (Figure 4.1C) (Conti and Holtberg, 2011). Despite sharp declines in the carbon intensity of the US energy sector, concurrent increases in energy demand have resulted in only weak declines in US monthly fossil fuel emissions over the same time period (Figure 4.1D).

Notwithstanding its plan to withdraw from the Paris Climate Agreement in 2020, the US remains a substantial contributor to global carbon emissions and reductions in the US will be important to meet global mitigation goals. As of 2019, 23 US states have set their own greenhouse gas reduction targets, and hundreds of US cities have also set similar goals (Krause, 2011; Lutsey and Sperling, 2008; Deetjen et al., 2018). Forecasting US emissions over short timescales, from a few months to a few years, may provide insight into such policy decisions surrounding emissions mitigation. The model structure behind these forecasts additionally provides relevant information about the key drivers of emissions and thus the most influential levers available to politicians seeking climate remedies.

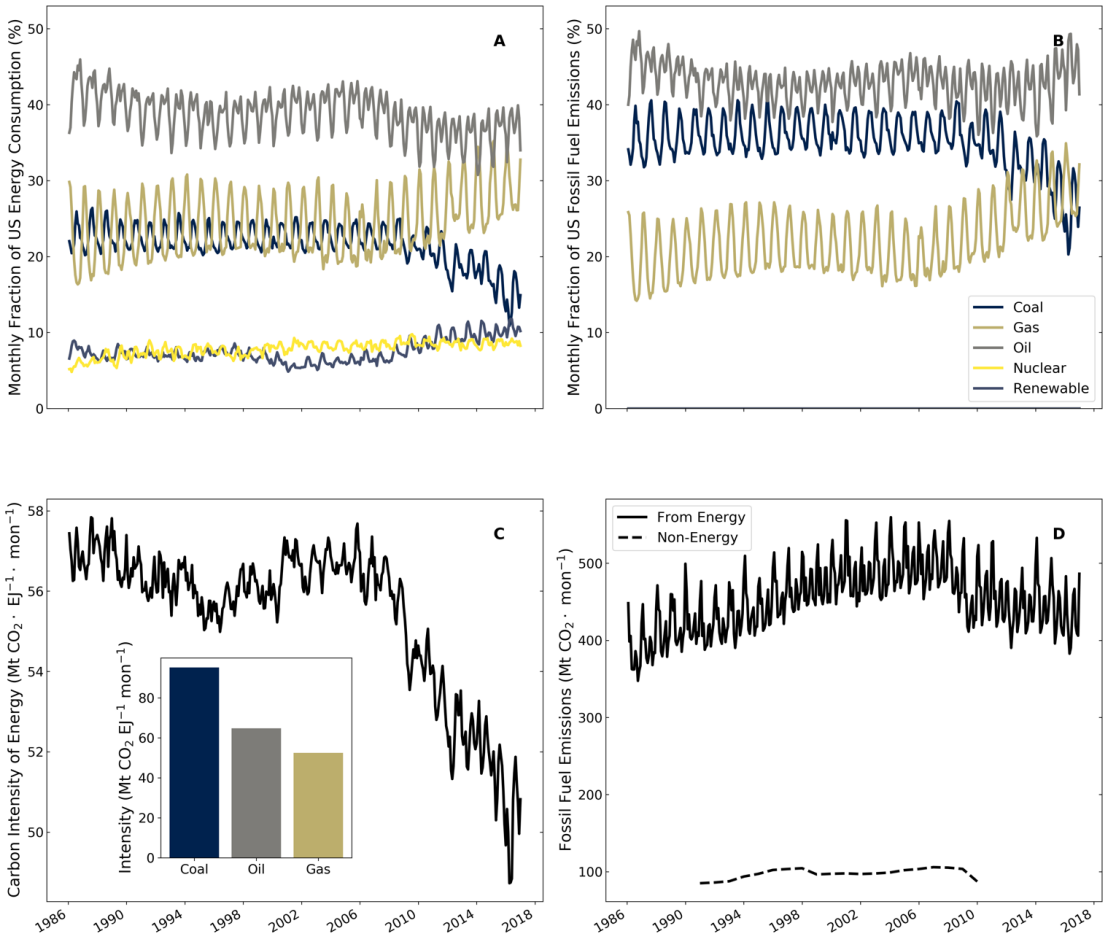

Figure 4.1: Panels A and B show the relative percent of primary energy consumption (A) and energy-related fossil fuel emissions (B) from oil, coal, and natural gas in the United States from 1987 to 2017 (EIA 2018). Panel C shows the decline in the carbon intensity of energy over the same period. It should be noted that this calculation only includes carbon dioxide emissions from energy. Inset into this panel is the mean carbon intensity of energy values for each fuel type over this period. Panel D shows total carbon dioxide emissions from energy compared with carbon dioxide emissions from non-energy sources such as cement and limestone manufacturing. Carbon emissions from energy make up approximately 98% of US annual carbon dioxide emissions (Conti and Holtberg, 2011).

Despite the global significance of US emissions, there are limited US-specific forecasts in the literature. The US Energy Information Administration (EIA) publishes annual forecasts out to two years ahead in their Monthly Energy Outlook publication based on projections of fossil fuel use from the energy and economic model. Emmanuel Silva improved on these results by combining the EIA forecast with a singular spectrum analysis model

(Silva, 2013). The Global Carbon Project also publishes US-specific emissions forecasts out to the end of the current year as part its overall estimation of the annual global carbon budget. However, these forecasting approaches are relatively complex, and they have not been systematically evaluated with respect to input variables or model form. Further, most past work has focused on annual predictions, making it more different to capture covariances between climate or socioeconomic driver variables that may emerge on shorter timescales.

Here we explore the usefulness of a set of readily-available predictors in a vector autoregression (VAR) model for making out-of-sample forecasts of monthly US carbon dioxide emissions over time scales of up to two years. VAR models have been widely used in time series forecasting including forecasting climate and weather variables (Hassani et al., 2018; Liu et al., 2018; Shahin et al., 2014), and a variety of economic outcomes (Kumar, 2010; Patnaik, 2010; Adomavicius et al., 2012; Kolodzeij and Kaufmann, 2014). They have also previously been used to forecast CO_2 emissions in other regions as well as understand structural drivers of emissions trends (Magazzino, 2016; Wen and Zhang, 2018; Xiumei et al., 2011; Xu and Lin, 2016a,b), however to our knowledge no previous analyses have applied this technique to emissions in the United States, nor has previous autoregression forecasting work addressed the complexities around different time delays in data availability for relevant predictors.

The rest of this chapter is organized as follows. In Section 2 we describe our data sources and processing as well as model development, selection, and validation approach. In Section 3 we evaluate the performance of the best model on out-of-sample forecasts during our test period at monthly and annual temporal resolutions. Finally, in Section 4 we compare our model to existing forecasts and discuss broader implications of this work, and in Section 5 we summarize our overall conclusions from this analysis.

4.2 Methods

4.2.1 Data selection and processing

We focused our forecasting efforts on carbon dioxide emissions from energy since these make up the vast majority of fossil fuel emissions in the United States and are also the most variable (Figure 4.1D). We selected potential predictors based on data that were frequently updated, freely available, and provided at a monthly resolution or better, so forecasts following this approach can be continually updated and can include sub-annual predictions. This allowed us to generate rolling forecasts using ever more recent data, despite delays in emissions data availability.

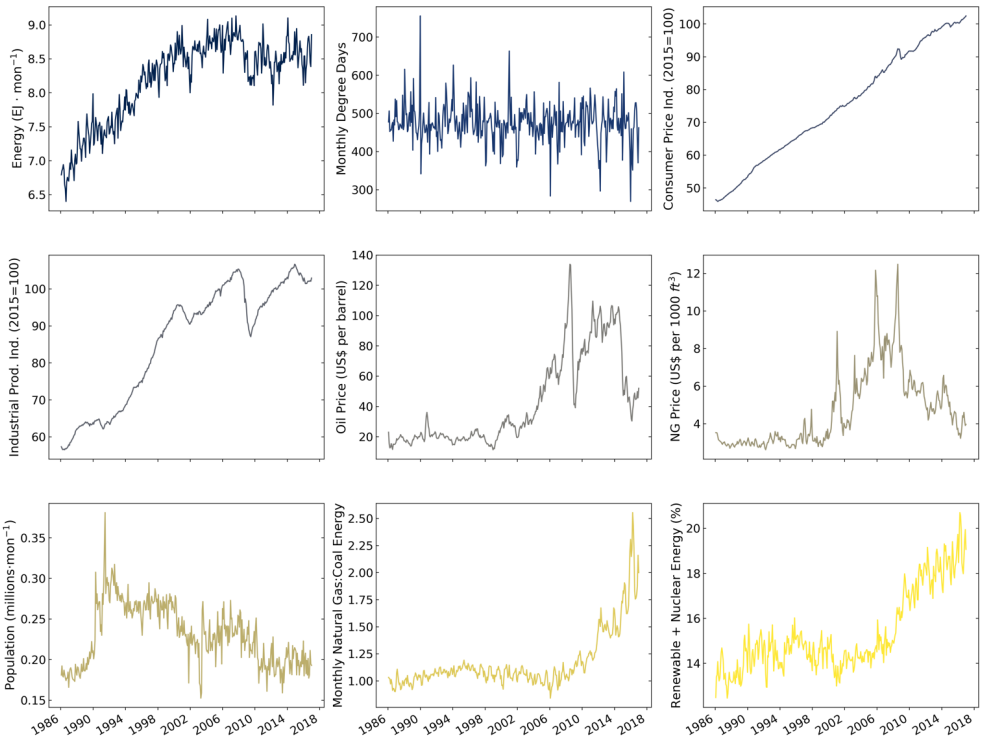

Figure 4.2: Monthly US data for the nine predictors used in this analysis, shown over the period from 1986-2016. Data is shown with the seasonal cycle removed from energy, degree days, population, the natural gas to coal ratio, and the renewable and nuclear energy fraction to be consistent with the data used for model fitting and forecasting.

Using this criteria we chose a set of nine predictors that are all readily available

online through the EIA and U.S. Federal Reserve (Table 4.1): monthly energy consumption, oil price, natural gas price, degree days, industrial production index, consumer price index, the natural gas to coal energy ratio, the fraction of energy from non-fossil fuel sources (hereafter, non-fossil), and population. Fossil fuel emissions data we also retrieved the EIA. To aid in forecasting we then removed a mean annual seasonal cycle in our analysis (Figure 4.2). Of all the predictors, energy was the most strongly correlated with contemporary emissions, followed by the industrial production index and natural gas price (Figure 4.3).

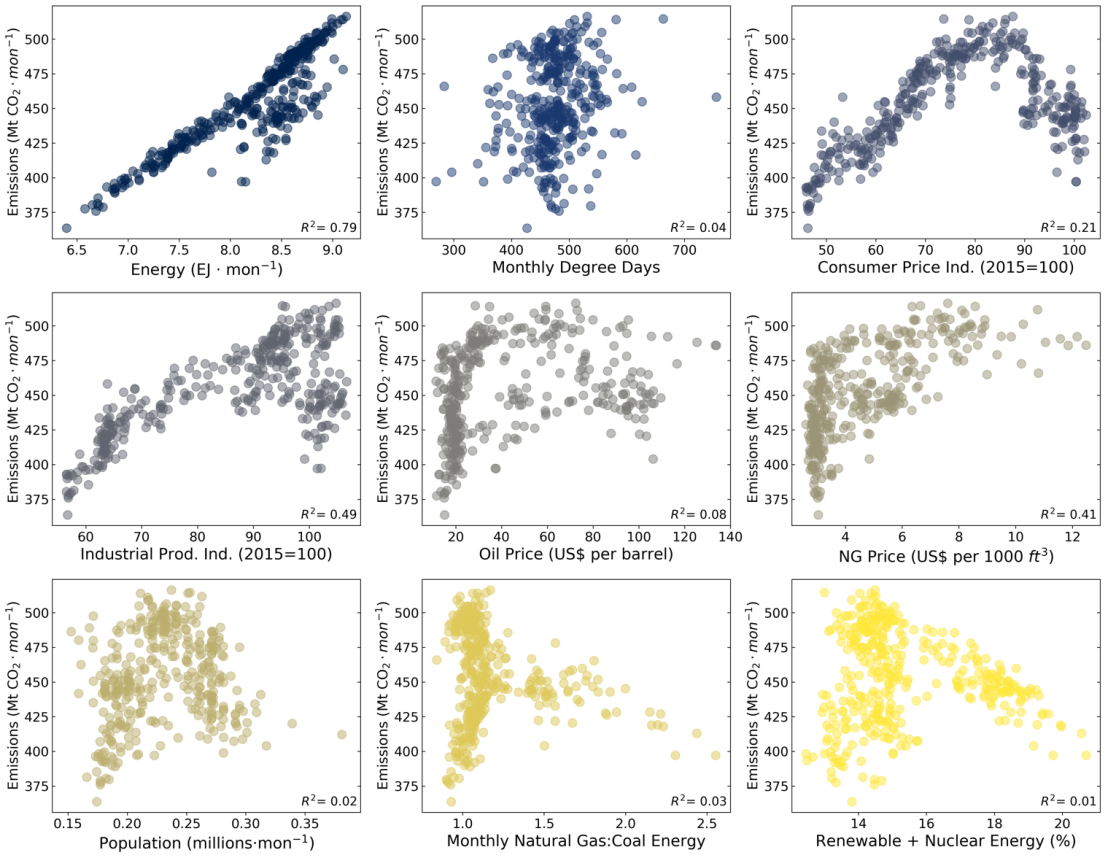

Figure 4.3: Contemporary correlations between US carbon dioxide emissions from energy and the set of nine predictors assessed in this study over the period from 1986-2016. We removed the seasonal cycle to better correspond with our subsequent analysis.

Also important for their forecasting relevance were the time delays in availability of each predictor. While the latest fossil fuel emissions data in the United States lags the present by around three months, as does energy data, economic variables such as the

Table 4.1: Data availability and temporal lags for emissions data and economic, climate, and energy predictor data. The column 'Temporal Lag' corresponds to the time in months that the latest data available lags the present day. For example, the latest energy data available in January 2019 was from September 2018. Population data is shown with an asterisk as the available data is actually also forecasted data from the US Census Bureau.

Predictor	**Timespan**	**Temporal lag**	**Data source**
Fossil Fuel Emissions	1973-2019	3 months	Energy Information Administration (Repice, 2019)
Industrial Productivity Index	1919-2019	2 months	The St. Louis Federal Reserve (Board of Governors of the US Federal Reserve System, 2019)
Consumer Price Index	1960-2019	1 month	The St. Louis Federal Reserve (Organization for Economic Co-operation and Development, 2019)
Oil Price	1946-2019	1 month	Energy Information Administration (Federal Reserve Bank of St. Louis, 2019)
Natural Gas Price	1984-2019	1 month	Energy Information Administration (2019)
Population∗	1959-2019	0 months	The St. Louis Federal Reserve (U.S. Census Bureau, 2019)
Energy Consumption	1973-2019	3 months	Energy Information Administration (Repice, 2019)
Non-Fossil Fraction	1973-2019	3 months	Energy Information Administration (Repice, 2019)
Degree Days	1973-2019	0 months	Energy Information Administration (Repice, 2019)

industrial production index are available with only a one or two month delay, and climate variables like degree days can be calculated up to the present (Table 4.1).

4.2.2 Model selection and design

The variable availability of each predictor created data gaps which needed to be filled up to the present day before forecasting emissions forward in time (Figure 4.4). For example, on January 1, 2020, to forecast the total carbon dioxide emissions for the rest of that January,

the model would be able to use emissions and energy data from up through September 2019, degree day data up through December 2020, and industrial production index values up through November 2020. To handle these varied lags in availability, we first hindcasted over the CO_2 emissions data lag using the other variables as they remained available and the gaps in data were filled with modeled values. This provided a full set of predictor data up until the forecast start date. Then fully out-of-sample forecasts were made using this hindcasted set (Figure 4.4).

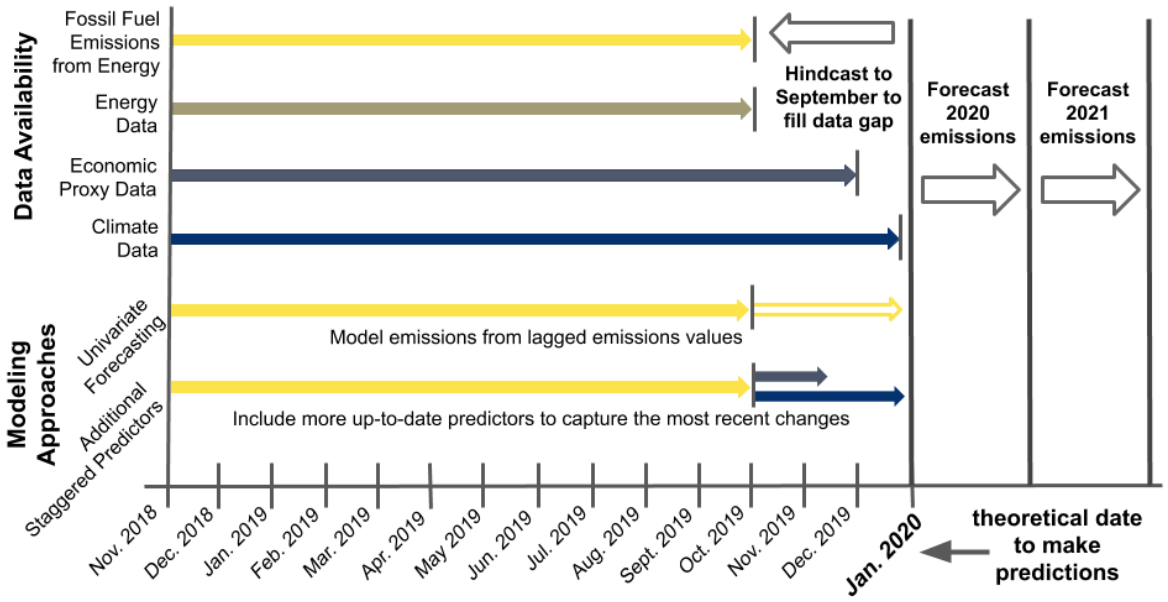

Figure 4.4: Theoretical timeline of US data availability (top) and modeling approaches (bottom) for making forecasts and hindcasts from Jan. 1, 2020. Economic data is shown lagging the present by two months, although some data, such as the consumer price index, is available on only a 1-month lag.

Model training and selection was done over a training period from 1986 to 2006, while data from our test period (2007-2016) was reserved for forecast evaluation. The best predictor set for the vector autoregression model was selected based on the out-of-sample mean absolute percent error (MAPE), root mean squared error (RMSE), and the R^2 value across eight years of hindcasted data over the last part of our training period. We compared

these metrics across out-of-sample monthly and annual hindcasts using all combinations of our nine predictors. Several sets of predictors we evaluated performed similarly well based on these three metrics, but the model with the best values across all three used only degree days and the industrial production index with six months of lagged values for each. This VAR(6) system is shown below:

$$V_t = \beta_1 \cdot V_{t-1} + ... + \beta_6 \cdot V_{t-6} + \epsilon \cdot \nu_t \tag{4.1}$$

where $V_t = (\text{emissions}_t, \text{deg. days}_t, \text{ind. prod. index}_t)$, β_1 through β_6 are coefficient matrices, and $\epsilon \cdot \nu_t$ is the vector of white noise residuals. The number of lags was selected automatically using Aikaike's Information Criterion (AIC).

We evaluated the predictive ability of this model against several simpler benchmark models: a univariate autoregression model, simple univariate and multivariate linear regression models using a mean of the most recent available values of each variable as predictors, and, finally, a baseline persistence model. For all models which used the mean of recent values as a predictor, we used the mean of the past six months of available monthly data. So, for example, the forecasted persistence value for April 2020 emissions made in January 2020, would be the mean of the CO_2 emissions values from April-September 2019. The linear regression model used a mean of six months of recent emissions data as a predictor, and the multiple linear regression model added the means of six months of recent degree days and industrial production index values on top of past emissions data to that model.

We also evaluated the performance of different sets of predictors on longer timescales. Over the training period several vector autoregression models were able to beat the performance of our autoregression and persistence models on out-of-sample forecasts of up to nine months, but this result was inconsistent and did not carry through into the test period.

4.2.3 Model evaluation

We used a rolling window cross-validation approach to compare the performance of our models over the ten successive years of our test period (2007-2016) (Bergmeir and Benítez, 2012). This best simulates real use of this forecasting system while maintaining equal sized training sets for comparison between forecasts. To assess forecast accuracy, our data was trained on twenty-year periods, and then we computed test forecasts over various time horizons using the last point of the training set as the forecast origin. In practice his meant that for a one-month forecast, we hindcasted over the three months of the fossil fuel emissions data lag from the last month of the training data to reach a theoretical 'current month' and from there we forecasted ahead the desired one month. So in total four months of emissions values were estimated, but three of those months were computed using current data from other predictors, and only the final month was forecasted using purely lagged values.

We also evaluated the model performance on annual timescales for which we focused on three time periods: end-of-year hindcasts, and forecasts with one year and two years lead times. The end-of-year prediction was generated by making a hindcast as described in the previous section up through the end of the current year and aggregating these monthly results with the monthly emissions data as available during the earlier part of the year. Annual and two-year forecasts were made as 12 and 24-month forecasts and the final 12 months of forecast results from each were then summed to an annual total. Our complete model and code is available at: `https://github.com/dawnlwoodard/fossil_forecast`.

4.3 Results

Our best fit VAR model using degree days and the industrial production index (Eqn. 4.1) was able to outperform persistence and univariate autoregression models up through a four-month forecast. Plotted monthly results from a one-month forecast over the test period show that the forecast closely follows the non-seasonal data, though the model overshoots

during periods of sharp decline, such as the 2008 economic crash (Figure 4.5). The best performance of this model relative to our autoregression and persistence models was with hindcasted predictions, where both degree days and the industrial production index were available more recently than emissions and this contemporary information improved model accuracy (Table 4.2).

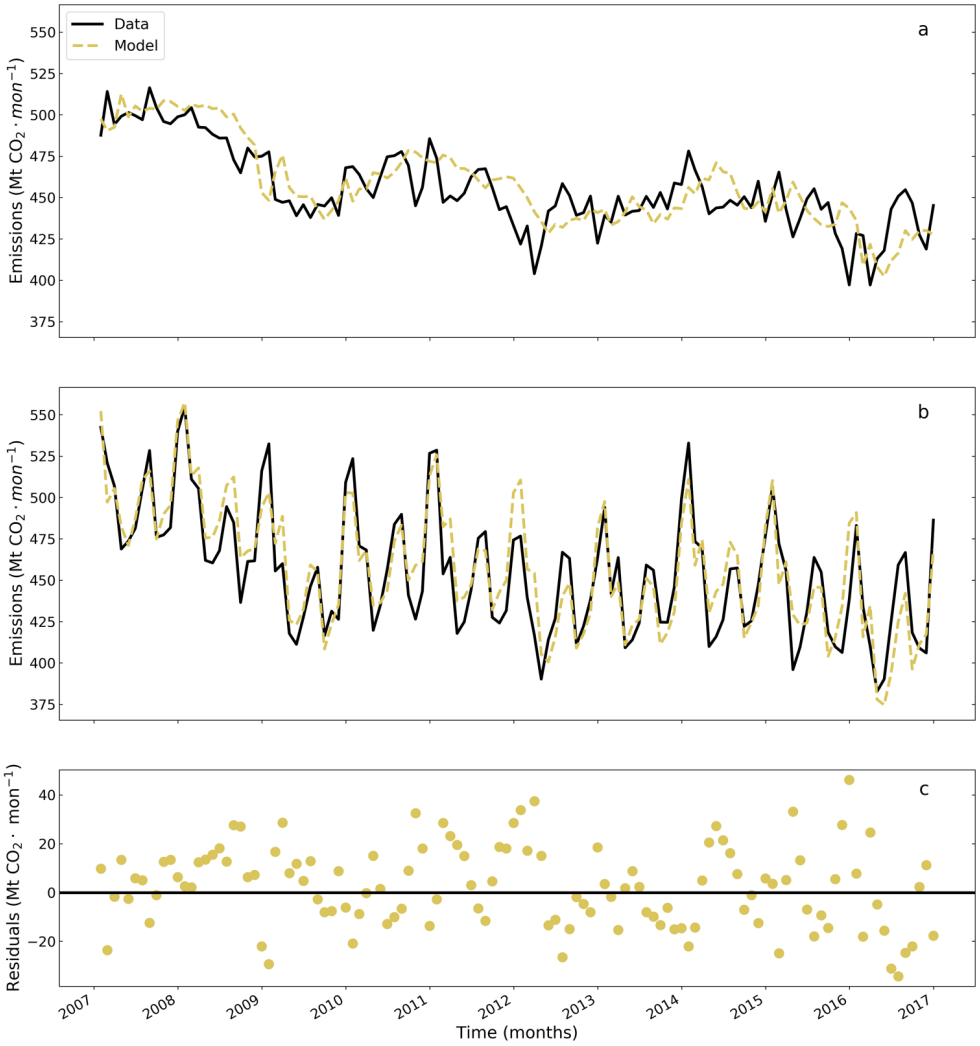

Figure 4.5: One-month forecast results for both the data with the seasonal cycle removed (a) and the full time series with the seasonal cycle added back (b) and the corresponding residuals for this forecast (c). The model forecast is from a vector autoregression model with degree days and the industrial production index as exogenous predictors.

There were also a few other sets of predictors with which our VAR model could

Table 4.2: Out-of-sample statistics and characteristics for a one-month forecast over the model test period from a subset of the models evaluated The first set of statistics (columns 3-5) are from a one-month ahead forecast, while the final three columns give annual statistics from a year where the last three months are hindcasted with the given model.

Predictors		**1-Month Forecast**			**End-of-Year Hindcast**		
	Lags	**MAPE** (%)	**RMSE**	**R^2**	**MAPE** (%)	**RMSE**	**R^2**
Persistence							
Emissions	—	3.46	19.08	0.70	0.60	44.03	0.96
Linear Regression							
Emissions	—	3.43	18.80	0.70	0.56	40.04	0.96
Multiple Linear Regression							
Emissions, degree days	—	3.42	18.78	0.70	0.56	40.04	0.96
Emissions, industrial production index	—	3.39	18.61	0.71	0.56	40.04	0.96
Emissions, degree days, industrial production index	—	3.37	18.54	0.71	0.56	40.04	0.96
Univariate Autoregression							
Emissions	17	3.40	19.00	0.71	0.58	40.85	0.96
Vector Autoregression							
Emissions, degree days	13	3.22	17.58	0.74	0.33	26.61	0.98
Emissions, industrial production index	11	3.21	18.13	0.72	0.70	43.84	0.94
Emissions, degree days, industrial production index	6	3.19	17.13	0.75	0.38	28.60	0.99

outperform the baseline persistence model, but only up through a few months at most, and we found that univariate autoregression did either worse or no better than persistence over all time periods (Figure 4.6, Table 4.2). Multivariate and univariate linear regression models without multiple autoregression terms were similar in accuracy to persistence up through monthly forecasts of a year or more. We found that long term forecasts with our VAR model were too variable to have high accuracy, and the best performing model beyond four month forecasts (eight months from available emissions data) was our benchmark persistence model (Figure 4.6).

Annual VAR results were consistent with these findings from our monthly analysis. While over the training period several VAR models were able to beat our benchmark models

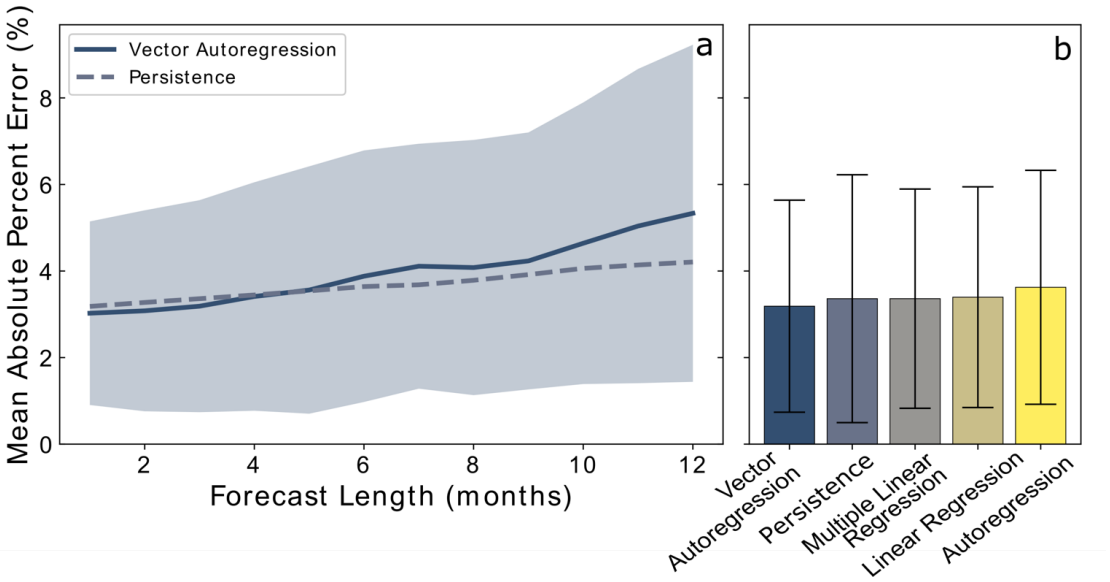

Figure 4.6: Forecast error across models by length of forecast. Panel a) shows the vector autoregression model accuracy over the test period across a range of forecast lengths given by the mean absolute percent error (solid blue line) ± one standard deviation (lighter blue shading). The persistence model is shown for comparison (dashed blue line). Panel b) shows the MAPE for a 1-month forecast using vector autoregression, multiple linear regression, persistence, linear regression, and autoregression. The VAR and MLR models used CO_2 emissions, degree days, and industrial production index as predictors, while the others used only emissions.

over annual out-of-sample forecasts, this did not hold true in the test period, and forecast accuracy was only high (and an improvement over persistence) for our end-of-year annual forecast, but declined substantially for the one and two-year forecasts (Figure 4.7).

4.4 Discussion

4.4.1 Lessons for prediction

This approach demonstrates that fossil fuel emissions can be predicted over the short term with similar or better accuracy than more data-intensive existing forecasts using relatively little data and a simple statistical approach. Using several combinations of predictors, we found our vector autoregression was able to improve on a univariate autoregression model up through a four-month forecast, when the additional predictors became less relevant.

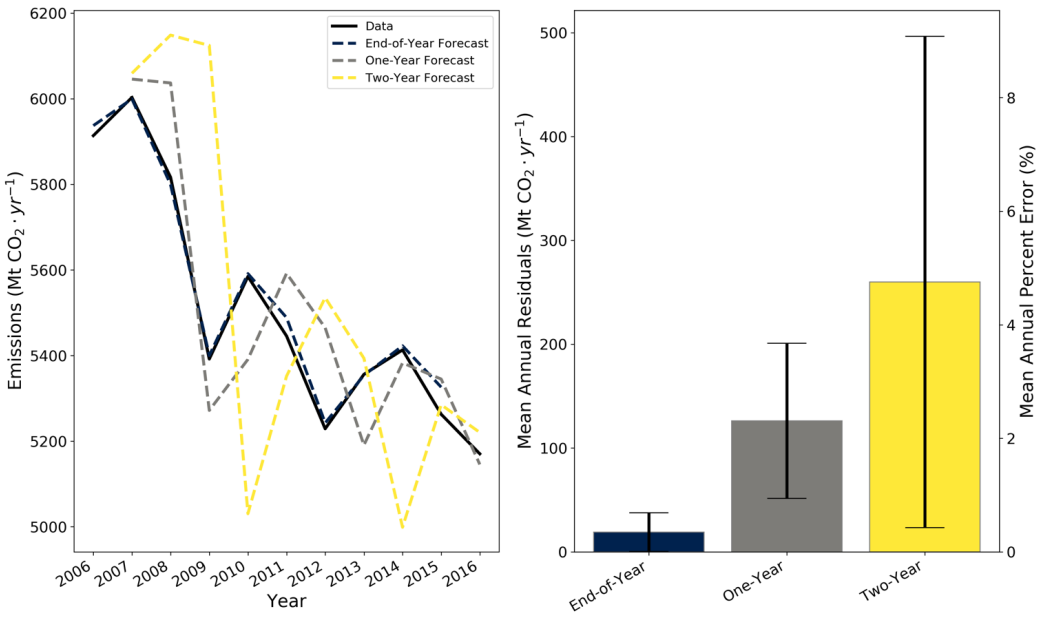

Figure 4.7: Out-of-sample annual forecasts over three time intervals: hindcasting over the last three months of each year (October-December), forecasting over the following year (a 12-month forecast plus a 3-month hindcast), and finally out to a second year ahead. Monthly results were aggregated to annual values for each forecast interval. Panel A shows these annual results over the test period from 2006-2016 and the corresponding mean annual residuals are given in B.

Several predictors stood out as most significant for this forecasting task: degree days, non-fossil energy fraction, and the industrial production index. These appeared in all or nearly all of the top 10 percent of models based on out-of-sample mean absolute percent error (Table 4.3), and the relationship of these particular predictors to fossil fuel emissions has also been supported by some previous analyses, for example, Meng et al. (2018); Aliprandi et al. (2016); Considine (2000).

We compared the performance of separate vector autoregression models using emissions and these three predictors, with the addition of oil price, across individual years to better understand their relative contributions to emissions forecasts (Figure 4.8). We selected four recent years where our autoregression model struggled to fully capture the dynamics of the emissions data and took our one-month ahead forecasts from each those years from each different model to evaluate. Different predictors were each able to improve accuracy in

Table 4.4: Frequency of occurrence of each predictor in the best 25 VAR models. All combinations of all predictors were compared over 1-month ahead forecast intervals based on the mean absolute percent error over 10 years of out-of-sample forecasts.

Predictor	Frequency in top 25 best models
Non-fossil fraction	25
Degree days	25
Industrial production index	19
Natural gas: coal	9
Oil price	8
Population	8
Consumer price index	5
Natural gas price	5
Energy	4

different years. The only variable that improved model performance over the final months of the Great Recession in 2009 was the industrial production index, while over the same time period a univariate model significantly overshot the data. In 2010 our autoregression model underpredicted the data, and the non-fossil fraction was the only predictor successful at closing the mid-year gap. In 2011, oil price was singularly useful in improving performance over the spring and fall where the autoregression model was somewhat overshooting the data. Finally, in 2015, the industrial production index was again the most useful variable at reducing the overshoot in the autoregression model toward the end of the year. This analysis is not causal but does point to the relevance of different predictors over different timeframes.

4.4.2 Comparison with other modeling approaches

Our methodology is relatively simple and involves far fewer data streams than other current approaches, but we were able to match or beat the performance of the EIA model annual end-of-year forecasts in most of the years available for comparison (Figure 4.9). Our best fit model from our training period had a mean absolute error of 0.59 percentage points from 2009 to 2015, compared to the EIA mean absolute error of 0.74 percentage points over the same period. Not only could our best fit model hit this benchmark, but so could vector autoregression models using any other combinations of predictors, as long as the

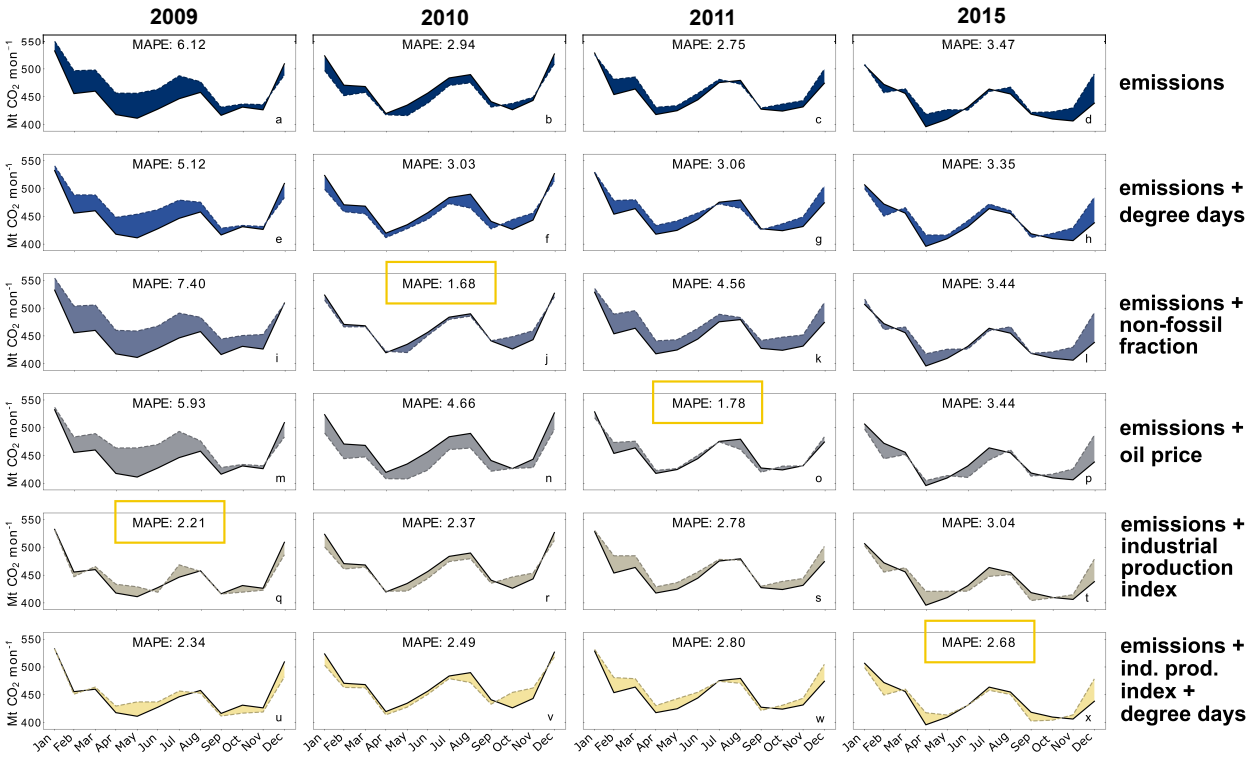

Figure 4.8: One-month ahead monthly forecasts compared against data for five different models over four recent years, selected based on years when our univariate autoregression model had relatively lower accuracy. Panels a-d show 12 one-month ahead forecasts (a year each) of the autoregression model for comparison, and the following rows show different VAR models using degree days (e-h), non-fossil energy fraction (i-l), oil price (m-p), and the industrial production index (q-t) as additional predictors for fossil fuel emissions. Finally, the bottom row (u-x) is the best-fit VAR model used in this analysis.

set of predictors included up-to-date degree day data. However, the high variability in the long-range forecast results of our vector autoregression models decreased the model accuracy compared to the smoother EIA forecast results at one and two-year timescales. To make this comparison as accurate as possible our predictions were made over the same timeframe as the EIA and with the same data availability that the EIA would have access to at the time of their forecast.

The Global Carbon Project also produces estimates of US fossil fuel emissions out to the end of the year from mid-year. In 2015 their Global Carbon Budget report estimated a decrease in fossil fuel emissions of 1.5% from 2014 (Friedlingstein et al., 2019), compared

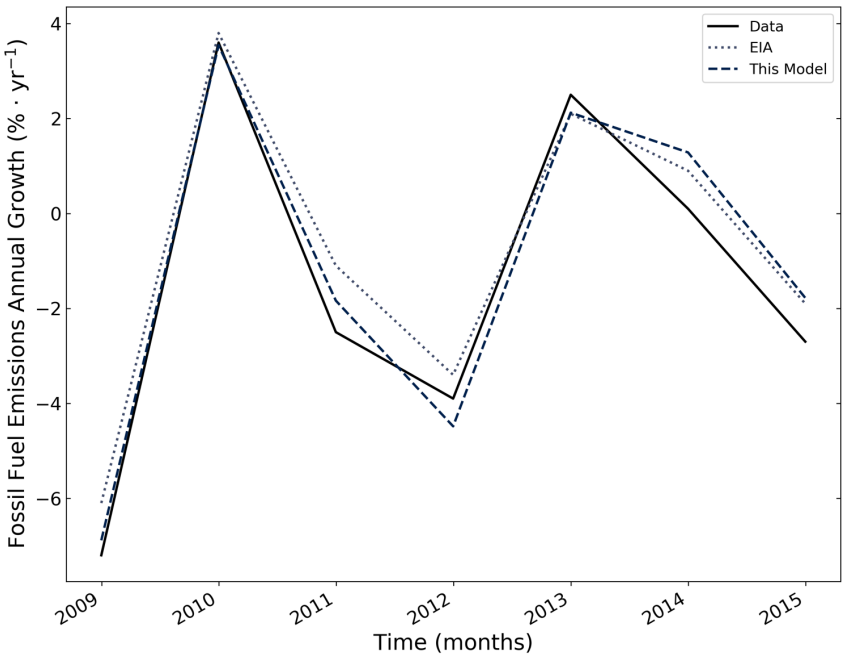

Figure 4.9: Best model (dashed) end-of-year annual forecast compared to the US Energy Information Administrations (dotted) end-of-year forecast. EIA predictions are from the Short Term Energy Outlook and made in January of each year. Our model predictions are from our best-fit VAR model with degree days and industrial production index values, made by hindcasting over October, November, and December of each year. Baseline annual percent emissions change is shown in black.

to the actual decrease of 2.8%, while our model estimated a decrease of 1.8%, though due to the high variability of the accuracy of our model as well as the models from the Global Carbon Project and the EIA, comparison over a single year gives little idea of the relative forecasting power of either model. Additionally, the methodology and timescale of the GCP model is somewhat less comparable to ours.

4.4.3 Lessons for global predictability

Although our focus was on only United States emissions, our findings have additional relevance for predicting global emissions on short time scales. Globally, the challenge of emissions data lagging the present is much more pronounced than in the US, increasing the relevance of substantially more up-to-date predictors such as degree days and various economic indi-

cators. While emissions data globally lags the present by a year or more, economic data is available with only a few months delay. Additionally, while in the United States energy data is available on the same time lag as fossil fuel data, energy data from several other major emitters is far more up-to-date than the CO_2 emissions data. These two predictors are strongly correlated, meaning that in our US model their equivalent temporal availability made energy data much less relevant (Table 4.3), since emissions data could always be used over the same timeframe, but globally this more recent energy data from certain countries may be an important asset to making accurate global predictions.

4.5 Conclusions

Modern climate policy necessitates a high level of understanding of the drivers of fossil fuel emissions and can be aided by accurate emissions forecasts. While more complex data-driven models outperformed our results in the long term, there is potential for more rapidly deployed hindcasts and forecasts using readily-available predictors to improve emissions forecasts over shorter timescales. This is particularly relevant globally as data lags are significantly longer in other countries and the hindcasting power of the approach discussed here may be able to help fill these gaps ahead of actual emissions data releases.

Using freely available and frequently updated monthly predictor variables we were able to produce forecasts over several months that could outperform more complex existing forecast systems as well as our benchmark univariate models, despite worse performance over longer timescales. This forecasting approach can be employed to support more rapid estimation of near-term emissions for use in carbon-cycle analyses and climate policy and can be extended globally to reduce much longer lags in emissions reporting.

Chapter 5
Conclusions

In this dissertation I set out to advance understanding of fossil fuel emissions in the near and long term in order to improve integrated assessment modeling efforts and projections of climate change from Earth system models. On long timescales I was interested in exploring the interconnected relationship between fossil fuel emissions and climate and how these relationships could be represented in models. I also sought to bridge the gap between the natural carbon cycle community, which has done extensive work evaluating carbon cycle feedbacks on land and in the ocean but lacks the ability to represent similar feedbacks in human systems, and the integrated assessment modeling community, which has made important progress representing economic and energy systems and producing fossil fuel emissions trajectories, but has almost no discussion in the literature of feedbacks in their models. On shorter timescales, I was interested in exploring the predictability of fossil fuel emissions which can be used to provide more up-to-date estimates and near-term forecasts to help close the carbon cycle budget and to inform climate policy.

In Chapter 2 my findings demonstrated the relevance of economically-driven carbon cycle feedbacks, showing that compared to natural carbon-climate feedbacks, these anthropogenic feedbacks on carbon dioxide emissions are potentially equally important to consider in terms of their magnitude and climate impacts. This analysis also found that the most significant feedback mechanism was the relationship between climate and the economy, which drove an overall negative net feedback on fossil fuel emissions, in contrast to natural carbon-climate feedbacks, which are net positive. However, the damage function behind this

climate-economic relationship also had the highest uncertainty of any of the components of the model, and the range has significant implications for future climate.

My hope is that the work from this chapter will prompt further discussion of the as-of-yet very limited representation of economic carbon cycle feedbacks in models and will be motivation for more models to intentionally consider where economic feedbacks may impact their findings. From conversations with several integrated assessment modeling groups I know that efforts are underway to include more such couplings in models. The other critical next step from this work is reducing the uncertainty in the climate-economy relationship through further empirical analyses, including efforts reconcile the disparity between small-scale local and regional economic damage estimates and national and global scale statistical findings such as from Burke *et al.* (2015).

In Chapter 3 I have developed an inclusive framework for estimating carbon cycle feedbacks in models, including both fossil fuel and land use anthropogenic feedbacks, which have previously been excluded from analyses. I applied this framework to evaluate carbon feedbacks in two different simple models, providing concrete examples of estimating feedback parameters of interest. The results from this analysis also demonstrated the importance of model structure in representing economic feedbacks, as I found that the ability of the economy to dynamically respond to climate impacts weakened the climate feedback on fossil fuel emissions. Additionally, through a carbon cycle feedback analysis on the DICE-Burke model, I illustrated the limitations of the model's very simplified carbon cycle, which has important consequences in light of the frequent use of this model and other similar models in climate policy.

This work has laid out the additional steps needed to apply a carbon cycle feedback analysis framework to models that include carbon feedbacks outside of the natural carbon cycle. As integrated assessment models continue to add couplings between climate and economic systems, and some researchers are even coupling Earth system models with integrated assessment models, this framework structure can facilitate inter-model comparisons

of anthropogenic carbon feedbacks to assist in model development and reduce uncertainties. Additionally, it can be applied to evaluate the existing representation of natural carbon cycle feedbacks in these models and compare this to previous results from Earth system model feedback analyses to improve understanding of the impact of the typically simplified representation of natural carbon feedbacks in IAMs.

Finally, in Chapter 4 I built a model to forecast fossil fuel emissions in the U.S. using fewer data sources and a simpler model than existing forecasts over similar timescales. I found that using up-to-date predictors to fill in the data lag that exists for fossil fuel emissions data was able to substantially increase accuracy over models without these predictors, and allowed me to improve on the performance of more complex existing forecasts for U.S. emissions. This work suggests that for near-term carbon cycle hindcasts and forecasts out to a few months, a relatively simple statistical approach using a few predictors may be a useful tool to provide more accessible estimates of emissions compared to other current forecasting approaches for the U.S. These results also provide a stepping stone to building a hopefully more nimble global emissions forecasting system.

Bibliography

Ackerman, F., DeCanio, S. J., Howarth, R. B., and Sheeran, K. (2009). Limitations of integrated assessment models of climate change. *Climatic Change*, 95(3-4):297–315.

Ackerman, F. and Stanton, E. A. (2012). Climate Risks and Carbon Prices: Revising the Social Cost of Carbon. *Economics: The Open-Access, Open-Assessment E-Journal*, 6(2012-10):1.

Adomavicius, G., Bockstedt, J., and Gupta, A. (2012). Modeling Supply-Side Dynamics of IT Components, Products, and Infrastructure: An Empirical Analysis Using Vector Autoregression. *Information Systems Research*, 23(2):397–417.

Aivalioti, S. (2015). Electricity Sector Adaptation to Heat Waves. SSRN Scholarly Paper ID 2563037, Social Science Research Network, Rochester, NY.

Alhazmy, M. M. and Najjar, Y. S. H. (2004). Augmentation of gas turbine performance using air coolers. *Applied Thermal Engineering*, 24(2):415–429.

Aliprandi, F., Stoppato, A., and Mirandola, A. (2016). Estimating CO2 emissions reduction from renewable energy use in Italy. *Renewable Energy*, 96:220–232.

Ameri, M. and Hejazi, S. H. (2004). The study of capacity enhancement of the Chabahar gas turbine installation using an absorption chiller. *Applied Thermal Engineering*, 24(1):59–68.

Arora, V. K., Boer, G. J., Friedlingstein, P., Eby, M., Jones, C. D., Christian, J. R., Bonan, G., Bopp, L., Brovkin, V., Cadule, P., Hajima, T., Ilyina, T., Lindsay, K., Tjiputra, J. F., and Wu, T. (2013). Carbon–Concentration and Carbon–Climate Feedbacks in CMIP5 Earth System Models. *Journal of Climate*, 26(15):5289–5314.

Arora, V. K., Katavouta, A., Williams, R. G., Jones, C. D., Brovkin, V., Friedlingstein, P., Schwinger, J., Bopp, L., Boucher, O., Cadule, P., Chamberlain, M. A., Christian, J. R., Delire, C., Fisher, R. A., Hajima, T., Ilyina, T., Joetzjer, E., Kawamiya, M., Koven, C., Krasting, J., Law, R. M., Lawrence, D. M., Lenton, A., Lindsay, K., Pongratz, J., Raddatz, T., Séférian, R., Tachiiri, K., Tjiputra, J. F., Wiltshire, A., Wu, T., and Ziehn, T. (2019). Carbon-concentration and carbon-climate feedbacks in CMIP6 models, and their comparison to CMIP5 models. *Biogeosciences Discussions*, pages 1–124.

Arora, V. K. and Melton, J. R. (2018). Reduction in global area burned and wildfire emissions since 1930s enhances carbon uptake by land. *Nature Communications*, 9(1):1326.

Basha, M., Shaahid, S. M., and Al-Hadhrami, L. (2012). Impact of Fuels on Performance and Efficiency of Gas Turbine Power Plants. *Energy Procedia*, 14:558–565.

Beckage, B., Gross, L. J., Lacasse, K., Carr, E., Metcalf, S. S., Winter, J. M., Howe, P. D., Fefferman, N., Franck, T., Zia, A., Kinzig, A., and Hoffman, F. M. (2018). Linking models of human behaviour and climate alters projected climate change. *Nature Climate Change*, 8(1):79–84.

Behrenfeld, M. J., O'Malley, R. T., Siegel, D. A., McClain, C. R., Sarmiento, J. L., Feldman, G. C., Milligan, A. J., Falkowski, P. G., Letelier, R. M., and Boss, E. S. (2006). Climate-driven trends in contemporary ocean productivity. *Nature*, 444(7120):752.

Bergmeir, C. and Benítez, J. M. (2012). On the use of cross-validation for time series predictor evaluation. *Information Sciences*, 191:192–213.

Board of Governors of the US Federal Reserve System (2019). Industrial Production Index.

Boden, T., Marland, G., and Andres, R. (2017). Global, Regional, and National Fossil-Fuel CO2 Emissions. Technical report, Carbon Dioxide Information Analysis Center, Oak Ridge National Laboratory, U.S. Department of Energy, Oak Ridge, TN, USA.

Boer, G. J. and Arora, V. (2009). Temperature and concentration feedbacks in the carbon cycle. *Geophysical Research Letters*, 36(2).

Boer, G. J. and Arora, V. (2010). Geographic Aspects of Temperature and Concentration Feedbacks in the Carbon Budget. *Journal of Climate*, 23(3):775–784.

Boer, G. J. and Arora, V. K. (2012). Feedbacks in Emission-Driven and Concentration-Driven Global Carbon Budgets. *Journal of Climate*, 26(10):3326–3341.

Bolt, J. and van Zanden, J. L. (2014). The maddison project: collaborative research on historical national accounts. *The Economic History Review*, 67(3):627–651.

Bopp, L., Aumont, O., Cadule, P., Alvain, S., and Gehlen, M. (2005). Response of diatoms distribution to global warming and potential implications: A global model study. *Geophysical Research Letters*, 32(19).

Boyd, P. W. and Doney, S. C. (2003). The Impact of Climate Change and Feedback Processes on the Ocean Carbon Cycle. In Fasham, M. J. R., editor, *Ocean Biogeochemistry: The Role of the Ocean Carbon Cycle in Global Change*, Global Change — The IGBP Series (closed), pages 157–193. Springer Berlin Heidelberg, Berlin, Heidelberg.

Bullock, M. A. and Grinspoon, D. H. (1999). Global climate change on venus. *Scientific American*, 280(3):50–57.

Burke, M., Craxton, M., Kolstad, C. D., and Onda, C. (2016). Some research challenges in the economics of climate change. *Climate Change Economics*, 07(02):1650002.

Burke, M., Davis, W. M., and Diffenbaugh, N. S. (2018). Large potential reduction in economic damages under UN mitigation targets. *Nature*, 557(7706):549.

Burke, M., Hsiang, S. M., and Miguel, E. (2015). Global non-linear effect of temperature on economic production. *Nature*, 527(7577):235–239.

Burnard, K. and Bhattacharya, S. (2011). Power Generation from Coal. IEA Energy Papers, Organisation for Economic Co-operation and Development, Paris.

Ciais, P., Sabine, C., Bala, G., Bopp, L., Brovkin, V., Canadell, J., Chhabra, A., DeFries, R., Galloway, J., Heimann, M., et al. (2014). Carbon and other biogeochemical cycles. In *Climate change 2013: the physical science basis. Contribution of Working Group I to the Fifth Assessment Report of the Intergovernmental Panel on Climate Change*, pages 465–570. Cambridge University Press.

Ciscar, J.-C. and Dowling, P. (2014). Integrated assessment of climate impacts and adaptation in the energy sector. *Energy Economics*, 46:531–538.

Considine, T. J. (2000). The impacts of weather variations on energy demand and carbon emissions. *Resource and Energy Economics*, 22(4):295–314.

Conti, J. and Holtberg, P. (2011). Emissions of Greenhouse Gases in the United States 2009. Technical Report DOE/EIA-0573(2009), U.S. Energy Information Administration, Washington, D.C.

Cox, P. M., Pearson, D., Booth, B. B., Friedlingstein, P., Huntingford, C., Jones, C. D., and Luke, C. M. (2013). Sensitivity of tropical carbon to climate change constrained by carbon dioxide variability. *Nature*, 494(7437):341–344.

Crowther, T. W., Todd-Brown, K. E. O., Rowe, C. W., Wieder, W. R., Carey, J. C., Machmuller, M. B., Snoek, B. L., Fang, S., Zhou, G., Allison, S. D., Blair, J. M., Bridgham, S. D., Burton, A. J., Carrillo, Y., Reich, P. B., Clark, J. S., Classen, A. T., Dijkstra, F. A., Elberling, B., Emmett, B. A., Estiarte, M., Frey, S. D., Guo, J., Harte, J., Jiang, L., Johnson, B. R., Kröel-Dulay, G., Larsen, K. S., Laudon, H., Lavallee, J. M., Luo, Y., Lupascu, M., Ma, L. N., Marhan, S., Michelsen, A., Mohan, J., Niu, S., Pendall, E., Peñuelas, J., Pfeifer-Meister, L., Poll, C., Reinsch, S., Reynolds, L. L., Schmidt, I. K., Sistla, S., Sokol, N. W., Templer, P. H., Treseder, K. K., Welker, J. M., and Bradford, M. A. (2016). Quantifying global soil carbon losses in response to warming. *Nature*, 540(7631):104–108.

Davidson, E. A. and Janssens, I. A. (2006). Temperature sensitivity of soil carbon decomposition and feedbacks to climate change. *Nature*, 440(7081):165–173.

Deetjen, T. A., Conger, J. P., Leibowicz, B. D., and Webber, M. E. (2018). Review of climate action plans in 29 major U.S. cities: Comparing current policies to research recommendations. *Sustainable Cities and Society*, 41:711–727.

Devaraju, N., Bala, G., Caldeira, K., and Nemani, R. (2016). A model based investigation of the relative importance of CO2-fertilization, climate warming, nitrogen deposition and land use change on the global terrestrial carbon uptake in the historical period. *Climate Dynamics*, 47(1):173–190.

Díaz, S., Grime, J. P., Harris, J., and McPherson, E. (1993). Evidence of a feedback mechanism limiting plant response to elevated carbon dioxide. *Nature*, 364(6438):616–617.

Diffenbaugh, N. S. and Field, C. B. (2013). Changes in Ecologically Critical Terrestrial Climate Conditions. *Science*, 341(6145):486–492.

Dunne, J. P., John, J. G., Adcroft, A. J., Griffies, S. M., Hallberg, R. W., Shevliakova, E., Stouffer, R. J., Cooke, W., Dunne, K. A., Harrison, M. J., and et al. (2012). Gfdl's esm2 global coupled climate–carbon earth system models. part i: Physical formulation and baseline simulation characteristics. *Journal of Climate*, 25(19):6646–6665.

Erb, K.-H., Fetzel, T., Plutzar, C., Kastner, T., Lauk, C., Mayer, A., Niedertscheider, M., Körner, C., and Haberl, H. (2016). Biomass turnover time in terrestrial ecosystems halved by land use. *Nature Geoscience*, 9(9):674–678.

Farouk, N., Sheng, L., and Hayat, Q. (2013). Effect of ambient temperature on the performance of gas turbines power plant. *International Journal of Computer Science Issues*, 10(3).

Federal Reserve Bank of St. Louis (2019). Spot Crude Oil Price: West Texas Intermediate (WTI).

Field, C. B., Barros, V. R., Mach, K., and Mastrandrea, M. (2014). *Climate change 2014: impacts, adaptation, and vulnerability*, volume 1. Cambridge University Press Cambridge and New York.

Flato, G. M. (2011). Earth system models: an overview. *WIREs Climate Change*, 2(6):783–800.

Fleischer, E., Khashimov, I., Hölzel, N., and Klemm, O. (2016). Carbon exchange fluxes over peatlands in Western Siberia: Possible feedback between land-use change and climate change. *Science of The Total Environment*, 545-546:424–433.

Friedlingstein, P., Cox, P., Betts, R., Bopp, L., von Bloh, W., Brovkin, V., Cadule, P., Doney, S., Eby, M., Fung, I., Bala, G., John, J., Jones, C., Joos, F., Kato, T., Kawamiya, M., Knorr, W., Lindsay, K., Matthews, H. D., Raddatz, T., Rayner, P., Reick, C., Roeckner, E., Schnitzler, K.-G., Schnur, R., Strassmann, K., Weaver, A. J., Yoshikawa, C., and Zeng, N. (2006). Climate–Carbon Cycle Feedback Analysis: Results from the C4mip Model Intercomparison. *Journal of Climate*, 19(14):3337–3353.

Friedlingstein, P., Jones, M. W., O'Sullivan, M., Andrew, R. M., Hauck, J., Peters, G. P., Peters, W., Pongratz, J., Sitch, S., Quéré, C. L., Bakker, D. C. E., Canadell, J. G., Ciais, P., Jackson, R. B., Anthoni, P., Barbero, L., Bastos, A., Bastrikov, V., Becker, M., Bopp, L., Buitenhuis, E., Chandra, N., Chevallier, F., Chini, L. P., Currie, K. I., Feely, R. A., Gehlen, M., Gilfillan, D., Gkritzalis, T., Goll, D. S., Gruber, N., Gutekunst, S., Harris, I., Haverd, V., Houghton, R. A., Hurtt, G., Ilyina, T., Jain, A. K., Joetzjer, E., Kaplan, J. O., Kato, E., Klein Goldewijk, K., Korsbakken, J. I., Landschützer, P., Lauvset, S. K., Lefèvre, N., Lenton, A., Lienert, S., Lombardozzi, D., Marland, G., McGuire, P. C.,

Melton, J. R., Metzl, N., Munro, D. R., Nabel, J. E. M. S., Nakaoka, S.-I., Neill, C., Omar, A. M., Ono, T., Peregon, A., Pierrot, D., Poulter, B., Rehder, G., Resplandy, L., Robertson, E., Rödenbeck, C., Séférian, R., Schwinger, J., Smith, N., Tans, P. P., Tian, H., Tilbrook, B., Tubiello, F. N., Werf, G. R. v. d., Wiltshire, A. J., and Zaehle, S. (2019). Global Carbon Budget 2019. *Earth System Science Data*, 11(4):1783–1838.

Friedlingstein, P., Meinshausen, M., Arora, V. K., Jones, C. D., Anav, A., Liddicoat, S. K., and Knutti, R. (2013). Uncertainties in CMIP5 Climate Projections due to Carbon Cycle Feedbacks. *Journal of Climate*, 27(2):511–526.

Friedlingstein, P. and Prentice, I. (2010). Carbon–climate feedbacks: a review of model and observation based estimates. *Current Opinion in Environmental Sustainability*, 2(4):251–257.

Gregory, J. M., Jones, C. D., Cadule, P., and Friedlingstein, P. (2009). Quantifying Carbon Cycle Feedbacks. *Journal of Climate*, 22(19):5232–5250.

Gurney, K. R., Mendoza, D. L., Zhou, Y., Fischer, M. L., Miller, C. C., Geethakumar, S., and de la Rue du Can, S. (2009). High Resolution Fossil Fuel Combustion CO2 Emission Fluxes for the United States. *Environmental Science & Technology*, 43(14):5535–5541.

Haines, A. and Patz, J. A. (2004). Health Effects of Climate Change. *JAMA*, 291(1):99–103.

Hassani, H., Silva, E. S., Gupta, R., and Das, S. (2018). Predicting global temperature anomaly: A definitive investigation using an ensemble of twelve competing forecasting models. *Physica A: Statistical Mechanics and its Applications*, 509:121–139.

Hoffman, F. M., Randerson, J. T., Arora, V. K., Bao, Q., Cadule, P., Ji, D., Jones, C. D., Kawamiya, M., Khatiwala, S., Lindsay, K., Obata, A., Shevliakova, E., Six, K. D., Tjiputra, J. F., Volodin, E. M., and Wu, T. (2014). Causes and implications of persistent atmospheric carbon dioxide biases in Earth System Models. *Journal of Geophysical Research: Biogeosciences*, 119(2):141–162.

Hooss, G., Voss, R., Hasselmann, K., Maier-Reimer, E., and Joos, F. (2001). A nonlinear impulse response model of the coupled carbon cycle-climate system (NICCS). *Climate Dynamics*, 18(3-4):189–202.

Hsiang, S., Kopp, R., Jina, A., Rising, J., Delgado, M., Mohan, S., Rasmussen, D. J., Muir-Wood, R., Wilson, P., Oppenheimer, M., Larsen, K., and Houser, T. (2017). Estimating economic damage from climate change in the United States. *Science*, 356(6345):1362–1369.

Isaac, M. and van Vuuren, D. P. (2009). Modeling global residential sector energy demand for heating and air conditioning in the context of climate change. *Energy Policy*, 37(2):507–521.

Janssen, M. L. and Hall, G. L. (1980). Effect of Ambient Temperature on Radial Tire Rolling Resistance. Technical report, SAE International.

Johnson, V. H. (2002). Fuel used for vehicle air conditioning: a state-by-state thermal comfort-based approach. Technical Report 0148-7191, SAE Technical Paper.

Jones, A. D., Calvin, K. V., Shi, X., Di Vittorio, A. V., Bond-Lamberty, B., Thornton, P. E., and Collins, W. D. (2018). Quantifying Human-Mediated Carbon Cycle Feedbacks. *Geophysical Research Letters*, 45(20):11,370–11,379.

Jones, C., Robertson, E., Arora, V., Friedlingstein, P., Shevliakova, E., Bopp, L., Brovkin, V., Hajima, T., Kato, E., Kawamiya, M., Liddicoat, S., Lindsay, K., Reick, C. H., Roelandt, C., Segschneider, J., and Tjiputra, J. (2013). Twenty-First-Century Compatible CO2 Emissions and Airborne Fraction Simulated by CMIP5 Earth System Models under Four Representative Concentration Pathways. *Journal of Climate*, 26(13):4398–4413.

Kahn, M. E. (2005). The Death Toll from Natural Disasters: The Role of Income, Geography, and Institutions. *The Review of Economics and Statistics*, 87(2):271–284.

Kakaras, E., Doukelis, A., Prelipceanu, A., and Karellas, S. (2006). Inlet air cooling methods for gas turbine based power plants. *Journal of engineering for gas turbines and power*, 128(2):312–317.

Kemp, A. E. S. and Villareal, T. A. (2013). High diatom production and export in stratified waters – A potential negative feedback to global warming. *Progress in Oceanography*, 119:4–23.

Kjellstrom, T., Kovats, R. S., Lloyd, S. J., Holt, T., and Tol, R. S. J. (2009). The direct impact of climate change on regional labor productivity. *Archives of Environmental & Occupational Health*, 64(4):217–227.

Kolodzeij, M. and Kaufmann, R. K. (2014). Oil demand shocks reconsidered: A cointegrated vector autoregression. *Energy Economics*, 41:33–40.

Köne, A. Ç. and Büke, T. (2010). Forecasting of CO2 emissions from fuel combustion using trend analysis. *Renewable and Sustainable Energy Reviews*, 14(9):2906–2915.

Krause, R. M. (2011). An assessment of the greenhouse gas reducing activities being implemented in US cities. *Local Environment*, 16(2):193–211.

Krey, V., Masera, O., Blanford, G., Bruckner, T., Cooke, R., and Fisher-Vanden, K. (2014). *Climate Change 2014: Mitigation of Climate Change. Contribution of Working Group III to the Fifth Assessment Report of the Intergovernmental Panel on Climate Change*, chapter Annex II: Metrics & Methodology. Cambridge University Press, Cambridge, United Kingdom and New York, NY, USA.

Kriegler, E., Petermann, N., Krey, V., Schwanitz, V. J., Luderer, G., Ashina, S., Bosetti, V., Eom, J., Kitous, A., Méjean, A., Paroussos, L., Sano, F., Turton, H., Wilson, C., and Van Vuuren, D. P. (2015). Diagnostic indicators for integrated assessment models of climate policy. *Technological Forecasting and Social Change*, 90:45–61.

Kumar, M. (2010). A Time-Varying Parameter Vector Autoregression Model for Forecasting Emerging Market Exchange Rates. *International Journal of Economic Sciences and Applied Research*, III(2):21–39.

Lasslop, G., Coppola, A. I., Voulgarakis, A., Yue, C., and Veraverbeke, S. (2019). Influence of Fire on the Carbon Cycle and Climate. *Current Climate Change Reports*, 5(2):112–123.

Le Quéré, C., Andrew, R. M., Friedlingstein, P., Sitch, S., Hauck, J., Pongratz, J., Pickers, P. A., Korsbakken, J. I., Peters, G. P., Canadell, J. G., Arneth, A., Arora, V. K., Barbero, L., Bastos, A., Bopp, L., Chevallier, F., Chini, L. P., Ciais, P., Doney, S. C., Gkritzalis, T., Goll, D. S., Harris, I., Haverd, V., Hoffman, F. M., Hoppema, M., Houghton, R. A., Hurtt, G., Ilyina, T., Jain, A. K., Johannessen, T., Jones, C. D., Kato, E., Keeling, R. F., Goldewijk, K. K., Landschützer, P., Lefèvre, N., Lienert, S., Liu, Z., Lombardozzi, D., Metzl, N., Munro, D. R., Nabel, J. E. M. S., Nakaoka, S.-i., Neill, C., Olsen, A., Ono, T., Patra, P., Peregon, A., Peters, W., Peylin, P., Pfeil, B., Pierrot, D., Poulter, B., Rehder, G., Resplandy, L., Robertson, E., Rocher, M., Rödenbeck, C., Schuster, U., Schwinger, J., Séférian, R., Skjelvan, I., Steinhoff, T., Sutton, A., Tans, P. P., Tian, H., Tilbrook, B., Tubiello, F. N., van der Laan-Luijkx, I. T., van der Werf, G. R., Viovy, N., Walker, A. P., Wiltshire, A. J., Wright, R., Zaehle, S., and Zheng, B. (2018). Global Carbon Budget 2018. *Earth System Science Data*, 10:2141–2194.

Libecap, G. D. and Steckel, R. H. (2011). *The Economics of Climate Change: Adaptations Past and Present*. University of Chicago Press.

Liu, Y., Roberts, M. C., and Sioshansi, R. (2018). A vector autoregression weather model for electricity supply and demand modeling. *Journal of Modern Power Systems and Clean Energy*, 6(4):763–776.

Lohse-Busch, H., Duoba, M., Rask, E., Stutenberg, K., Gowri, V., Slezak, L., and Anderson, D. (2013). Ambient Temperature (20 °F, 72 °F and 95 °F) Impact on Fuel and Energy Consumption for Several Conventional Vehicles, Hybrid and Plug-In Hybrid Electric Vehicles and Battery Electric Vehicle. Technical report, SAE International.

Lombardozzi, D. L., Bonan, G. B., Smith, N. G., Dukes, J. S., and Fisher, R. A. (2015). Temperature acclimation of photosynthesis and respiration: A key uncertainty in the carbon cycle-climate feedback. *Geophysical Research Letters*, 42(20):8624–8631.

Long, S. P., Ainsworth, E. A., Leakey, A. D. B., Nösberger, J., and Ort, D. R. (2006). Food for Thought: Lower-Than-Expected Crop Yield Stimulation with Rising CO_2 Concentrations. *Science*, 312(5782):1918–1921.

Lopes, C., Kucera, M., and Mix, A. C. (2015). Climate change decouples oceanic primary and export productivity and organic carbon burial. *Proceedings of the National Academy of Sciences*, 112(2):332–335.

Lu, X., Kicklighter, D. W., Melillo, J. M., Reilly, J. M., and Xu, L. (2015). Land carbon sequestration within the conterminous United States: Regional- and state-level analyses. *Journal of Geophysical Research: Biogeosciences*, 120(2):379–398.

Lüthi, D., Le Floch, M., Bereiter, B., Blunier, T., Barnola, J.-M., Siegenthaler, U., Raynaud, D., Jouzel, J., Fischer, H., Kawamura, K., et al. (2008). High-resolution carbon dioxide concentration record 650,000–800,000 years before present. *Nature*, 453(7193):379.

Lutsey, N. and Sperling, D. (2008). America's bottom-up climate change mitigation policy. *Energy Policy*, 36(2):673–685.

Magazzino, C. (2016). CO2 emissions, economic growth, and energy use in the Middle East countries: A panel VAR approach. *Energy Sources, Part B: Economics, Planning, and Policy*, 11(10):960–968.

Mahowald, N. M., Randerson, J. T., Lindsay, K., Munoz, E., Doney, S. C., Lawrence, P., Schlunegger, S., Ward, D. S., Lawrence, D., and Hoffman, F. M. (2017). Interactions between land use change and carbon cycle feedbacks. *Global Biogeochemical Cycles*, 31(1):96–113.

McMichael, A. J., Woodruff, R. E., and Hales, S. (2006). Climate change and human health: present and future risks. *The Lancet*, 367(9513):859–869.

Meinshausen, M., Smith, S. J., Calvin, K., Daniel, J. S., Kainuma, M. L. T., Lamarque, J.-F., Matsumoto, K., Montzka, S. A., Raper, S. C. B., Riahi, K., Thomson, A., Velders, G. J. M., and Vuuren, D. P. P. v. (2011). The RCP greenhouse gas concentrations and their extensions from 1765 to 2300. *Climatic Change*, 109(1-2):213.

Meng, M., Fu, Y., and Wang, X. (2018). Decoupling, decomposition and forecasting analysis of China's fossil energy consumption from industrial output. *Journal of Cleaner Production*, 177:752–759.

Mideksa, T. K. and Kallbekken, S. (2010). The impact of climate change on the electricity market: A review. *Energy Policy*, 38(7):3579–3585.

Mohanty, B. and Paloso, G. (1995). Enhancing gas turbine performance by intake air cooling using an absorption chiller. *Heat Recovery Systems and CHP*, 15(1):41–50.

Monnin, E., Indermühle, A., Dällenbach, A., Flückiger, J., Stauffer, B., Stocker, T. F., Raynaud, D., and Barnola, J.-M. (2001). Atmospheric CO2 Concentrations over the Last Glacial Termination. *Science*, 291(5501):112–114.

Montañez, I. P., McElwain, J. C., Poulsen, C. J., White, J. D., DiMichele, W. A., Wilson, J. P., Griggs, G., and Hren, M. T. (2016). Climate, p CO 2 and terrestrial carbon cycle linkages during late Palaeozoic glacial–interglacial cycles. *Nature Geoscience*, 9(11):824–828.

Moore, J. K., Fu, W., Primeau, F., Britten, G. L., Lindsay, K., Long, M., Doney, S. C., Mahowald, N., Hoffman, F., and Randerson, J. T. (2018). Sustained climate warming drives declining marine biological productivity. *Science*, 359(6380):1139–1143.

Moss, R., Babiker, W., Brinkman, S., Calvo, E., Carter, T., Edmonds, J., Elgizouli, I., Emori, S., Erda, L., Hibbard, K., Jones, R. N., Kainuma, M., Kelleher, J., Lamarque, J. F., Manning, M., Matthews, B., Meehl, J., Meyer, L., Mitchell, J., Nakicenovic, N., ONeill, B., Pichs, R., Riahi, K., Rose, S., Stouffer, R., van Vuuren, D., Weyant, J., Wilbanks, T., vanYpersele, J. P., and Zurek, M. (2008). *Towards New Scenarios for the Analysis of Emissions: Climate Change, Impacts and Response Strategies*. Intergovernmental Panel on Climate Change Secretariat (IPCC), Geneva, Switzerland.

Moss, R. H., Edmonds, J. A., Hibbard, K. A., Manning, M. R., Rose, S. K., van Vuuren, D. P., Carter, T. R., Emori, S., Kainuma, M., Kram, T., Meehl, G. A., Mitchell, J. F. B., Nakicenovic, N., Riahi, K., Smith, S. J., Stouffer, R. J., Thomson, A. M., Weyant, J. P., and Wilbanks, T. J. (2010). The next generation of scenarios for climate change research and assessment. *Nature; London*, 463(7282):747–56.

Myhre, G., Highwood, E. J., Shine, K. P., and Stordal, F. (1998). New estimates of radiative forcing due to well mixed greenhouse gases. *Geophysical Research Letters*, 25(14):2715–2718.

Myhre, G., Shindell, D., Bréon, F.-M., Collins, W., Fuglestvedt, J., Huang, J., Koch, D., and et al. (2013). *Climate Change 2013: The Physical Science Basis: Working Group I Contribution to the Fifth Assessment Report of the Intergovernmental Panel on Climate Change*, chapter Anthropogenic and Natural Radiative Forcing. Cambridge University Press, Cambridge, United Kingdom and New York, NY, USA.

Nordhaus, W. D. (2017). Revisiting the social cost of carbon. *Proceedings of the National Academy of Sciences*, 114(7):1518–1523.

O'Connor, F. M., Boucher, O., Gedney, N., Jones, C. D., Folberth, G. A., Coppell, R., Friedlingstein, P., Collins, W. J., Chappellaz, J., Ridley, J., and Johnson, C. E. (2010). Possible role of wetlands, permafrost, and methane hydrates in the methane cycle under future climate change: A review. *Reviews of Geophysics*, 48(4).

Oda, T., Maksyutov, S., and Andres, R. J. (2018). The Open-source Data Inventory for Anthropogenic CO_2, version 2016 (ODIAC2016): a global monthly fossil fuel CO_2 gridded emissions data product for tracer transport simulations and surface flux inversions. *Earth System Science Data*, 10(1):87–107.

Oeschger, H., Siegenthaler, U., Schotterer, U., and Gugelmann, A. (1975). A box diffusion model to study the carbon dioxide exchange in nature. *Tellus*, 27(2):168–192.

Organization for Economic Co-operation and Development (2019). Consumer Price Index: Total All Items for the United States.

Otto, I. M., Reckien, D., Reyer, C. P. O., Marcus, R., Masson, V. L., Jones, L., Norton, A., and Serdeczny, O. (2017). Social vulnerability to climate change: a review of concepts and evidence. *Regional Environmental Change*, 17(6):1651–1662.

Pao, H.-T., Fu, H.-C., and Tseng, C.-L. (2012). Forecasting of CO2 emissions, energy consumption and economic growth in China using an improved grey model. *Energy*, 40(1):400–409.

Patnaik, A. (2010). Study of Inflation in India: A Cointegrated Vector Autoregression Approach. *Journal of Quantitative Economics*, 8(1).

Pedersen, B. P. and Larsen, J. (2009). Modeling of ship propulsion performance. Technical report, Institute of Marine Engineers, Mumbai, India.

Pendleton, L., Donato, D. C., Murray, B. C., Crooks, S., Jenkins, W. A., Sifleet, S., Craft, C., Fourqurean, J. W., Kauffman, J. B., Marbà, N., Megonigal, P., Pidgeon, E., Herr, D., Gordon, D., and Baldera, A. (2012). Estimating Global "Blue Carbon" Emissions from Conversion and Degradation of Vegetated Coastal Ecosystems. *PLOS ONE*, 7(9):e43542.

Peters, G. P., Andrew, R. M., Canadell, J. G., Fuss, S., Jackson, R. B., Korsbakken, J. I., Le Quéré, C., and Nakicenovic, N. (2017). Key indicators to track current progress and future ambition of the Paris Agreement. *Nature Climate Change*, 7(2):118–122.

Raupach, M. R., Marland, G., Ciais, P., Quéré, C. L., Canadell, J. G., Klepper, G., and Field, C. B. (2007). Global and regional drivers of accelerating CO2 emissions. *Proceedings of the National Academy of Sciences*, 104(24):10288–10293.

Raymond, P. A., Saiers, J. E., and Sobczak, W. V. (2016). Hydrological and biogeochemical controls on watershed dissolved organic matter transport: pulse-shunt concept. *Ecology*, 97(1):5–16.

Repice, R. (2019). Monthly Energy Review. Technical Report DOE/EIA0035, U.S. Energy Information Administration.

Riahi, K., van Vuuren, D. P., Kriegler, E., Edmonds, J., O'Neill, B. C., Fujimori, S., Bauer, N., Calvin, K., Dellink, R., Fricko, O., Lutz, W., Popp, A., Cuaresma, J. C., Kc, S., Leimbach, M., Jiang, L., Kram, T., Rao, S., Emmerling, J., Ebi, K., Hasegawa, T., Havlik, P., Humpenöder, F., Da Silva, L. A., Smith, S., Stehfest, E., Bosetti, V., Eom, J., Gernaat, D., Masui, T., Rogelj, J., Strefler, J., Drouet, L., Krey, V., Luderer, G., Harmsen, M., Takahashi, K., Baumstark, L., Doelman, J. C., Kainuma, M., Klimont, Z., Marangoni, G., Lotze-Campen, H., Obersteiner, M., Tabeau, A., and Tavoni, M. (2017). The Shared Socioeconomic Pathways and their energy, land use, and greenhouse gas emissions implications: An overview. *Global Environmental Change*, 42:153–168.

Rose, A. (2004). Defining and measuring economic resilience to disasters. *Disaster Prevention and Management: An International Journal*, 13(4):307–314.

Roson, R. and van der Mensbrugghe, D. (2012). Climate change and economic growth: impacts and interactions. *International Journal of Sustainable Economy*, 4(3):270–285.

Ruppel, C. D. and Kessler, J. D. (2017). The interaction of climate change and methane hydrates. *Reviews of Geophysics*, 55(1):126–168.

Santamouris, M., Cartalis, C., Synnefa, A., and Kolokotsa, D. (2015). On the impact of urban heat island and global warming on the power demand and electricity consumption of buildings—A review. *Energy and Buildings*, 98:119–124.

Sathaye, J., Dale, L., Larsen, P., Fitts, G., Koy, K., Lewis, S., and Lucena, A. (2011). Estimating Risk to California Energy Infrastructure from Projected Climate Change. Technical Report LBNL-4967E, Ernest Orlando Lawrence Berkeley National Laboratory, Berkeley, CA (US).

Schuur, E. a. G., McGuire, A. D., Schädel, C., Grosse, G., Harden, J. W., Hayes, D. J., Hugelius, G., Koven, C. D., Kuhry, P., Lawrence, D. M., Natali, S. M., Olefeldt, D., Romanovsky, V. E., Schaefer, K., Turetsky, M. R., Treat, C. C., and Vonk, J. E. (2015). Climate change and the permafrost carbon feedback. *Nature*, 520(7546):171–179.

Schwinger, J., Tjiputra, J. F., Heinze, C., Bopp, L., Christian, J. R., Gehlen, M., Ilyina, T., Jones, C. D., Salas-Mélia, D., Segschneider, J., Séférian, R., and Totterdell, I. (2014). Nonlinearity of Ocean Carbon Cycle Feedbacks in CMIP5 Earth System Models. *Journal of Climate*, 27(11):3869–3888.

Shahin, M. A., Ali, M. A., and Ali, A. B. M. S. (2014). Vector Autoregression (VAR) Modeling and Forecasting of Temperature, Humidity, and Cloud Coverage. In Islam, T., Srivastava, P. K., Gupta, M., Zhu, X., and Mukherjee, S., editors, *Computational Intelligence Techniques in Earth and Environmental Sciences*, pages 29–51. Springer Netherlands, Dordrecht.

Shakun, J. D. and Carlson, A. E. (2010). A global perspective on Last Glacial Maximum to Holocene climate change. *Quaternary Science Reviews*, 29(15):1801–1816.

Siegenthaler, U., Stocker, T. F., Monnin, E., Lüthi, D., Schwander, J., Stauffer, B., Raynaud, D., Barnola, J.-M., Fischer, H., Masson-Delmotte, V., and Jouzel, J. (2005). Stable Carbon Cycle-Climate Relationship During the Late Pleistocene. *Science*, 310(5752):1313–1317.

Silva, E. S. (2013). A combination forecast for energy-related co2 emissions in the united states. *International Journal of Energy and Statistics*, 01(04):269–279.

Smil, V. (2010). *Energy Transitions: History, Requirements, Prospects*. ABC-CLIO. Google-Books-ID: vLuT4BS_25MC.

Smith, T. M., Reynolds, R. W., Peterson, T. C., and Lawrimore, J. (2008). Improvements to NOAA's Historical Merged Land–Ocean Surface Temperature Analysis (1880–2006). *Journal of Climate*, 21(10):2283–2296.

Suarez, C. A., Edmonds, M., and Jones, A. P. (2019). Earth Catastrophes and their Impact on the Carbon Cycle. *Elements*, 15(5):301–306.

Thornton, P. E., Calvin, K., Jones, A. D., Di Vittorio, A. V., Bond-Lamberty, B., Chini, L., Shi, X., Mao, J., Collins, W. D., Edmonds, J., Thomson, A., Truesdale, J., Craig, A., Branstetter, M. L., and Hurtt, G. (2017). Biospheric feedback effects in a synchronously coupled model of human and Earth systems. *Nature Climate Change*, 7(7):496–500.

Tian, H., Yang, Q., Najjar, R. G., Ren, W., Friedrichs, M. A. M., Hopkinson, C. S., and Pan, S. (2015). Anthropogenic and climatic influences on carbon fluxes from eastern North America to the Atlantic Ocean: A process-based modeling study. *Journal of Geophysical Research: Biogeosciences*, 120(4):757–772.

Toggweiler, J. R. and Russell, J. (2008). Ocean circulation in a warming climate. *Nature*, 451(7176):286–288.

Tol, R. S. (2009). The economic effects of climate change. *The Journal of Economic Perspectives*, 23(2):29–51.

Torres, M. A., Moosdorf, N., Hartmann, J., Adkins, J. F., and West, A. J. (2017). Glacial weathering, sulfide oxidation, and global carbon cycle feedbacks. *Proceedings of the National Academy of Sciences*, 114(33):8716–8721.

Tréguer, P., Bowler, C., Moriceau, B., Dutkiewicz, S., Gehlen, M., Aumont, O., Bittner, L., Dugdale, R., Finkel, Z., Iudicone, D., Jahn, O., Guidi, L., Lasbleiz, M., Leblanc, K., Levy, M., and Pondaven, P. (2018). Influence of diatom diversity on the ocean biological carbon pump. *Nature Geoscience*, 11(1):27.

United Nations Department of Economic and Social Affairs, Population Division (2015). World Population Prospects: The 2015 Revision, DVD Edition. Technical report.

U.S. Census Bureau (2019). US Population by Month.

U.S. Energy Information Administration (2016). International Energy Outlook. Technical report, U.S. Department of Energy.

U.S. Energy Information Administration (2019). U.S. Natural Gas Citygate Price (Dollars per Thousand Cubic Feet).

Valentine, D. L., Kessler, J. D., Redmond, M. C., Mendes, S. D., Heintz, M. B., Farwell, C., Hu, L., Kinnaman, F. S., Yvon-Lewis, S., Du, M., Chan, E. W., Tigreros, F. G., and Villanueva, C. J. (2010). Propane Respiration Jump-Starts Microbial Response to a Deep Oil Spill. *Science*, 330(6001):208–211.

van der Mensbrugghe, D. (2010). Technical reference guide for ENVISAGE.

van Vuuren, D. P., Edmonds, J., Kainuma, M., Riahi, K., Thomson, A., Hibbard, K., Hurtt, G. C., Kram, T., Krey, V., Lamarque, J.-F., Masui, T., Meinshausen, M., Nakicenovic, N., Smith, S. J., and Rose, S. K. (2011). The representative concentration pathways: an overview. *Climatic Change*, 109(1):5.

Weitzman, M. L. (2012). GHG Targets as Insurance Against Catastrophic Climate Damages. *Journal of Public Economic Theory*, 14(2):221–244.

Wen, L. and Zhang, X. (2018). CO2 Emissions in China's Yangtze River Economic Zone: A Dynamic Vector Autoregression Approach. *Polish Journal of Environmental Studies*, 28(2):923–933.

Weyant, J. (2017). Some Contributions of Integrated Assessment Models of Global Climate Change. *Review of Environmental Economics and Policy*, 11(1):115–137.

Woodard, D. L., Davis, S. J., and Randerson, J. T. (2019). Economic carbon cycle feedbacks may offset additional warming from natural feedbacks. *Proceedings of the National Academy of Sciences*, 116(3):759–764.

World Bank national accounts data and OECD national accounts data files (2015). GDP (Constant 2005 US$). Technical report, The World Bank.

World Health Organization (2014). *Quantitative risk assessment of the effects of climate change on selected causes of death, 2030s and 2050s*. World Health Organization.

Wu, L., Liu, S., Liu, D., Fang, Z., and Xu, H. (2015). Modelling and forecasting CO2 emissions in the BRICS (Brazil, Russia, India, China, and South Africa) countries using a novel multi-variable grey model. *Energy*, 79:489–495.

Xiumei, S., Min, Z., and Ming, Z. (2011). Empirical Study on the Relationship between Economic Growth and Carbon Emissions in Resource-dependent Cities Based on Vector Autoregression Model. *Energy Procedia*, 5:2461–2467.

Xu, B. and Lin, B. (2016a). Assessing CO2 emissions in China's iron and steel industry: A dynamic vector autoregression model. *Applied Energy*, 161:375–386.

Xu, B. and Lin, B. (2016b). Reducing carbon dioxide emissions in China's manufacturing industry: a dynamic vector autoregression approach. *Journal of Cleaner Production*, 131:594–606.

YvonLewis, S. A., Hu, L., and Kessler, J. (2011). Methane flux to the atmosphere from the Deepwater Horizon oil disaster. *Geophysical Research Letters*, 38(1).

Zaehle, S., Jones, C. D., Houlton, B., Lamarque, J.-F., and Robertson, E. (2014). Nitrogen Availability Reduces CMIP5 Projections of Twenty-First-Century Land Carbon Uptake. *Journal of Climate*, 28(6):2494–2511.

Zahabi, S. A. H., Miranda-Moreno, L., Barla, P., and Vincent, B. (2014). Fuel economy of hybrid-electric versus conventional gasoline vehicles in real-world conditions: A case study of cold cities in Quebec, Canada. *Transportation Research Part D: Transport and Environment*, 32:184–192.

Zhou, T., Shi, P., Hui, D., and Luo, Y. (2009). Global pattern of temperature sensitivity of soil heterotrophic respiration (Q10) and its implications for carbon-climate feedback. *Journal of Geophysical Research: Biogeosciences*, 114(G2).

Zhou, Y., Clarke, L., Eom, J., Kyle, P., Patel, P., Kim, S. H., Dirks, J., Jensen, E., Liu, Y., Rice, J., Schmidt, L., and Seiple, T. (2014). Modeling the effect of climate change on U.S. state-level buildings energy demands in an integrated assessment framework. *Applied Energy*, 113:1077–1088.

Zhu, P., Zhuang, Q., Ciais, P., Welp, L., Li, W., and Xin, Q. (2017). Elevated atmospheric CO2 negatively impacts photosynthesis through radiative forcing and physiology-mediated climate feedback. *Geophysical Research Letters*, 44(4):1956–1963.

Zickfeld, K., Eby, M., Matthews, H. D., Schmittner, A., and Weaver, A. J. (2011). Nonlinearity of Carbon Cycle Feedbacks. *Journal of Climate*, 24(16):4255–4275.

Appendix A
Supplementary Methods for Chapter 2

A.1 Carbon cycle box model

Our analysis was based on a simple box model of the natural carbon cycle, onto which we added a temperature-sensitivity of fossil fuel emissions to account for economic carbon-climate dynamics. We constructed this base model using a single land pool, as well as a mixed layer and a deep ocean pools, and we included important natural carbon-concentration and carbon-climate feedbacks (Fig. 2.1, Table A.4). To improve accuracy of the natural carbon cycle, we tuned the model to CMIP5 multi-model mean output from previous analyses (Table A.5) and found that the tuned model was able to reproduce historical fluxes, though a weaker ocean uptake resulted in somewhat overestimating the atmospheric CO_2 growth rate (Fig. A.1B). Nevertheless, our cumulative results are within one standard deviation of the historical data up to 2005 (Friedlingstein et al., 2013). To estimate uncertainty on this model we tuned a 1% idealized run of our model to the CMIP5 multi-model mean gain found by Arora et al. (2013) plus one standard deviation and minus one standard deviation for the upper and lower bounds, respectively.

We modeled the atmosphere as a single, well-mixed carbon reservoir (C_A) with inputs from fossil fuel emissions (F_{FF}), land use change (F_{LUC}), and net carbon exchange with the land (F_L) and ocean (F_O).

$$\frac{(dC_A)}{dt} = F_{FF} + F_{LUC} - F_L - F_O \tag{A.1}$$

Our land model included only a single carbon pool (C_L) with carbon uptake from net primary productivity (NPP) and losses to the atmosphere from heterotrophic respiration (R_h) and land use change.

$$\frac{dC_L}{dt} = F_L = NPP - R_h - LUC \tag{A.2}$$

We initialized NPP and R_h to 60 Pg C y^{-1} and used an initial turnover time of 15 years. Our modeled NPP includes both sensitivity to atmospheric CO_2 as well as a temperature coupling.

$$NPP = NPP_0(1 + B \cdot ln\frac{C_A}{C_A(0)}) \cdot (1 + a_{land} \cdot (\Delta T_{air})^2 + b_{land} \cdot \Delta T_{air}) \tag{A.3}$$

We estimated the influence of temperature on NPP by fitting a polynomial to the mean response of NPP from CMIP5 earth system model to global mean surface air temperature changes from the idealized esmFdbk1 scenario. The esmFdbk1 scenario includes only temperature-driven effects on the carbon cycle, so this calculation excludes the direct impact of atmospheric carbon dioxide concentrations on photosynthesis. We used a Q10 function to model the temperature sensitivity of heterotrophic respiration.

$$R_h = \frac{1}{\tau_b} \cdot Q10^{\frac{T_{air} - T_{air}(0)}{10}} \cdot C_L \tag{A.4}$$

We also added a sensitivity of the turnover time to land use change emissions in order to better match the dynamics of the observed land sink. For comparison, Erb et al. (2016) estimated a modern value of 0.51 for this effect of land use change on turnover time, while our value over the period from 2000 to 2010 is, on average, 0.84.

$$\tau_b = \tau_b(0) \cdot \frac{C_L(0) - \Sigma LUC}{C_L(0)} \tag{A.5}$$

Our ocean carbon cycle separately tracks mixed layer (C_{OM}) and deep ocean carbon (C_{OD}) pools and includes fluxes into each deep ocean box F_{ODi} and between the mixed layer and atmosphere (F_{AO} and FF_{OA}) and the mixed layer and deep ocean (F_{MD} and F_{DM}). The net ocean flux, F_O, is the difference between the atmosphere-ocean exchange fluxes, F_{AO} and F_{OA}.

$$\frac{dC_{OM}}{dt} = F_{AO} - F_{OA} + F_{DM} - F_{MD} \tag{A.6}$$

We used a global mean air-sea gas transfer velocity (k_{gas}) and the partial pressure difference of CO_2 between the atmosphere and the ocean mixed layer to estimate the net ocean-atmosphere carbon flux.

$$F_{AO} = k_{gas} \cdot \frac{C_A}{2.12} \tag{A.7}$$

$$F_{OA} = k_{gas} \cdot \frac{C_A(0)}{2.12} \cdot (1 + R \cdot \frac{C_{OM} - C_{OM}(0)}{C_{OM}(0)}) \tag{A.8}$$

The model included a Revelle factor (R) that was tuned to 11.5 to estimate the amount of anthropogenic CO_2 equilibrated with dissolved inorganic carbon at each time step. We represented fluxes in the deep ocean with a box diffusion model following Oeschger et al. (1975), though we used only 25 total deep ocean boxes and allowed our diffusivity constant K_{deep} to decrease linearly with depth starting from an initial value of 2500 yr^{-1} and reaching 125 yr^{-1} in the deepest box. We simulated temperature-driven stratification impacts on ocean carbon uptake by allowing the diffusivity constant to also vary as a function of temperature. The flux in box i is equal to the flux exchange between box j and the surrounding boxes i and k.

$$F_{ODj} = k_{ij} \cdot C_{ODi} - k_{ji} \cdot C_{OD} + k_{kj} \cdot C_{OD} - k_{jk} \cdot C_{ODj} \tag{A.9}$$

The deep ocean exchange parameter from any box i to the next lower box j is a function of the deep ocean diffusivity value K_{deep} and the box height h.

$$k_{ij} = K_{deep} \cdot \frac{1}{0.5 \cdot (h_j + h_i) \cdot h_i)} \tag{A.10}$$

The diffusivity value for the shallowest deep ocean box at time t is calculated by modifying the initial value for that parameter by the change in temperature at the current time step (Eqn. A.11) such that diffusivity slows with warming. The magnitude of the temperature effect on diffusivity is controlled by the parameter f_{mod}. Deeper ocean diffusivity values decrease proportional to the ocean depth down to a fixed lower bound K_{min} (Eqn. A.12).

$$K_{deep}(t) = K_{deep}(0) \cdot (1 - f_{mod} \cdot \Delta T) \tag{A.11}$$

$$K_{deep_i} = K_{deep}(t) - \frac{i \cdot (K_{deep}(t) - K_{min}}{nboxes} \tag{A.12}$$

In the absence of an economic carbon feedback, the model assumed fossil fuel and land use change emissions were exogenously defined by the business-as-usual representative concentration pathway (RCP8.5) (Moss et al., 2008, 2010). We initialized the model at a pre-industrial base temperature of 15 °C and 283 ppm of atmospheric CO_2 and iterated from 1800 to 2100 using a forward Euler integration scheme. The set of tuned parameters used in this model are given in Table A.4. The model computed radiative forcing at each time step (Myhre et al., 1998) and used an impulse response function (Hooss et al., 2001) fit to the mean CMIP5 earth system models 4xCO_2 experiment to obtain the consequent global mean surface air temperature change at each time step.

A.2 Simulation design

To add an economic carbon feedback to our natural model, we included a sensitivity of fossil fuel emissions, calculating a temperature-adjusted emissions term at each time step. Initially, we adjusted emissions from the baseline data by some fraction f_{FFT} in $^{\circ}C^{-1}$,

$$F_{FFadj} = F_{FFdata} + f_{FFT} \cdot \Delta T \cdot F_{FFdata} \tag{A.13}$$

where F_{FFdata} is the baseline RCP8.5 fossil fuel emissions data and F_{FFadj} is the calculated temperature-adjusted emissions. To derive Figure 2.4, we allowed f_{FFT} to vary over a wide range of values (shown along the x-axis of Figure 2.4) and calculated the carbon-climate gain from the model results. We tested both a linear and quadratic relationship with temperature, but the results were comparable over the range of f-values used in the simulation.

To analyze the impact on the carbon cycle from specific economic-temperature relationships from the literature, we designed a set of eight decoupled and coupled scenarios used in the rest of our analysis (Table A.1). The first two scenarios are similar to those used in the natural carbon cycle literature (for example Arora et al. 2013 and Friedlingstein et al. 2006). Our No Feedbacks scenario does not allow the land, ocean, and human modules to see increasing temperatures, so only carbon-concentration feedbacks are active. Our Net Natural scenario corresponds to the Fully-coupled scenario from previous literature on the natural carbon cycle, and all the natural carbon-climate and carbon-concentration feedbacks included in our model are activated in this scenario. In this case we refer to this scenario as 'Net Natural' because it only includes the natural carbon cycle feedbacks and does not include a coupling between fossil fuel emissions and temperature. We reserve the label 'Fully Coupled' in our analysis to refer to the scenario which includes both economic and natural carbon cycle feedbacks.

The four partially-coupled economic feedback scenarios in our model draw upon

synthesis described in the main text and in the following sections. We used the Kaya Identity (Eqn. 2.1) to isolate individual economic factors and their contribution to the feedback. Our 'Net Economic' scenario is the economic parallel to the 'Net Natural' scenario, representing the net impact of economic carbon-climate feedback drivers. This scenario includes only temperature effects on per capita GDP and on the carbon intensity of energy as a conservative estimate, in order to avoid potential double-counting of temperature effects on population and energy intensity of GDP that are already included in the relationship we used for GDP and temperature. We focused here only on the carbon-climate feedback, so the impact of an economic carbon-concentration feedback was not explicitly included in any scenario, though a carbon concentration feedback with crop yield could have the potential to offset some of the negative temperature impacts on GDP (Long et al., 2006).

As a baseline for socio-economic development we harmonized data from a combination of sources over the period from 1800 to 2100 (Fig. A.2, Table A.6). Our baseline future scenario data used throughout this analysis was from the business-as-usual RCP8.5 scenario (Moss et al., 2008, 2010). We assumed for simplicity that this baseline data did not already include any temperature-sensitivity, which is inaccurate for all historical data, but as our goal was a comparison with natural feedbacks the error introduced from this assumption should be relatively small. The assumption does hold true for future data since GCAM does not include any climate-emissions coupling.

It is additionally important to note that there are many more potential interactions between model terms than are considered here. We have focused in this analysis on isolating effects from each term to quantify the individual contributions, but in reality, energy, GDP, and population all may exert mutual influence on each other, and this and other more complex market dynamics will play a role in determining the overall size of an economic carbon feedback. The consideration of these effects is best suited for future analysis within integrated assessment models.

A.3 Estimating the gain of the climate-carbon feedback

We estimated the gain, g, of a carbon-climate feedback using the approach described by Friedlingstein et al. (2006) who used atmospheric carbon accumulation from an emissions-forced Fully-coupled (C_A^{FC}) and an uncoupled simulation (C_A^{UC}) to calculate this value, so that

$$g = \frac{\Delta C_A^{FC} - \Delta C_A^{UC}}{\Delta C_A^{FC}} \tag{A.14}$$

where C_A^{UC} and C_A^{FC} correspond to the change in atmospheric carbon in an emissions-forced simulation with and without carbon-climate feedbacks, respectively. To calculate the natural carbon-climate feedback gain we use

$$g = \frac{\Delta C_A^{netnatural} - \Delta C_A^{nofeedbacks}}{\Delta C_A^{netnatural}} \tag{A.15}$$

while to calculate the net economic carbon-climate feedback gain we use

$$g = \frac{\Delta C_A^{neteconomic} - \Delta C_A^{nofeedbacks}}{\Delta C_A^{neteconomic}} \tag{A.16}$$

The gain values in Figure 2.4 are calculated using a fully coupled scenario with all-natural carbon-climate feedbacks active and constant, while the strength of the economic feedback is allowed to vary over a range. When the economic feedback is zero, this is equivalent to our Net Natural scenario. When the strength of the economic feedback is at -3.1% change in emissions per °C, this is then equivalent to our Fully Coupled baseline scenario as used in the rest of the paper. This is calculated as

$$g = \frac{\Delta C_A^{fully-coupled} - \Delta C_A^{no-feedbacks}}{\Delta C_A^{fully-coupled}} \tag{A.17}$$

A.4 Climate-economy relationships

A.4.1 Influence of climate on population

Rising future temperatures are expected to increase human mortality due to extreme weather events, floods, diseases, heat stress, and food and water scarcity (McMichael et al., 2006; Haines and Patz, 2004). McMichael et al. estimated that from the combined effects of climate change 154,000 people died in the year 2000 alone, though the impacts vary widely by region, with southern Africa seeing the highest impacts and Europe, Russia, and most of North America experiencing the lowest (2006).

The literature indicates strongly that temperature has an inverse relationship with population, so we assigned this to a negative sign in Figure 2.1. Although some lives are saved due to relief from cold temperatures, the deaths from heat, drought, extreme weather events, fires, and other results of a warming planet are expected to dominate this feedback, keeping the overall sign of this relationship negative.

To model climate-related mortality as a function of climate warming, we used mid-century estimates of climate-induced mortality and global mean surface air temperature change. In a recent analysis, the World Health Organization estimated that 250,000 annual deaths would be attributable to climate change by 2030-2050 based on the future scenario SRES A1b (World Health Organization, 2014). This finding included deaths from heat exposure, diarrhea, malaria, and childhood undernutrition. We used the corresponding average temperature change between 2030 and 2050 projected under SRES A1B to calculate a linear sensitivity scalar, f_{PT} (199,283 deaths yr^{-1} $°C^{-1}$), of annual deaths per °C of warming. This scalar was used in the Population scenario in our model to calculate a temperature-adjusted population value at each time step by adding the net population change from the baseline scenario and subtracting the product of the temperature change and the population-temperature sensitivity scalar, f_{PT} (Fig A.3A). The new population value was then used to calculate the corresponding temperature-adjusted fossil fuel emissions based on the Kaya

Identity. All other components of the Kaya Identity were left at baseline values in this scenario.

A.4.2 Temperature impacts on per capita gross domestic product

We drew from the literature on integrated assessment model damage functions to understand the response of GDP to climate warming. Such damage functions include a variety of economic impacts including effects on sea level rise, tourism, heat stress, agriculture, human health, energy systems, and various other sectors. Due to climate change, resources will have to be diverted from research and development and investment in capital and instead put towards countering climate change impacts, while other key resources will be permanently lost including some ecosystems, species, and human lives (McMichael et al., 2006; Libecap and Steckel, 2011). There are also direct temperature impacts on human productivity, particularly in climate-exposed sectors of the economy such as construction and agriculture (Kjellstrom et al., 2009). A study by Roson *et al.* decomposed these climate impacts, finding the most significant to be heat stress, sea level rise, and tourism, with substantial regional variation in the relevance of other factors (2012). Based on the literature we expect this overall relationship between temperature and GDP to be negative, as no estimates we are aware of suggest a global net economic benefit from climate change. There may, however, be some regions that do see a different sign and experience an overall economic boost from global warming (Tol, 2009).

Our model used the damage function described in Burke et al. (2015) as a baseline estimate of the temperature sensitivity to climate warming (Fig. A.3B). Damage functions in many modern integrated assessment models place impacts at around one or two percent of GDP by the end of the century (Tol, 2009), but there has been little empirical basis for these estimates (Burke et al., 2016; Weitzman, 2012). The work by Burke et al. (2015) emerged from an attempt to unify micro and macro-level studies of climate damages and used historical economic data to develop a non-linear model of climate impacts on GDP. The

authors found that the sensitivity of GDP to climate warming may be considerably higher than predicted by other damage functions, estimating a 23% loss in global GDP by 2100. Although empirical estimates are subject to problems when going out of sample, there are no temperature changes projected over the next century under RCP8.5 that exceed the highest values of temperature anomalies already seen locally in various countries over the past half century (Burke et al., 2015).

We included the DICE2016 damage function as a lower bound in our model, modifying GDP levels at each time step by a loss of 0.236% per degree Celsius squared (Nordhaus, 2017). Our upper bound came from the highest impact scenario in the Burke et al. (2015) analysis. Because the Burke relationship includes effects of temperature on energy demand and climate mortality, these terms in the Kaya Identity are not included separately in our Fully Coupled scenario. However, for the sake of understanding their potential contributions we did analyze each in their own individual scenarios.

A.4.3 Temperature impact on the energy intensity of GDP

To estimate the impacts of climate warming on energy demand, we assessed changes in heating and air conditioning use. These two drivers respond in opposite directions to warming, with their net balance determining whether the overall impact of climate change yields a positive or negative effect on energy demand. In current integrated assessment models, energy impacts from climate change are considered primarily for residential heating and cooling.

As with the GDP-climate relationship, there is a wide variety of estimates of this energy demand-temperature sensitivity in available models. Of a set of IAMs reviewed by Ciscar and Dowling (2014), the results varied from estimating positive to negative overall economic effects from climate-driven changes in energy demand. Isaac and Van Vuuren used the model IMAGE to project future residential energy demand under climate change, estimating a 34% decrease in heating use and a 72% increase in air conditioning use by 2100, although they found the overall impacts to nearly balance on a global scale (2009).

Empirical estimates of these damages lean toward overall negative outcomes. For example, Santamouris et al. (2015) analyzed fifteen studies on the impact of temperature on electricity consumption, finding an increase of between 0.5% and 8.5% per °C. However, this sign could be driven positive if climate-driven reductions in heating use dominated over increases in air conditioning use.

We considered these energy demand effects in our model on the energy intensity of GDP term in the Kaya Identity (Energy Intensity scenario). We assumed that at a fixed economic output level, the energy demand associated with that output may increase or decrease based on a relationship with temperature. We adapted Isaac and Van Vuuren's model (2009) to calculate heating and cooling-driven energy demand in 14 different regions, which we then aggregated to global estimates of total residential energy demand. Heating energy demand is calculated based on a population, per capita floor area, population-weighted heating degree days, and useful energy heating efficiency, combined with a time-dependent parameter for the efficiency of heating broken down by energy carrier. Air conditioning energy demand is calculated from the number of households, the penetration of air conditioners in a region, and the unit energy consumption, combined with a time-dependent parameter for technological improvements. We ran this model with and without temperature sensitivity of energy demand turned on, and the difference of these two runs allowed us to isolate the climate impacts on residential energy demand from the purely economic and demographic ones. To account for the commercial sector, which has similar heating and cooling energy use, we increased this temperature relationship by 56% (U.S. Energy Information Administration, 2016). We then used a polynomial fit with temperature on the difference of these two scenario runs to model the overall sensitivity of energy demand to climate change (Eqn. A.18; Fig. A.3C).

$$E_{adj}(t) = E_{data}(t) - 0.74\Delta T(t)^3 + 6.77\Delta T(t)^2 - 7.25\Delta T(t) \tag{A.18}$$

In our box model, we used this relationship to calculate a temperature-adjusted

energy demand value at each time step from the baseline data. The subsequent temperature-adjusted fossil fuel emissions value is then calculated through the Kaya Identity, with all other terms held to baseline data. As a qualitative estimate of uncertainty, we used high and low bounds of +50% and -50% of our baseline estimate, recognizing that significant uncertainties exist in the current understanding of this relationship in the literature.

A.4.4 Temperature impact on carbon intensity of energy

Energy production may be vulnerable to climate change through several avenues. Thermo-electric power plants are sensitive to increasing air and water temperatures and lose efficiency as temperature rises (Sathaye et al., 2011; Basha et al., 2012; Burnard and Bhattacharya, 2011; Farouk et al., 2013; Mohanty and Paloso, 1995). Electricity distribution also loses efficiency due to changes in resistance of power lines (Santamouris et al., 2015), while the transportation sector may benefit somewhat due to decreased air resistance, despite negative effects on vehicle tire pressure and air conditioning use (Janssen and Hall, 1980; Lohse-Busch et al., 2013; Johnson, 2002; Pedersen and Larsen, 2009; Zahabi et al., 2014).

Climate impacts on energy production have consequences for the carbon intensity of energy in the future. If the same demand needs to be met, the response of energy production to climate warming leads to changes in the energy supplied per unit of fossil fuel emissions. Efficiency reductions with warming, for example, would lead to less energy output per unit of fossil fuel emissions. We assumed in this analysis that transportation and electricity production are the only temperature-sensitive components of the energy sector, and this temperature-sensitive fraction of primary energy is increasing over time as access to electricity and economic well-being increases (Fig. A.4A). As this temperature insensitive proportion decreases, the potential for a stronger effect of temperature on energy production increases. This may be offset by technological advances in efficiency, but the model here uses contemporary production efficiencies. As a result, the relevance of the climate response of energy production will grow over the next century.

In our model, we estimated a linear temperature relationship for each component of transportation and electricity production from the literature (Table A.7). Combining these impacts, the model reduces energy supply due to changes in power line resistance, thermoelectric power plant efficiency, and transportation efficiency at higher temperatures. For each of coal, oil, and natural gas electrical production the baseline portion of energy produced by that fuel type is adjusted by the production efficiency changes multiplied by the temperature change from preindustrial. This is then adjusted again by temperature-sensitive distribution losses. Transportation losses are estimated as the linear combination of truck, car, train, and boat temperature-sensitive efficiency changes. The upper and lower ranges from Table A.7 were used as upper and lower bounds for this analysis.

These various effects sum to a small net loss in energy supply, and thus a net increase in the carbon intensity of energy per degree of warming (Fig. A.3D). This sign of the response of carbon intensity of energy to temperature could be driven negative if future technological changes reduced the vulnerability of thermoelectric power plants and electricity distribution systems to temperature such that transportation efficiency improvements dominated the overall feedback.

Separating out the electricity component, Fig. A.4B shows the relative contribution of each to the overall climate-driven losses in electricity production. Coal dominated this feedback because it is the largest fraction of fossil fuel electricity production, which suggests that improvements in the cooling efficiency of coal fired power plants would play a significant role in reducing this impact in the future.

Future changes in water availability and likelihood of extreme weather events are also potential contributors to climate impacts on energy production in thermoelectric power plants, but these were ignored in our model for simplicity. The inclusion of this effect would likely strengthen the carbon intensity of energy feedback. We also did not include any temperature-related changes to primary energy supply such as oil refining or natural gas extraction, since these are more directly affected by extreme weather events than by rising

temperatures, and extreme weather events were not included in our model.

Renewable energy production is likely to see impacts from climate change as well (Mideksa and Kallbekken, 2010), but these energy sources were not included in our model. We made the simplifying assumption that temperature-related losses in energy supply were replaced by increased production of that same energy source, meaning that changes in renewable energy production would not significantly impact fossil fuel emissions. If changes in renewable capacity are replaced by fossil fuels instead this would increase the strength of the carbon intensity feedback, but if, on the other hand losses, in fossil fuels are replaced by more renewables, it would be expected to decrease.

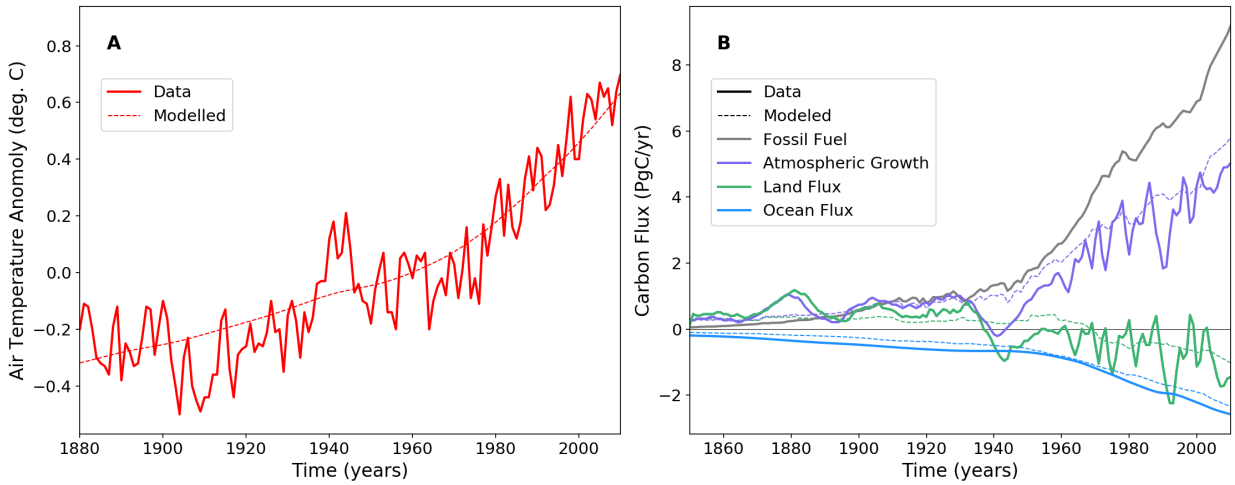

Figure A.1: Comparison of historical data to model results. Panel A shows our modeled temperature curve (solid) against historical data (dashed). Panel B compares model results (dashed) with all included ocean and land carbon cycle feedbacks against observed fluxes (solid) over the past two centuries. Observed air temperature anomaly data is from NOAA (Smith et al., 2008) , atmospheric CO_2 data is from the RCP8.5 historical data archives (Meinshausen et al., 2011), while data for the observed ocean and residual land sink is from Hoffman *et al.* (2014).

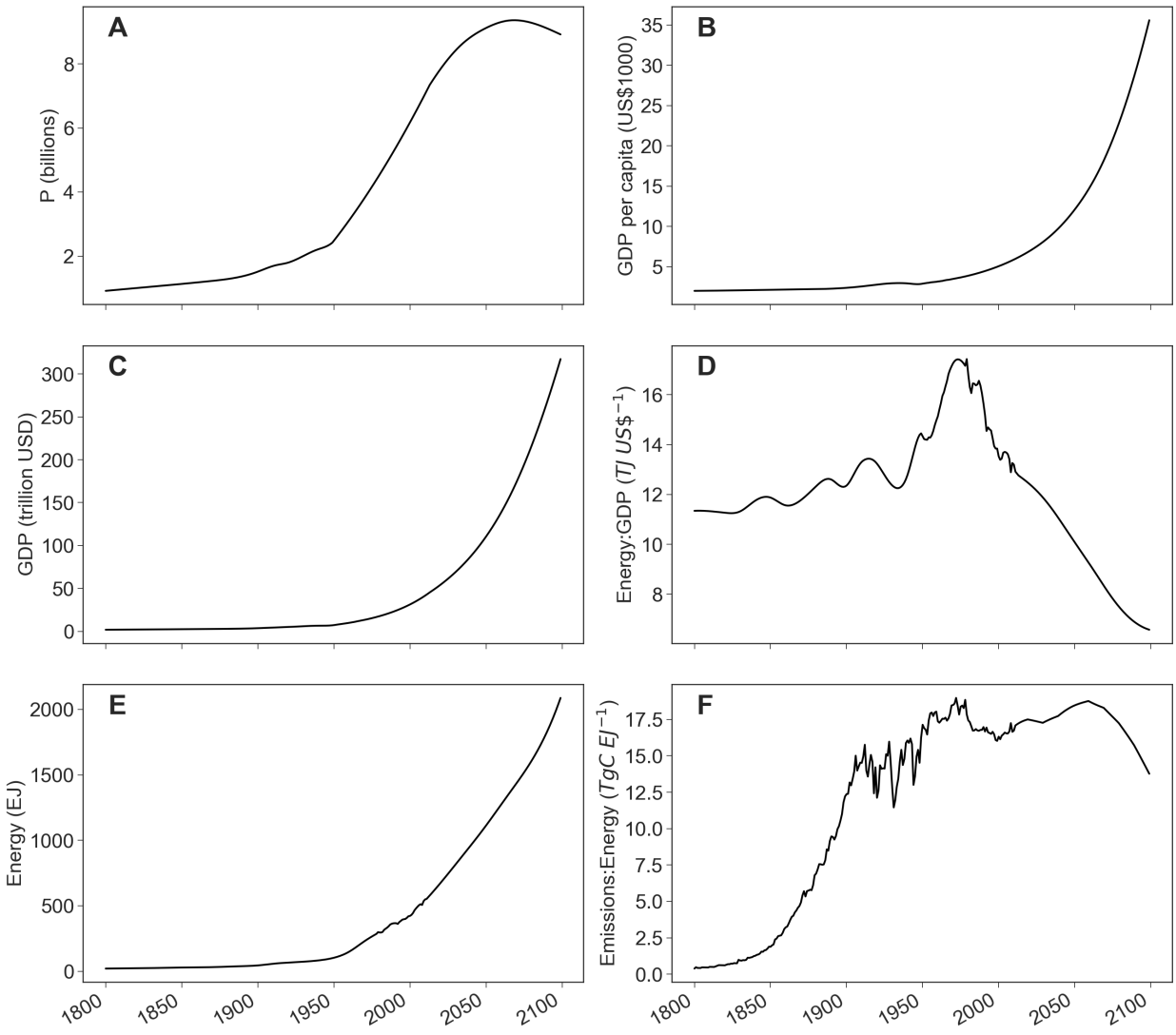

Figure A.2: Breakdown of the Kaya Identity and socioeconomic data used to calculate it. The left column presents the harmonized socioeconomic data used in the model, while the right shows the three calculated components of the Kaya Identity: per capita GDP, energy intensity of GDP, and carbon intensity of energy. The data sources for this figure are described in Table A.6.

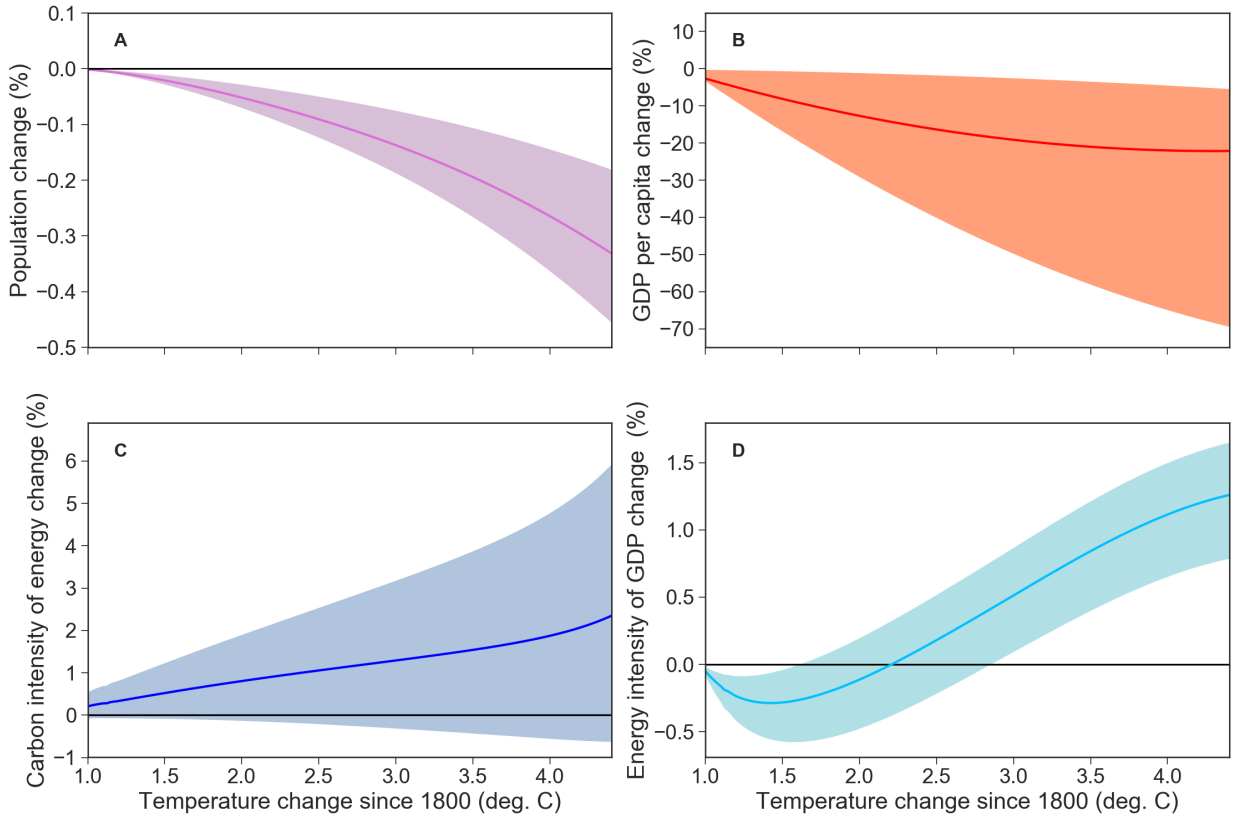

Figure A.3: Temperature relationships for each economic model component. We used the Net Natural scenario in our model under RCP8.5 to adjust each component by temperature at each time step without any economic feedback to fossil fuel emissions. Temperature changes are given from 1800 - 2100 for the RCP8.5 scenario. Overall energy supply decreased with temperature, causing carbon intensity of energy to increase with temperature, contributing to a positive feedback effect. Higher temperature increased energy demand, and thus energy intensity of GDP, which also created a positive feedback in our model. Climate mortality created a very slight negative relationship between population and temperature, contributing to a negative feedback effect. Upper and lower bounds are 50% on population and energy demand effects, for energy supply and GDP upper and lower bounds were taken from the literature. Climate damages to GDP represent the most significant relationship, but also the widest spread. The maximum impact shown was calculated using the highest impact scenario from Burke *et al.* (2015), while the minimum used the DICE2016 damage function (Nordhaus, 2017).

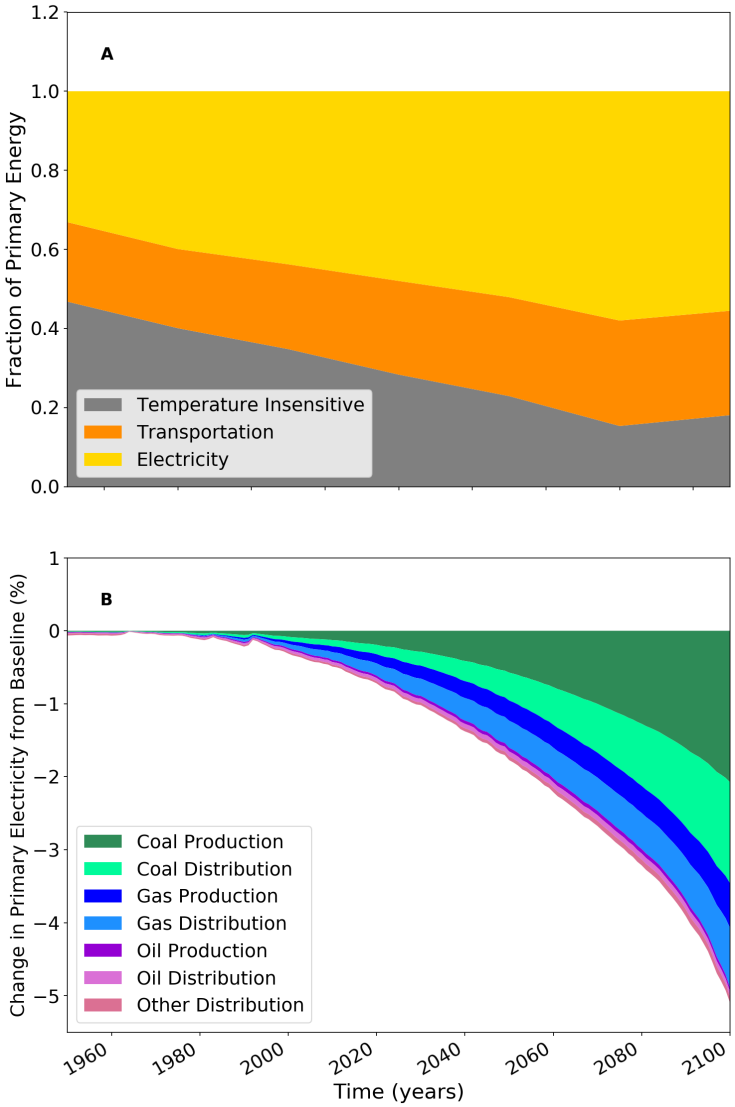

Figure A.4: Change in the future fraction of temperature-sensitive primary energy and breakdown of electricity production component drivers in our model. Panel **A** shows fractional change in the proportions of primary energy in GCAM data. We assumed that the two colored components, transportation and electricity production, were temperature-sensitive in our model. All other components of primary energy are lumped into the gray 'Temperature Insensitive' portion shown. Panel **B** shows the individual effects on each component of the electricity production feedback with temperature under RCP8.5. Coal, oil, and natural gas thermoelectric power generation were separated from the temperature-driven impacts on electricity distribution for each component. While the distribution losses per degree are the same across fuel types, the fraction of energy being distributed by each fuel type differed in our model. 'Other distribution' refers to temperature-related electricity distribution losses incurred from any other carbon-emitting fuel source. Renewables were not included in this analysis, because we made the simplifying assumption that losses in fossil fuel-based electricity production were replaced by increasing production of electricity from a fossil fuel source and similarly, renewable losses were replaced by renewables. In other words, like replaced like.

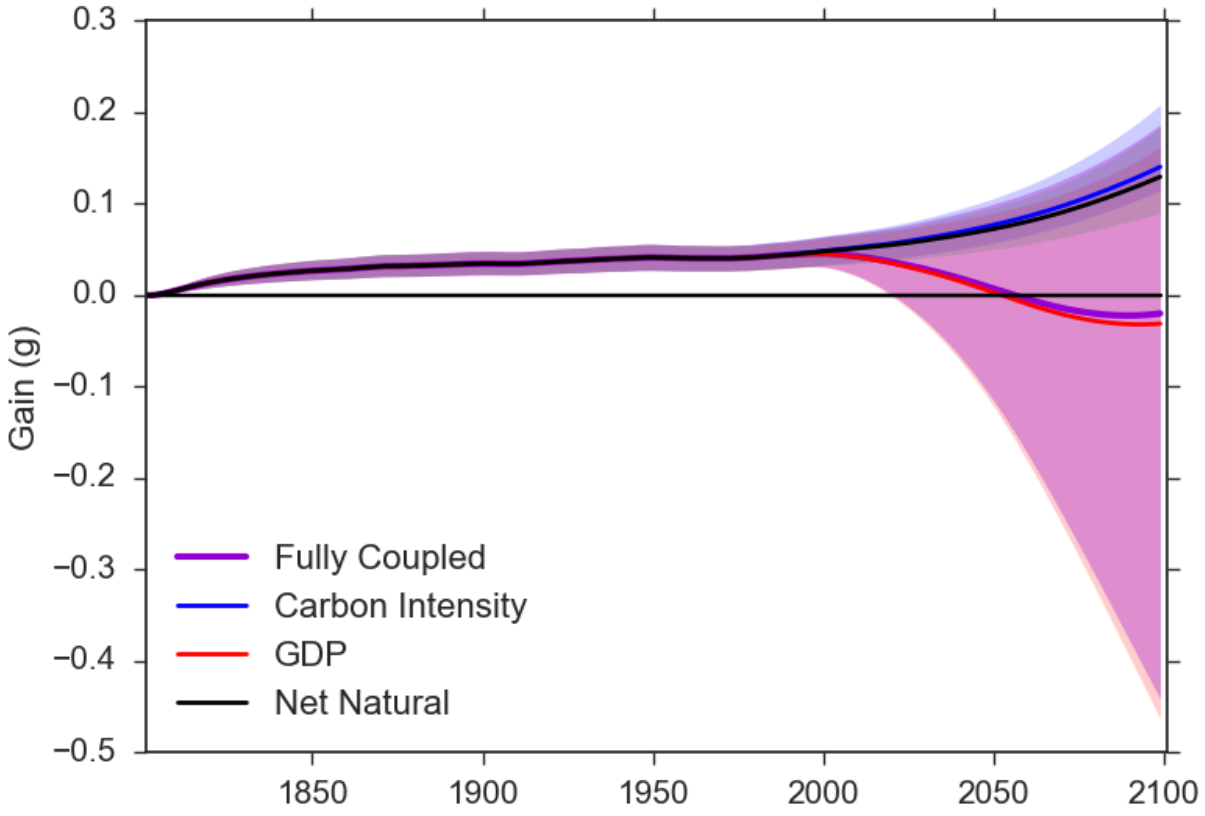

Figure A.5: Cumulative carbon-climate feedback gain over time in the Fully Coupled and Net Natural scenarios from our model. Also shown are the components from GDP and Carbon Intensity that contribute to the overall change in the gain from the Net Natural to the Fully Coupled scenario. Until the mid-21st century the positive gain from the natural carbon cycle effects dominates, but by the middle of the 21st century economic feedbacks dominate, pulling the overall gain negative. Background colors show the uncertainty associated with each scenario.

Table A.1: Descriptions and coupled components of the seven scenarios used in the model to calculate carbon feedbacks. The first columns show which components were coupled to which driver. A value of 'ΔT' indicates that the carbon-climate feedback indicated by the column was included, while a value of 'CO_2' indicates that carbon-concentration feedback processes were included. A blank value means that the component was treated as an exogenous input and the original source data was used. All scenarios included land and ocean coupling with atmospheric carbon dioxide. To calculate the contribution of each economic component to the total feedback effect we isolated each in its own scenario as well as investigating their overall effect in the Net Economic scenario. All feedbacks included in our model were combined in the Fully Coupled scenario.

Scenario	**Land Flux**	**Ocean Flux**	**Human Flux Driver (F_H)**				**Description**
	(F_L)	**(F_O)**	**P**	**G/P**	**E/G**	**F/G**	
No Feedbacks	CO_2	CO_2	—	—	—	—	Only ocean and land carbon-concentration feedbacks
Net Natural	ΔT, CO_2	ΔT, CO_2	—	—	—	—	Only ocean and land carbon-concentration and carbon-climate feedbacks
Population	CO_2	CO_2	ΔT	—	—	—	No Feedbacks + population carbon-climate feedbacks
GDP	CO_2	CO_2	—	ΔT	—	—	No Feedbacks + GDP carbon-climate feedbacks
Energy Intensity	CO_2	CO_2	—	—	ΔT	—	No Feedbacks + energy demand carbon-climate feedbacks
Carbon Intensity	CO_2	CO_2	—	—	—	ΔT	No Feedbacks + energy supply carbon-climate feedbacks
Net Economic	CO_2	CO_2	—	ΔT	—	ΔT	No Feedbacks + economic carbon-climate feedbacks
Fully Coupled	ΔT, CO_2	ΔT, CO_2	—	ΔT	—	ΔT	All carbon-concentration and carbon-climate feedbacks

Table A.2: Changes in each component of the Kaya Identity in our Fully Coupled scenario compared to the baseline projected data in years 2030 and 2100. By 2030 none of the temperature effects have impacted these components by over 1 percent, but by 2100 we see a decrease in GDP of 22% percent and an increase in the energy intensity of GDP and the carbon intensity of energy by less than 3% each.

	2030			**2100**		
Kaya Component	Baseline Projection	Fully-coupled	Percent Difference	Baseline Projection	Fully-coupled	Percent Difference
Population (billion)	8.4	8.4	-0.03%	8.9	8.9	-0.34%
Per capita GDP (US$1000)	8.2	7.4	-9.6%	36	28	-22%
Energy intensity of GDP (EJ/US$)	99	99	-0.25%	59	60	1.1%
Carbon intensity of energy (Pg C/EJ)	0.02	0.02	0.62%	0.01	0.01	2.4%

Table A.3: Temperature and carbon cycle results from all scenarios in our model under RCP8.5. Values are listed as base (min, max), though for the Population scenario the effects were too small for the differences to be seen at this precision. All values are cumulative over the period from 1800 to 2100. Including an economic feedback (Fully Coupled scenario) lowered temperature by over a quarter of a degree and reduced atmospheric carbon by 220 Pg C compared to the Net Natural scenario. The net economic feedback also reduced the carbon-climate feedback gain (g) in our Fully Coupled scenario to -0.02 from 0.13 in our Net Natural scenario.

Scenario	ΔT_{air} (C)	ΔC_A (Pg C)	ΔC_H (Pg C)	ΔC_O (Pg C)	ΔC_L (Pg C)	Gain (g)
No Feedbacks	**4.25** (3.98, 4.54)	**1311** (1192, 1438)	**2238** (2238, 2238)	**649** (583, 724)	**278** (462, 76)	—
Net Natural	**4.55** (4.17, 4.98)	**1506** (1311, 1761)	**2238** (2238, 2238)	**566** (556, 518)	**166** (372, -41)	**0.1294** (0.0903, 0.1836)
Population	**4.25** (3.97, 4.54)	**1310** (1190, 1437)	**2236** (2234, 2237)	**648** (583, 724)	**277** (462, 76)	**-0.001** (-0.002, -0.001)
GDP	**3.94** (3.23, 4.50)	**1119** (761, 1407)	**1934** (1507, 2194)	**577** (427, 714)	**237** (320, 73)	**-0.172** (-0.567, -0.022)
Energy Intensity	**4.25** (3.99, 4.54)	**1317** (1201, 1439)	**2246** (2238, 2252)	**650** (586, 723)	**279** (465, 76)	**0.004** (0.000, 0.007)
Carbon Intensity	**4.27** (3.97, 4.59)	**1327** (1189, 1478)	**2262** (2232, 2296)	**654** (582, 738)	**281** (461, 80)	**0.012** (0.003, 0.027)
Net Economic	**3.96** (3.22, 4.55)	**1130** (759, 1445)	**1952** (1505, 2250)	**582** (426, 727)	**240** (319, 77)	**-0.160** (-0.570, 0.005)
Fully Coupled	**4.23** (3.35, 4.99)	**1286** (813, 1768)	**1940** (1474, 2246)	**514** (407, 519)	**140** (253, -41)	**-0.020** (-0.466, 0.187)

Table A.5: List of key model parameter values. Starred values have been tuned to fit to CMIP5 model results from previous analysis as described in the text. We initialized atmospheric carbon, net primary productivity, and air temperature to approximate pre-industrial values: 283 ppm, 60.0 $\frac{PgC}{yr}$, and 15.0 °C, respectively.

Parameter	Value
Ocean area	3.61e14 m^2
Mixed layer depth*	100 m
Ocean depth	3800 m
k_{gas}*	0.06 yr^{-1}
τ_{md}*	7.0 years
f_{mod}	0.15 $°C^{-1}$
τ_{b0}*	15.0 years
β*	0.65
a_{land}*	-0.002 $°C^{-2}$
b_{land}	-0.013 $°C^{-1}$
Revelle factor*	11.5
Q10*	1.1

Table A.6: Tuned model results compared to previous analysis. The first two rows show the comparison of the carbon cycle in our model to the analysis by Arora et al. (2013) of CMIP5 model carbon cycle feedbacks in the run that includes all natural feedbacks under one percent per year CO_2 increase up through a quadrupling of CO_2. The final two rows compare our model to the CMIP5 model carbon cycle results from Friedlingstein et al. (2013) using the RCP8.5 scenario. Carbon cycle changes under RCP8.5 are calculated from 1850-2100, and temperature change is calculated as the average from 2081-2099 relative to 1986-2005. Results over the 1% runs are calculated as the change over the 140-year period. Columns 4 and 5 are the cumulative changes in land and ocean carbon storage, and column 6 is the change in atmospheric carbon over the period. All our model values have been tuned to within one standard deviation of the results from each of these analyses.

Scenario	**Analysis**	Δ**T** (°C)	$\Delta\mathbf{C_L}$ (Pg C)	$\Delta\mathbf{C_O}$ (Pg C)	$\Delta\mathbf{C_A}$ (Pg C)
Idealized 1% run	Arora et al. (2013)	4.76	499±275	613±50	1805
	This model	5.02	504	649	1805
RCP8.5	Friedlingstein et al. (2013)	3.9±0.9	91±218	557±112	985±97
	This model	3.2	177	563	994

Table A.7: Sources of socioeconomic baseline data used for this analysis. For all but fossil fuel and land use change emissions, three different datasets were used in order to cover the full period of interest. All datasets were harmonized to the modern data of each using the ratio of the slopes at the end points of overlap. The future data are projected values by the Global Change Assessment Model corresponding to the GCAM rendition of business-as-usual scenario RCP8.5.

Variable	Data Source	Time span used
Population	Maddison Project (Bolt and van Zanden, 2014)	1800-1960
	United Nations (2015)	1960-2014
	GCAM (Moss et al., 2008, 2010)	2014-2100
GDP	Maddison Project (Bolt and van Zanden, 2014)	1800-1970
	World Bank (2015)	1971-2014
	GCAM (Moss et al., 2008, 2010)	2014-2100
Energy	Vaclav Smil (2010)	1800-1980
	US Energy Information Administration (2019)	1980-2014
Fossil Fuel Emissions	GCAM (Moss et al., 2008, 2010)	2014-2100
	CDIAC (Boden et al., 2017)	1800-2014
	GCAM (Moss et al., 2008, 2010)	2014-2100
Land Use Change Emissions	RCP8.5 Harmonized Emissions Data (Meinshausen et al., 2011)	1800-2100

Table A.8: Individual components of the carbon-climate feedback on the carbon intensity of energy. For our base model the best estimate of each component was used to adjust the corresponding fraction of energy at each time step when multiplied by the temperature change at that time step. The range was used to model upper and lower bounds. For transportation, we used upper and lower bounds of ± 100% due to the high uncertainty of this relationship.

Component	**Best estimate (% per $^{\circ}C$)**	**Range (% per $^{\circ}C$)**	**References**
Coal	-1.05	(-1.5, -0.6)	(Aivalioti, 2015; Sathaye et al., 2011; Burnard and Bhattacharya, 2011)
Natural Gas	-0.75	(-1, -0.3)	(Aivalioti, 2015; Basha et al., 2012; Farouk et al., 2013; Mohanty and Paloso, 1995; Kakaras et al., 2006; Alhazmy and Najjar, 2004; Ameri and Hejazi, 2004)
Oil	-0.75	Same as NG	(Basha et al., 2012)
Distribution	-0.87	(-1.4, -0.33)	(Aivalioti, 2015; Sathaye et al., 2011)
Transportation	0.0406	(0, 0.08)	derived from (Janssen and Hall, 1980; Lohse-Busch et al., 2013; Johnson, 2002; Pedersen and Larsen, 2009; Zahabi et al., 2014)